THE UNIVERSITY OF MANITOBA

PERIPHERAL SITE LIGAND-MEDIATED EFFECTS ON ACETYLCHOLINESTERASE

BY

© BULENT MUTUS

A THESIS
SUBMITTED TO THE FACULTY OF GRADUATE STUDIES
IN PARTIAL FULFILMENT OF THE REQUIREMENTS FOR THE DEGREE
OF DOCTOR OF PHILOSOPHY

DEPARTMENT OF CHEMISTRY

WINNIPEG, MANITOBA
1981

PERIPHERAL SITE LIGAND-MEDIATED EFFECTS ON ACETYLCHOLINESTERASE

BY

BULENT MUTUS

A thesis submitted to the Faculty of Graduate Studies of the University of Manitoba in partial fulfillment of the requirements of the degree of

DOCTOR OF PHILOSOPHY

dedicated to my mother and father

Emel and Cemil Mutus

ACKNOWLEDGEMENTS

I would like to express my deep appreciation to my supervisor Dr. G. Tomlinson of the Department of Chemistry, University of Winnipeg, for his thoughtful guidance, encouragement, patience and enthusiasm for the project and for biochemistry in general.

I would also like to thank Dr. H.E. Duckworth, president of the University of Winnipeg, for financial support. Dr. F.W. Barth, for unlimited use of the research facilities. Dr. B.D. Roufagalis, Department of Pharmaceutical Sciences, University of British Columbia; Dr. F.C. Stevens, Department of Biochemistry, University of Manitoba; Dr. H.W. Duckworth and Dr. J.C. Jamieson of the Department of Chemistry, University of Manitoba, for critical evaluation of the thesis.

Mr. I. McLennan, Mr. D.V. Duncan and Ms. M. Mooibroek for assistance in parts of the project.

Mr. G. Baird and Mr. G. Reinfeld of Technical Services, University of Winnipeg for their expertise. Mr. W. Danchura for assistance in computer programming. Ms. Marliss Ziprick for typing the thesis.

And a special thanks to Barbara for all her help, assistance and love during this period in our lives.

TABLE OF CONTENTS

ABSTRACT

Acetylcholinesterase (acetylcholine acetyl-hydrolase E.C. 3.1.1.7), in addition to the anionic subsite of the catalytic site, possesses a class of peripheral anionic sites. The functional consequences of peripheral site occupation were investigated by steady-state and pre-steady-state kinetic studies, using affinity purified acetylcholinesterase isolated from the electric organs of Electrophorus electricus and Torpedo californica.

The existence of a peripheral anionic region on E. electricus acetylcholinesterase, as well as the peripheral site-specificity of the cationic ligands propidium, gallamine, Mg^{2+} and Zn^{2+}, was established by fluorescence binding and displacement experiments.

Steady-state kinetics indicated that the enzyme existed in two distinct kinetic states stabilized at either low or high ionic strength. The peripheral site ligands gallamine, propidium, Mg^{2+} and Ca^{2+} were shown to convert the low ionic strength form of the enzyme (E) to the high ionic strength form (E_a). The cation Zn^{2+} was shown to have two opposing effects on the steady-state hydrolysis rates: an instantaneous activation as well as a slow inactivation of the enzyme. This may be a general metal ion effect with consequences which depend upon the relative affinities of the various binding sites for a particular metal ion.

The pre-steady-state kinetics enabled a more comprehensive study of the effects of peripheral site occupation on

the proposed kinetic mechanism of acetylcholinesterase. Organic peripheral site activators were shown to activate both the carbamoylation (k_2) and the decarbamoylation (k_3) rate constants whereas inorganic activators were shown to activate only the decarbamoylation rate constant (k_3), suggesting the existence of discrete binding sites for organic and inorganic activators.

Another group of peripheral site ligands Zn^{2+}, d-Tubocurarine, Hg^{2+} and Cd^{2+}, induced the conversion of acetylcholinesterase to an inactive form. This inactivation was partially reversible, but a slow metal-cation/O_2-dependent irreversible step was evident.

The kinetics of the metal-induced inactivation at low ionic strength were characterized by two slow, first order processes differing by approximately an order of magnitude. At high ionic strength the inactivation rates were monophasic with a rate constant identical to the faster rate observed at low ionic strength. The fast and the slow rates were attributed to the inactivation of activated (E_a) and active (E) forms of the enzyme, respectively. Therefore the biphasic inactivation kinetics at low ionic strength can be explained by the dual action of inactivating-metal ions: 1) A rapid conversion of active enzyme (E) to the activated (E_a) form and 2) A concomitant slow conversion of the two enzyme forms (E, E_a), with differing rates to inactive states.

The inactivation produced by La^{3+} was unlike that observed with the other inactivating metal ions, in that the inactivation

was not complete within four orders of magnitude of La^{3+} concentration and the inactivation profiles were characterized by a plateau region.

A ligand binding model has been proposed to account for the observed peripheral site ligand-induced kinetic states in acetylcholinesterase. This model was particularly successful in accommodating the La^{3+} inactivation results.

A search for free thiol groups in acetylcholinesterase was initiated. Both T. californica and E. electricus enzymes were modified by reaction with DTNB and N-dansylaziridine, two thiol-specific reagents. A fluorescent, ninhydrin positive compound with identical R_f values to those of dansyl-s-aminoethyl cysteine was isolated from the hydrolysates of the enzyme modified with N-dansylziridine. While strongly suggestive of the presence of thiol groups in acetylcholinesterase conclusive proof must await further characterization of this compound. Acetylcholinesterase was most reactive towards N-dansylaziridine in the inactive state (E_i), partially reactive in the active (E) state and least reactive in the activated (E_a) state, further illustrating the existence of at least three peripheral site ligand-induced conformational states in acetylcholinesterase.

LIST OF ABBREVIATIONS

AcCh	acetylcholine
AcSCh	acetylthiocholine
AcChase	acetylcholinesterase
iPr_2PF (DFP)	diisopropylfluorophosphate
DPA	N,N-dimethyl-2-phenyl-aziridinium
TDF	p-(trimethyl ammonium)benzene diazonium fluoroborate
2-PAM	pyridine-2-aldoxime methiodide
M7C	1-methyl-7-dimethylcarbamoyloxy-quinolinium
M7H	1-methyl-7-hydroxyquinolinium
DMB	decamethonium bromide
	p-Chloromercuribenzoic acid
DTNB	5,5'-dithiobis-(2-nitrobenzoic acid)
TEA	tetraethylammonium
EDTA	ethylenediamine tetraacetic acid
N-DAZ	N-dansylaziridine
NPA	p-nitrophenylacetate
NEM	N-ethylmaleimide
Ac	acyl
Pr	propyl
Bu	butyl
Et	ethyl

LIST OF TABLES

LIST OF FIGURES

INTRODUCTION

1) Historical background:

The pharmacological effects of acetylcholine were first demonstrated in 1906 (1). Evidence at that time suggested that acetylcholine was released from certain nerve endings and crossed the interneural gap, acting as a "chemical transmitter". This led Stedman *et al*. (2) to propose the existence of a specific enzyme for the hydrolysis of acetylcholine. An esterase was first isolated from horse serum (2). However, subsequent investigations (3, 4, 5) indicated that this esterase was non-specific for choline esters. Alles and Hawes, in 1940, were able to isolate an esterase specific for choline esters from the erythrocytes (6).

Nachmansohn and Rothenberg (7, 8) extended the search to conducting tissues of various animals, and were successful in identifying many choline specific esterases. The esterases isolated from electric tissues of *Torpedo californica* and *Electrophorus electricus* demonstrated extremely high rates of hydrolysis: one milligram of crude preparation was able to hydrolyze 70 g of acetylcholine per hour. The enzyme-catalyzed rates of hydrolysis of choline esters were in the order of Ac > Pr > Bu (9). From all of these investigations it was apparent that a choline ester-specific esterase existed in all of the conductive tissues examined. The main characteristics of these esterases were summarized as follows: 1. A high affinity for acetylcholine; 2. A well defined maximal velocity; 3. Decreased rates of hydrolysis of choline esters

with increased length of the acyl chain (in the order Ac > Pr > Bu). Augustinson and Nachmansohn (10) proposed that esterases displaying these characteristics be named acetylcholinesterase.

2) The role of Acetylcholine, Acetylcholine receptor and Acetylcholinesterase in electrical activity of the cholinergic neurons:

i) Acetylcholine:

Acetylcholine (AcCh) is generally accepted as the chemical transmitter at the cholinergic synapse and at the neuromuscular junction. This hypothesis has been arrived at through many experiments (mainly performed at the neuromuscular junction) that suggest; (1) that AcCh is released presynaptically, (2) that its action is at the postsynaptic site, and (3) that enough AcCh is released to initiate a muscle response. Some of these experiments are summarized below:

Dale, Feldberg and Vogt (11) were able to detect AcCh in perfusion fluid whenever the nerve was stimulated, in experiments where an esterase inhibitor (eserine) was used to prevent the hydrolysis of the released AcCh. The presynaptic release of AcCh was demonstrated by several experiments. Dale et al. (11) showed that in denervated muscle no AcCh was released. Upon stimulation of motor nerves in the presence of curare, which prevents the depolarization of muscle fibers, nerve impulses were shown to reach the axon terminals (12) and the usual amount of AcCh was released (11). Even when muscle fibers were cut away, AcCh was still released upon stimulation

of the nerve (13). On the other hand, the release of AcCh was shown to be greatly diminished under conditions that prevent depolarization of neurons such as low Ca^{+2} or high Mg^{+2} concentrations (13).

End plate regions of muscle were shown to be very specific "detectors" of AcCh; as low as 10^{-16} moles of AcCh applied externally were shown to depolarize muscle fibers (14).

It was further observed that neurons in the resting state secreted small but detectable amounts of transmitter from their terminals, causing miniature end plate potentials (mepps) (15, 16). When the neuromuscular preparations were bathed in low Ca^{+2} solutions, the observed end plate potential was very small. Upon increasing the concentration of Ca^{+2} the end plate potential increased in integral multiples of the mepps rather than in continuously graded amounts. This led Katz and his colleagues (15, 16) to introduce the idea of quantal release of AcCh from nerve terminals. Katz and Miledi (17, 18) were able to demonstrate that Ca^{+2} is the link between the action potential and the secretion of AcCh. Neither Na^{+} influx nor the K^{+} efflux associated with the action potential was required for AcCh release (19).

The site of action of Ca^{+2} as well as the mechanism of transmitter release is not yet known. Shortly after the demonstration of quantal release, synaptic vesicles were found in nerve terminals (20, 21), which led to the suggestion that each vesicle corresponds to a quantum of AcCh. Subsequent studies have demonstrated that both AcCh and norepinephrine

are associated with vesicles similar to those found near the nerve terminals (22). The amount of AcCh represented by a quantum has been estimated to be in the range 0.2 to 3.0 x 10^5 molecules (22). For the vesicle hypothesis to be correct each vesicle should at least contain this amount of AcCh. Measurement of AcCh content of vesicles have yet to be made but Sheriden, Whittaker and Israel (23), using crude vesicle preparations of known AcCh content, have calculated that each vesicle of 80 nm diameter contains approximately 4 x 10^4 molecules of AcCh. However, the present data are too uncertain to provide firm evidence for or against the vesicle hypothesis. The mechanism by which AcCh enters and is released from the vesicles is also unclear.

Another model for nerve excitability has been proposed by Nachmansohn (24-27). In the proposed "integral model of nerve excitability" AcCh is not a neurotransmitter but instead acts intra-cellularly within the presynaptic and postsynaptic membranes. K^+ instead of AcCh is thought to be the neurotransmitter released into the synaptic cleft. Central to this model is the presence within the presynaptic and postsynaptic membranes of a protein complex termed the basic excitation unit (BEU). BEU's are thought to be ionic gateways surrounded by a protein complex comprised of an AcCh storage protein, AcCh-receptor and acetylcholinesterase.

The key processes in this model are as follows:

a) AcCh is released from the storage site by a proper stimulus, and is translocated to the AcCh-receptor.

b) The receptor is thought to bind Ca^{+2} in its resting state. When AcCh is bound, Ca^{+2} is released, resulting in a conformational change. This leads to permeability changes in the gateway (the AcCh-receptor is thought to comprise a part of the gateway). The permeability changes result in the efflux of K^{+} ions, into the synaptic cleft.

c) AcCh is translocated to acetylcholinesterase where it is hydrolyzed.

d) After the destruction of AcCh the receptor assumes its resting conformation (Ca^{+2} bound state), resulting in the closure of the gateway.

e) K^{+} released into the cleft then triggers the same process postsynaptically, resulting in the propagation of the impulse.

The integral model of Nachmansohn is very hypothetical. Therefore its general acceptance must await further experimental evidence.

ii) Acetylcholine receptor:

Although the AcCh - receptor and the enzyme acetylcholinesterase display many similarities in ligand binding properties, they are distinct proteins. The properties of acetylcholinesterase will be discussed at length throughout the Introduction. At this point it is appropriate to describe some of the properties of the AcCh-receptor.

The AcCh-receptor isolated from T. californica or E. electricus is composed of five subunits; two smaller ones for the binding of AcCh and three different larger ones whose

function is not well understood (28-36).

The evidence for the AcCh-receptor being a transmembrane protein has been given (37). The molecule appears to span the postsynaptic membrane, protruding about 5 nm from the inner surface. Its diameter viewed face on, is about 8.5 nm with a 2.5 nm pit at the centre which narrows to form an 0.65 nm ion pore (37).

Binding studies using AcCh-analogues indicate the presence of an anionic site. As well there seems to be a region of hydrophobic interaction with the ligand about 1 nm from the anionic site (28).

A wide variety of AcCh analogues (agonists) have been shown to depolarize post-synaptic membranes of skeletal muscle and the electroplax of electric fish. Also a larger number of compounds have been found that are inhibitors (antagonists) of the AcCh-induced depolarization.

Not all agonists induce the same degree of depolarization (38). These results were explained in terms of a two-state allosteric model (39). In the proposed model the receptor was thought to exist in two conformational states which are in equilibrium: an active state which increases permeability and an inactive state. In the resting membrane the equilibrium would favor the inactive state. Agonists were thought to bind to the active state whereas antagonists would bind to the inactive state. Another interesting observation was the desensitization of the AcCh-receptor. Prolonged incubation with acetyl-, carbamoyl- or succinyl-choline resulted in an

observed decrease in the effectiveness of the agonists (40). This phenomenon was explained by an agonist-induced slow conformational change of the receptor from the agonist sensitive (low affinity) to an agonist desensitized (high affinity) form. This was subsequently demonstrated by Rang and Ritter (41, 42) by equilibrium dialysis measurements. Desensitization by antagonists could not be demonostrated under these experimental conditions. As a result antagonists were assumed to bind to the desensitized form of the receptor. The desensitization kinetics were still adequately treated under the two state model (38, 40). However, direct measurements utilizing the intrinsic fluorescence of the membrane bound AcCh-receptor (43, 44) and fluorescent probes (44, 45), suggested that both agonists and antagonists induced slow conformational changes upon prolonged contact with the receptor. More recently, Quast et al. (46) studying [^{125}I]α-bungarotoxin-receptor complex formation in the presence of various ligands, have also demonstrated that both agonists and antagonists "desensitized" the receptor; furthermore, agonist- and antagonist-induced slow conformational changes were implicated. The desensitization kinetics were no longer adequately treated by the two state model (46, 28, 40). A more appropriate model for agonist-antagonist induced desensitization of the receptor is illustrated in Figure I.

In this model agonists induce a fast conformational change to the active or depolarized state; this is followed by a slow-conformational change to the desensitized state of the receptor.

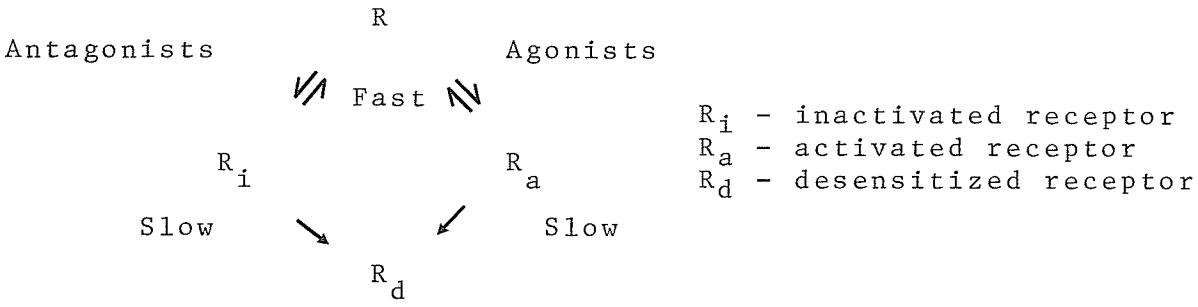

FIGURE I

Antagonists on the other hand, induce a fast conformational change to an inactive state followed by a slow conformational change to the desensitized state of the receptor. Further evidence for ligand induced conformational changes comes from the chemical modification of the receptor. AcCh-receptor has been shown to possess an easily-reduced disulphide in the vicinity of the AcCh binding site (28). Reduction of this disulphide bridge alters the pharmacological properties of the AcCh-receptor (22, 28). In the desensitized state, an agonist-dependent decrease in the rates of reduction of the disulphide bridge was observed (47). The rates were lowered 80-fold by AcCh; 64-fold by n-butrylcholine; 43-fold by succinylcholine; 21-fold by carbamylcholine; 15-fold by phenyltrimethylammonium; and 12-fold by tetramethylammonium. This order roughly parallels the depolarizing ability of these agonists. The decrease in the rates of reduction were explained in terms of agonist-induced conformational changes that result in the disulphide bond being protected from the reducing agents (47).

AcCh-receptor is essentially irreversibly blocked by

several neurotoxins isolated from various snake venoms. These toxins are small peptides with molecular weights of 7000 to 8000 daltons. The dissociation constant for α-toxin type II from Naja naja with E. electricus AcCh-receptor is 1 nm whereas the dissociation constant for Naja nigricolis α-toxin type I with T. californica AcChase is 0.1 nM (28). These toxins have no effect on the acetylcholinesterase activity (22, 28). The mode of toxin binding to the receptor is not understood. However, it seems to be very specific. Modification of one tryptophan residue in cobra neurotoxin or in erabulotoxin results in the loss of binding ability to the receptor (28).

The total membrane protein fraction of E. electricus electric tissues contains 15% AcCh-receptor, 43% AcChase and 39% ATPase (28).

The receptor can be solubilized from the membrane by non-ionic detergents and/or bile salts, and can be further purified on affinity gels to which toxins have been covalently linked (28). The purification and properties of the AcCh-R are summarized in Tables I and II (28, 29). AcCh-R is thought to be a pentameric complex with a molecular weight of 255,000 daltons. The subunit stoichiometry is (4×10^4: 5×10^4:6×10^4:6.5×10^4 daltons) 2:1:1:1. The 4×10^4 dalton dimeric subunit contains the cholinergic ligand binding site.

The function of the remaining subunits is not well established. It is known that all four subunits are present in the outer surface of the membrane. It remains to be determined

TABLE I (28). Purification of Acetylcholine receptor by affinity chromatography.

Gel Ligand	Eluting Ligand	Specific Activity (μ mol sites/g protein)	Mol.Wt.SDS-PGE[a] (10^3 daltons)
	E. electricus		
N.naja toxin	Benzoquinonium	7.5	42, 54
N.n.siam.toxin	Hexamethonium	11	160
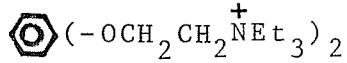	Fladexil	4.5	43, 48
	Decamethonium	4.5	44, 50
	Carbamylcholine	4	40, 47, 53
	T. californica		
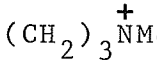	NaCl gradient	6	26, 35, 42
N.n.siam toxin	Carbamylcholine gradient	3.3	
N.n. siam toxin	Carbamyl choline		

[a] SDS-PGE: Sodium dodecyl sulphate - polyacrylamide gel electrophoresis.

TABLE II (29). Properties of purified T. californica Acetylcholine receptor.

	Structure
Subunit composition	40×10^3; 50×10^3; 60×10^3; 65×10^3 (daltons)
Subunit stoichiometry	2:1:1:1
Molecular mass	255×10^3 daltons
	Physical Properties
S value	9s; 13.7s as dimer
Stokes radius	72 A°
Isoelectric point	4.9
Specific activity	1 α-bungarotoxin per 110×10^3 daltons

which of these subunits comprise the ion channel and which are transmembrane in nature (29). Purified AcCh-receptor has been successfully reconstituted into bilayers (48). Antibodies to AcCh-receptor have been raised in rabbits, these have been shown to complex with AcCh-receptor but not with acetylcholinesterase (28). Recently m-RNA for AcCh-receptor has been isolated (49).

iii) Acetylcholinesterase:

In animals, acetylcholinesterase (AcChase) is present in various tissues which include muscle, in the synaptic cleft and the postsynaptic and axonal membranes of cholinergic neurons (and in some neurons not known to be cholinergic), as well as the erythrocyte and placental membranes. In muscle, AcChase activity is 3 to 6 times higher in end plate regions (50). The highest concentrations of AcChase are found in the electric organs of electric fish. These organs are phylogenetically derived from muscle. Within these tissues AcChase is found in several molecular forms. The largest of these molecular species is one comprizing 12 catalytic subunits attached via a collagen-like tail to the extracellular basal lamina. AcChase occurs in tetrameric, dimeric and monomeric globular soluble forms within myoneural tissue or the synaptic cleft. Particulate forms of AcChase are also found within excitable axonal membranes, both pre- and postsynaptically (24, 51).

AcChase plays an integral part in the maintenance of ionic currents in nervous tissues. Its role is the rapid destruction (80 μsec/molecule) of the depolarizing agent,

AcCh, thereby restoring excitable membranes to their resting state. Introduction of anticholinesterase drugs to the synapse or to the neuromuscular junction results in the blockage of electrical activity. The role of AcChase in axonal conduction seems harder to delineate. The main difficulties have been in the assay and the subsequent inhibition of the total AcChase activity in the axon, which is extremely well protected with such physical barriers as the nodes of Ranvier and the myelin sheath. Previous attempts to determine the role of AcChase in axonal conduction have involved the exposure of nerves to various reversible and irreversible AcChase inhibitors. The effects of such inhibitors on electrical activity were then correlated with AcChase levels, determined by homogenization of the tissues. The results obtained in this way have been very inconsistent (52, 53, 54) and contradictory. More recently, Kremzner and Rosenberg (55), working with the intact giant squid axon, have demonstrated that the inhibition of 99% of AcChase activity with the inhibitor, tertiary anologue of phosphine (TP), had no observable effect on electrical conduction. Diisopropylfluorophosphate (iPr_2PF), on the other hand, was shown to block enzymic and electrical activity. However, this was thought to result from the non-specific action of DFP on the axon.

Unfortunately, the evidence to date is not very conclusive, but indications are that there is no simple and direct relationship between axonal conduction and AcChase activity.

3) Methods of isolation, purification and assay of Acetylcholinesterase:

i) Isolation and purification of Acetylcholinesterase:

Various methods of extraction, isolation and purification are summarized in Table III.

Method 1) results in well defined homogeneous AcChase populations with one obvious drawback; the time of extraction. With method 2) 18s, 14s and 11s species are isolated. However, the lack of careful controls has given rise to conflicting reports on the distribution of these species (56). Method 3) seems to be the method of choice: It is fast and has consistently resulted in the extraction of 18s and 14s species which can, easily and in high yields, be converted to the 11s globular form by the action of proteases.

ii) Assay methods:

See Table IV.

4) Structure of Acetylcholinesterase:

The most recent model proposed for the enzyme attached to the basal lamina, based on electron micrographic evidence (82, 83, 84) and on the analysis of the degradative species (60, 65), is an asymmetric structure with a globular head containing 12 catalytic subunits. The subunits are arranged as three tetramers. Within each tetramer, two subunits are linked by disulphide bridges, while the remaining two are attached to a collagen-like tail *via* disulphide bridges. The collagen-like tail is estimated to have a molecular weight

Table III. Methods of purification of acetylcholinesterase.

Step	Procedure	Yield %	Specific activity[a] %	Sedimentation coefficient of the species isolated
I.	*E. electricus* (57, 68)			
1.	Immersion of tissue slices in toluene (2 yrs)			
2.	Homogenization in $(NH_4)_2SO_4$			
3.	Centrifugation			
4.	3 x $(NH_4)_2SO_4$ precipitation/centrifugation	15	20	11s
II.	*E. electricus* (69)			
1.	Immersion of tissue slices in toluene (2 yrs)	100	3	
2.	Homogenization			
3.	Centrifugation			
4.	Supernatant chromatographed on benzyl aminoethyl cellulose	73	4	
5.	Concentration	68	5	
6.	Sephadex G-100 chromatography	54	9	
7.	Celex-P chromatography	36	50	
8.	DEAE-cellulose chromatography	24	90	
9.	DEAE-cellulose chromatography	9	100	10.8s
III.	*E. electricus* (59)			
1.	Homogenization in 2M NaCl	N/A		
2.	Centrifugation			
3.	$(NH_4)_2SO_4$ precipitation			
4.	Centrifugation			
5.	Pellet dialysed against $CsCl_2$			
6.	Centrifugation			
7.	Dialysis			
8.	Lyophilization			
9.	Saline sucrose gradient centrifugation		60	18.5s;14.2s; 9.2s

Table III. Continued.

Step	Procedure	Yield %	Specific activity[a] %	Sedimentation coefficient of the species isolated
AFFINITY CHROMATOGRAPHY				
IV. *E. electricus*				
	1. 1M NaCl extraction of fresh tissue 2. Affinity chromatography Gel ligand: 9-[γ-N-(Sepharose-4B-6-aminocaproyl)-γ-aminopropylamino acridinium]	60	50	17.8s; 13.8s
V. *E. electricus* (70)				
	1. Toluene extraction (2 yrs) 2. Homogenization in 5% $(NH_4)_2SO_4$/centrifugation 3. 2 x precipitation in 5% $(NH_4)_2SO_4$/centrifugation 4. Affinity chromatography			
	Gel ligand: 1) Sepharose-4B-6-(aminocaproyl)-phenyltrimethyl ammonium	65-75	100	11s
	2) Sepharose-4B-6-(aminocaproyl)-phenyltrimethyl ammonium	40-50	60	11s
VI. *T. californica* (64)				
	1. Homogenization of fresh tissue in 0.04M $MgCl_2$/0.1M NaCl	100		
	2. Centrifugation			
	3. Supernatant digested with trypsin for 8 minutes; reaction stopped by the addition of soybean trypsin inhibitor.	90		
	4. Centrifugation.			
	5. Affinity chromatography			
	Gel ligand: Sepharose-4B-6-(aminocaproyl)-6-(aminocaproyl)-m-phenylenetrimethyl ammonium	46	60	10.8s

[a] Expressed as a % of the highest specific activity obtained 10000 Ellman assay units/mg of protein.

Table IV. Assay methods.

Method	Description of Assay	Comments	References
1) pH STAT	Titration of H^+ released during ester hydrolysis; dual syringe modification enables activity measurement at constant level of substrate concentration.	Non-specific; least sensitive; can be used with particulate or soluble enzymes.	71, 72
2) SPECTROPHOTOMETRIC			
a) Ellman Assay	Detection of the mercaptide released from thioester substrate acetylthiocholine with a chromophoric oxidizing agent DTNB.	Substrates limited to thioesters; possible modification of AcChase with DTNB has been reported (76).	73, 74, 75
b) p-nitrophenylacetate	Release of the chromophore nitrophenylate anion is detected at 400 nm.	Non-specific; low solubility in H_2O.	77, 56
ACTIVE SITE TITRANTS			
3) 1-methyl-7-dimethyl carbamoyloxy quinol	Fluorogenic, transient kinetic burst in the formation of carbamyl enzyme can be directly related to enzyme active site concentration.	Very sensitive; soluble; stable also can be used to evaluate K_S, carbamoylation and decarbamoylation rate constants.	79, 64
4) Diisopropylfluorophosphate [^{32}P]	Phosphorylation of the active site serine leads to inactive enzyme; assayed by method of residual activity or radiometrically.	Non-specific; will react with any serine hydrolase.	56
5) DEPQ-7$^+$	Fluorogenic; M7H released upon phosphorylation is proportional to amount of enzyme.	Inhibitor reacts rapidly and completely, diethyl phosphoryl-enzyme stable.	80

of 1 x 10^5 daltons (60, 65). The sedimentation coefficient of this enzyme form is 18s and 16s for E. electricus and T. californica AcChase, respectively.

The major force involved in the interaction of the enzyme tail with the membrane surface appears to be electrostatic (63, 85), and seems to be related to the low ionic strength aggregation of the 18s, 14s and 8s forms of the enzyme (65, 85). The 18s, 14s, and 11s forms are identical kinetically (81).

Proteolysis of the 18s (16s) species yields the globular 11s species with 14s and 8s tailed forms produced as degradative intermediates (Figure 2). The same degradative pattern is obtained from the tailed enzyme containing 12 catalytic

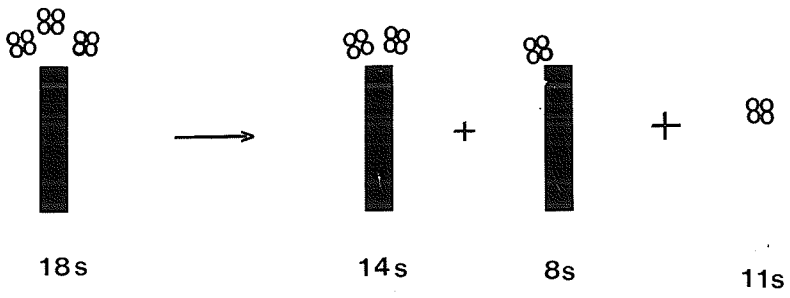

FIGURE 2

subunits isolated from the rat (51), the chicken (58, 86, 87), the bovine superior cervical ganglion (51), and the human muscle (62), thus supporting the universality of the proposed structure for the "native" AcChase, associated with the basal lamina. However, there is growing evidence for AcChase forms *in vivo* that are not associated with the basal lamina. Studies on non-degraded fresh extracts of AcChase from chicken, rat, human and more recently from *T. californica* have indicated that the major components of AcChase in these tissues are globular, non-tailed monomers, dimers and tetramers in the case of the rat, human and chicken and dimers in the case of the *T. californica* AcChase (Table V). The non-tailed native forms are identical with respect to their catalytic properties and the molecular weight of the catalytic subunit (51, 64, 88). The biological significance of the multiple molecular species found *in vivo* is not clear.

The globular 11s AcChase is very stable and does not aggregate in low or high ionic strength media. For these reasons it is the form most widely used in kinetic studies of AcChase.

The reported molecular weights of the 11s species are quite variable (Table VI). Initially, varying degrees of degradation from different autolytic and proteolytic conditions (see section 3) were thought to be responsible for the inconsistency of the reported molecular weights. However, this suggestion was disproven experimentally. Samples of the enzyme purified, after solubilization with trypsin or by autolysis (up to 4 years), resulted in molecular weights of 3×10^5

TABLE V. Sedimentation coefficients of rat, human, chicken and T. californica AcChase molecular forms.

Form	Sedimentation coefficient, S			
	Chicken(88)	Rat(88)	Human(88)	T. californica(88)
G_1	4	3.5	3.5	-
G_2	6.5	6	6	-
G_4	11.5	9.9	11	-
A_2	-	-	-	8
A_4	-	8.8	9.5	-
A_8	14.8	13	13.3	14
A_{12}	20	16.7	16.7	18

G = globular, non-tailed forms.
A = asymmetric, tailed forms.
Subscripts indicate the number of catalytic subunits.

TABLE VI. Reported molecular weights of 11s AcChase from *E. electricus*.

Mol. Wt. (daltons)	Reference
230,000	69
330,000	68
260,000	92
335,000	58

$\pm$ 1.0 x 10^4 daltons (85) for the 11s species. The differences in the solubilization procedures only became apparent after denaturation or subsequent disulphide reduction. The enzyme fraction exposed to autolysis for long periods of time had lower molecular weights (5.0 x 10^4 daltons) for the catalytic subunits. These fractions were shown to contain a non-catalytic, 2.5 x 10^4 dalton species, whereas the fractions exposed to minimal proteolysis had larger (7.0-7.5 x 10^4 dalton) catalytic subunits. The obvious conclusion then must be that the differences in molecular weight of the 11s species have arisen in the analysis of the data, and do not reflect the preparations themselves (56).

Catalytically active monomers and dimers of the enzyme have been isolated (90). Their catalytic properties (K_{app}, V_{max}) were identical to the tetrameric 11s enzyme. However, the phosphorylated enzyme was reactivated (with 2-PAM) 2.5 times faster than the dimer or the monomer (90).

The amino acid sequence of the active site region of AcChase from E. electricus has been determined (91). The sequence in the region of the reactive serine is: Gly-Gly-Glu-Ser*-Ser-Glu-Gly-Ala-Ala-Gly (asterisk indicates the serine that is reactive towards [^{32}P]-iPr_2PF) (91).

The amino acid compositions of AcChase from three different sources are given in Table VII.

Torpedo and eel enzymes appear to be quite distinct with respect to their amino acid content (64).

The presence of carbohydrate in the E. electricus enzyme

TABLE VII. Amino acid and carbohydrate composition of AcChase.

	T. californica[a] (64)	*E. electricus*[b] (70)	Difference[c] %	Bovine Erythrocyte (56)
Residue				
½ Cys	10[d]	10.6	-7.8	25
Asp	74	84.7	-15.7	46
Met	20	17.5	+9.8	9
Thr	28	29.2	-4.6	31
Ser	55	44.1	+17.9	63
Glu	75	66.9	+17.7	65
Pro	35	38.4	-7.0	27
Gly	54	56.2	-4.2	76
Ala	29	40.3	-31.6	61
Val	44	45.6	-19.2	42
Ile	28	24.3	-4.6	16
Leu	61	55.5	+4.4	43
Tyr	18	23.5	-32.2	20
Phe	38	34.2	+15.1	20
His	20	14.8	+36.1	9
Lys	34	29.6	+15.6	36
Arg	31	33.4	-7.5	5
Trp	19	12.9	+39.0	-
Hexosamine	19	N/A		
Sialic acid	2.9			
Hexose	11.1			

[a] Calculations based on 82,500 dalton subunit.
[b] Calculations based on 76,000 dalton subunit.
[c] Difference in amino acid content is taken as the difference between species (*T. californica* - *E. electricus*) divided by the average.
[d] Mol amino acid/ mol protein.

has been demonstrated qualitatively (92). 7.9% of T. californica enzyme (by weight) is made up of carbohydrates (as hexosamine, sialic acid and hexose) (64).

AcChase reportedly contains no free thiol groups (56) but the number of half-cysteine groups per tetramer range between 5 and 12 (60, 64, 70, 92). The globular 11s form of AcChase has been crystallized (92, 94), but due to crystal size and quality, X-ray crystallographic analysis of the enzyme has not yet been undertaken.

5) Catalysis:

The catalytic site of AcChase is thought be comprised of an anionic subsite to which the positively charged quaternary ammonium group of the natural substrate AcCh binds, and an esteratic site, which is acetylated at a serine hydroxyl group during esterolysis.

i) The Anionic subsite:

The anionic subsite, as the name implies, is thought to possess a net negative charge to accommodate the positively charged quaternary ammonium group of AcCh. Strong evidence for this postulate comes from studies using isosteric charged and uncharged substrates and inhibitors of the enzyme (95, 96): Substrates and inhibitors possessing a positive charge were hydrolyzed 10 times more quickly and bound 30 times more tightly, respectively, than their uncharged analogues.

The methyl groups of AcCh were also found to be important in the binding process. The binding of a series of inhibitors,

(obtained starting with ethanolamine and replacing H-atoms with methyl groups), increased the binding by a factor of seven for the first two methyl groups and 3-fold for the last (approximately 150-fold overall) (7). However, increasing the hydrophobicity of the substrates resulted in weaker substrate binding (97). Recently Hasan et al. (98) have questioned a negatively charged "anionic site". The authors pointed to the fact that methyl groups contribute approximately 5 times more to the binding than does the negative charge (95, 96). A suggestion was also made that the higher reactivity of AcCh as compared to uncharged analogues might be due to the coulombic attraction of OH^- rather than to a binding effect. Experimentally, Hasan et al. (98) were able to demonstrate a linear relationship between $\log(k_{cat}/K_{app})$ and the total molal volume of the substrates. AcCh and its uncharged analogues all fell on a straight line. A closer examination of their data reveals that the K_{app} value used (98) for AcCh is 3 to 6 fold higher than the values previously reported (56). When the data are replotted (using the accepted K_{app} value for AcCh) the experimental point for AcCh deviates significantly from the linear relationship obtained for the uncharged substrates.

The bimolecular rate constants for the association of AcCh and N-methyl-acridinium with the enzyme have been estimated to be 4.29×10^9 M^{-1} sec^{-1} and 1.1×10^{10} M^{-1} sec^{-1}, respectively (99). These values are the highest reported for the interactions of small ligands with a specific binding site. The net negative charge on the enzyme catalytic site was estimated to

have a value of $Z_E = -9$ and led to the suggestion that negatively charged groups near the catalytic site, in addition to the anionic site,are responsible for trapping of cationic ligands (99).

Studies on the effect of aromatic cations on the intrinsic enzyme fluorescence have indicated the presence of a tryptophan residue at a maximum distance of 0.5 nm from the primary site of cation binding (100).

Several irreversible "alkylating inhibitors" directed towards the anionic site have been reported. Belleau and Tani, (101) were the first to report the irreversible alkylation of the AcChase active sites by the compound N,N-dimethyl-2-phenylaziridinium (DPA). The enzyme so modified became a poor catalyst for AcCh but a better catalyst for several neutral acetic acid esters such as indophenylacetate (102-105). Studies using ^{14}C-DPA revealed that 2 molecules of the inhibitor were incorporated per AcChase monomer. The double labelled AcChase (bis-DPA) lost 50% of its label upon exposure to pH 9.5 for 1 hr (101). Further investigations indicated that bis-DPA enzyme was labelled both at the anionic subsite of the catalytic site and at peripheral anionic sites (see below), as indicated by the failure of d-tubocurarine (a peripheral anionic-site-specific ligand, see below) to inhibit indophenylacetate hydrolysis. Mono-DPA labelled enzyme, obtained by the exposure of bis-DPA-AcChase to pH 9.5 was inhibited by d-tubocurarine but anionic competitive inhibitors of native AcChase had no effect on indophenylacetate hydrolysis (106), indicating that in mono-

DPA-AcChase only the anionic subsite of the catalytic site was blocked. Another anionic site alkylating agent, first introduced by Wolfsy and Michaeli (107), p-(trimethylammonium)benzene diazonium fluoroborate (TDF), was found to inhibit erythrocyte AcChase. The effects of TDF on E. electricus AcChase was characterized by an initial fast step, which corresponded to the incorporation of 2 molecules of TDF per tetrameric enzyme, and resulted in the inactivation of AcChase towards all substrates. This was followed by a slow reaction with TDF, and the restoration of AcChase activity towards indophenylacetate (108, 109).

ii) The Esteratic site:

The dominant feature of the esteratic site is the presence of a reactive serine hydroxyl that can be readily phosphorylated. Owing to this feature AcChase is classified as a serine hydrolase. The amino acid sequence about the reactive serine shows significant homology in the case of chymotrypsin, trypsin, elastase and thrombin (91). The three dimensional structure of α-CT has been shown to possess a system of hydrogen bonds formed by a serine hydroxyl, a histidine imidazole and a carboxyl group in a linear array.

A catalytic mechanism based on this system has been proposed (Scheme I) (56). The characteristics of the mechanism have been determined by studying the kinetics of α-chymotrypsin in solution. In these studies acylation has been assumed to be the microscopic reverse of deacylation (110). The reaction, in both directions, shows general base catalysis by a group with

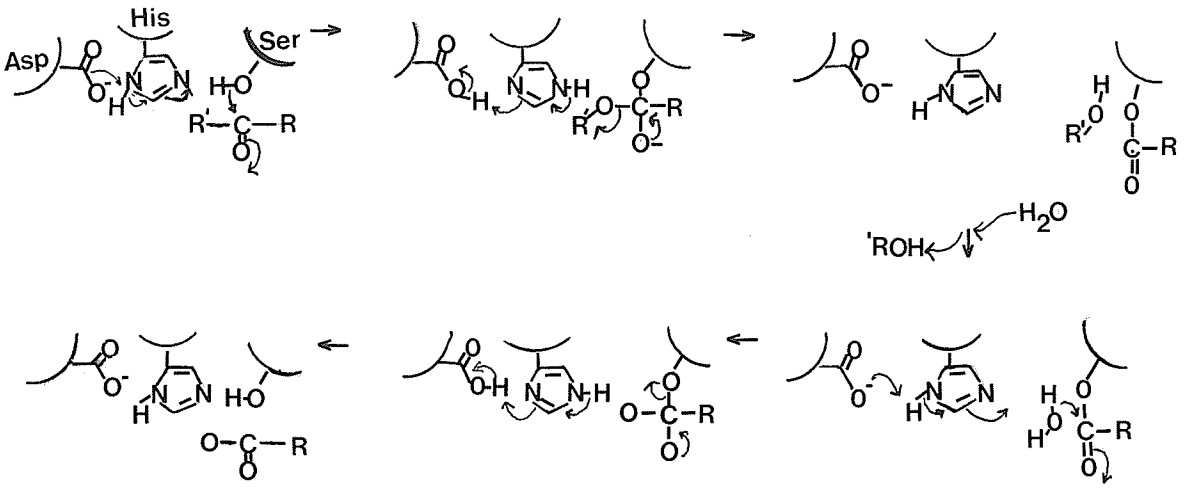

SCHEME I

an approximate pKa of 6.8 and is thought to be due to the imidazole deprotonating serine hydroxyl and thereby permitting the formation of a hypothetical tetrahedral intermediate (Scheme I), which decomposes to give rise to the acetyl-enzyme.

In the absence of a 3-dimensional structure for AcChase, Scheme I is assumed to be operative. Although both AcChase and α-chymotrypsin display bell-shaped activity vs. pH profiles and the lower apparent pKa is between 6 and 7 (7, 72, 111, 112) there are important differences in the kinetic behaviour to suggest that modifications to the proposed mechanism (Scheme I) are required to adequately account for the kinetic behaviour of AcChase. A mechanism which describes the AcChase catalysed hydrolysis of a variety of substrates including esters of acetic acid, esters or acylhalides of phosphoric, carbamic and methyl sulphonic acids is given below (Scheme II).

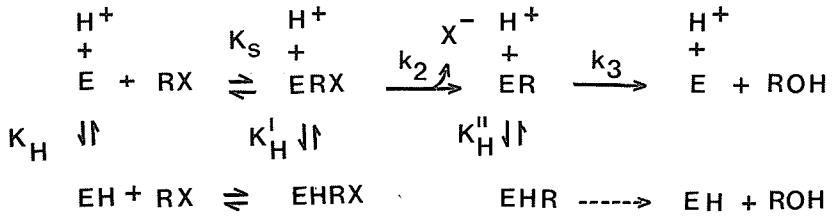

SCHEME II

E, ERX and ER are the free enzyme, the enzyme substrate complex, and the acyl enzyme, respectively. EH, EHRX, and ERH are the corresponding unreactive (imidazole protonated) species.

Unlike the acetyl enzyme, the covalent enzyme intermediate resulting from the reaction with carbamates, organophosphates or methanesulphonates is hydrolysed extremely slowly, if at all. These compounds act as extremely potent inhibitors of AcChase. A steady-state kinetic treatment of the above Scheme (II) permits the definition of the following terms.

$$v = k_{cat}\, E_o\, [S_o]/K_{app} + [S_o] \qquad [1]$$

$$k_{cat} = \text{turnover number} = k_2k_3/(k_2 + k_3) \qquad [2]$$

$$\text{if } k_2 >> k_3 \quad \text{then } k_{cat} \simeq k_3$$

$$K_{app} = (k_{-1} + k_2)k_{cat}/k_1k_2 \qquad [3]$$

$$k_{cat}/K_{app} = k_1k_2/(k_{-1} + k_2) \qquad [4]$$

$$\text{if } k_2 >> k_{-1} \quad \text{then}$$

$$k_{cat}/K_{app} \simeq k_1 \qquad [5]$$

assuming $K_H = K'_H = K''_H$

$$1/v = \frac{1}{k_{cat}[E_o]} \left\{ 1 + \frac{K_{app}}{[RX]} (1 + \frac{[H^+]}{K_H}) \right\} \quad [6]$$

Thus the parameter k_{cat} represents the effect of pH on the deacetylation (k_3) whereas k_{cat}/K_{app} represents the effect of pH on the acylation step (k_2).

The pH dependance of various kinetic parameters of the erythrocyte AcChase catalyzed hydrolysis of cationic and neutral acetic acid esters are summarized in Table VIII. The k_{cat} of these substrates, similar in size and structure, varies as much as 50-fold (Table VIII). The pH dependance of k_{cat} for the substrates for which deacetylation is rate limiting (i.e. $k_2 >> k_3$) indicate an apparent pKa value of 6.3. However, with substrates for which acetylation is rate limiting (i.e. $k_2 << k_3$), the apparent pKa values range from 5.2 to 5.5 and never reach 6.3. The same sort of pattern is observed for the pH dependence of k_{cat}/K_{app}. The apparent pKa for AcCh is 6.3 but for the remaining substrates the apparent pKa values vary from 5.3 to 6.25. These results are in sharp contrast to those obtained with α-chymotrypsin (113), where only a very slight decrease in the observed pKa of 6.8, is observed with substrates that approach maximal k_{cat}/K_{app} values.

Rosenberry (56, 114) has explained this anomalous pH dependence by suggesting that the induced-fit model of catalysis is operative in AcChase. The induced-fit model of catalysis formulated by Koshland and Neet (115), is a general model for

enzyme-substrate interactions in which the initial binding of substrate induces a conformational change to a highly reactive enzyme-substrate complex. To account for the anomalous pH dependance, Rosenberry (56, 114) has extended Scheme II to include additional induced-fit intermediates $(ERX)'$ and $(EHRX)'$ as shown in Scheme II. The parameters k_{cat} and K_{app} are now given by eq. [7] and [8].

$$k_{cat} = \frac{k_2}{K_i' + 1 + \frac{k_2}{k_3}} \qquad [7]$$

$$K_{app} = \frac{K_s K_i'}{K_i' + 1 + \frac{k_2}{k_3}} \qquad [8]$$

where K_i' is the induced-fit equilibrium constant $K_i' = k_{-1}'/k_1'$. As can be seen K_i' enters into both eq. [7] and [8]. K_i' is assumed to be very large for poor substrates (i.e. those that can not induce a conformational change) and small for good substrates that have similar K_{app} and are similar in size and structure (Table VIII).

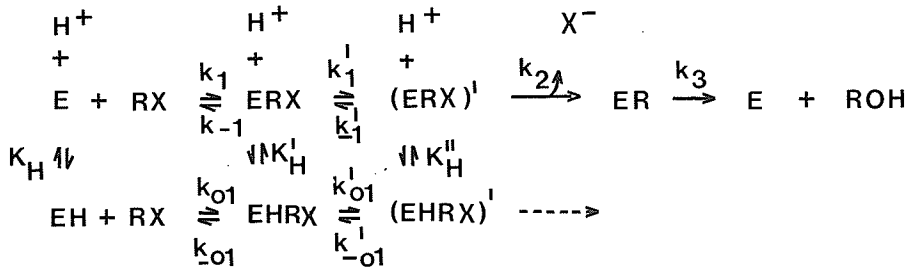

SCHEME III

The equilibrium formulation of induced-fit (Scheme III). still fails to account for the observed pH effects: Under equilibrium conditions the apparent pKa is equal to the actual

TABLE VIII. The pH dependance of hydrolysis of cationic and neutral acetic acid esters with Bovine Erythrocyte AcChase (56).

Substrate	Relative k_{cat} (pH 7.5)	Rate Limiting Step: A ≡ acylation D ≡ deacylation	pKa	
			k_{cat}/K_{app}	k_{cat}
CATIONIC				
Acetylcholine	1.00	D	6.7	6.32
Acetylthiocholine	0.83	D	-	6.18
Diethylbutylaminoethyl acetate	0.16	A	6.25	5.50
Dipropylmethylaminoethyl acetate	0.05	A	6.2	5.2
Dimethylaminoethyl acetate	0.36	A	5.85	5.5
Methylaminoethyl acetate	0.10	A	5.90	5.20
4-Trimethylaminobutyl acetate	0.02	A	5.88	5.46
NEUTRAL				
Phenyl acetate	1.13	D	5.55	6.35
Isoamyl acetate	0.10	A	5.5	5.5
Methyl acetate	-	A	5.3	-

pKa of the general base involved in acylation step (k_2). For the apparent pKa to deviate below the actual pKa, k_2 must no longer be rate limiting for acylation. This can only happen if k_2 is larger than k_{-1}. Under these circumstances ERX is no longer in equilibrium with ERX' and k_1' becomes rate limiting (56, 114). Rosenberry (56, 114) was able to show that under these circumstances anomalous pH dependence, as observed with AcChase, could result. The parameters resulting from the non-equilibrium formulation of Scheme III (equations [9], [10], [11])

$$k_c = \frac{k_a\, k_3}{k_a + k_3} \qquad [9]$$

$$K_{app} = \frac{K_s\, k_{cat}\, (k_{-1} + k_2)}{k_a\, (k_1' + k_{-1}' + k_2)} \qquad [10]$$

$$k_a = \frac{k_{-1}'\, k_2}{k_{-1}' + k_1' + k_2} \qquad [11]$$

were combined with the general steady-state rate expression, and the following assumptions were made: (1) EHRX is completely equilibrated with (ERX)'; (2) $k_{01}' = k_1'$; (3) $K_H = K_H' = K_H''$. Under these circumstances the apparent pKa was given by equation [12].

$$K_a(\text{apparent}) = K_H\, (1 + \frac{k_2}{k_{-1}}) \qquad [12]$$

The true K_H is decreased to the apparent K_a by the extent k_2 exceeds k_{-1}.

Further evidence for the induced-fit model of catalysis being operative in AcChase came from the effects of D_2O on the

hydrolysis of acetic acid esters (114). Serine hydrolases usually show deuterium isotope effects of 2 to 3 for k_{cat}/K_{app} when the acid/base catalyzed step (k_2) is thought to be rate limiting. Since the induced-fit step (k_1' in Scheme III) involves an enzyme conformational change, it should have low deuterium effects. Therefore substrates for which this step is rate limiting (i.e. $k_2 > k_{-1}'$) should have the lowest deuterium effects and the lowest apparent pKa values for k_{cat}/K_{app}. On the other hand substrates capable of inducing this conformational change should not be rate limited by k_1' (i.e. $k_2 \simeq k_{-1}'$) and should show a greater deuterium isotope effect and near "normal" apparent pKa for k_{cat}/K_{app}. This was in fact the case; D_2O effects of 1.3 and 1.4 were observed for phenyl acetate and isoamylacetate respectively, these substrates had apparent pKa values of 5.5 and 5.6. Methylacetate and p-nitrophenylacetate gave corresponding deuterium effects of 1.9 and 2, respectively, these substrates had apparent pKa's for k_{cat}/K_{app} 6 to 6.25 (114).

iii) Catalytic site inhibitors of Acetylcholinesterase:

In view of the anionic nature of the AcCh binding site, it is to be expected that a wide variety of cationic substances might function as inhibitors of AcChase. Simple, pure competitive inhibition is seldom observed, however, an often-considerable uncompetitive component of inhibition is generally found. This phenomenon may in some cases be reasonably explained in terms of the formation of a ternary complex of the inhibitor and the acetyl enzyme.

Ternary complex formation has been implicated in the inhibition of AcChase by choline, carbachol (116, 117), the substrates AcCh and AcSCh (117), fluoride ion (118, 119, 120) and in synergistic inhibition displayed by naphthalene derivatives and some aromatic cations (121).

Fluoride ions are thought to inhibit AcChase by binding at or near the esteratic site (118, 119, 120). The pH dependence of F^- binding to free enzymes and to the enzyme substrate complex has been found to be identical. However a different pH dependence is observed for the acyl-enzyme. These observations have led to the suggestion that the site of F^- attachment is altered via conformational changes accompanying acetylation (56, 118-120).

Synergistic inhibition of AcChase by certain naphthalene derivatives and aromatic cations has been demonstrated (121). Napthylacetate and 2-PAM when present in combination have been shown to result in much lower inhibition constants than those observed for the inhibitors individually. Ternary complex formation and synergistic inhibition are thought to be the result of conformational changes induced by aromatic cation binding at the anionic subsite of the catalytic site. In the resultant conformation a second inhibitor molecule is thought to bind at or near the esteratic site giving rise to a dead-end complex (56, 121).

Naturally occurring carbamate inhibitors such as eserine (physostigmine) and its analogues were originally considered to be competitive inhibitors of cholinesterases. Goldstein

(122), studying the inhibition of plasma cholinesterases by eserine and related compounds was the first to suggest that these substances react covalently with the enzyme. Subsequently, various esters of dimethyl carbamic acid were shown to react with AcChase to form a common intermediate whose breakdown was the rate determining step in the hydrolysis (123, 124). This intermediate was assumed to be the dimethyl carbamoyl-enzyme, analogous to the acetyl-enzyme formed during the AcChase catalyzed hydrolysis of acetic acid esters. The evidence for the same enzyme active site being involved in the hydrolysis of carbamate and acetate esters was given by Rosenberry and Bernhard (79). In this study the carbamoylation reaction was studied using the fluorogenic carbamoylating agent 1-methyl-7-dimethylcarbamoyloxyquinolinium (M7C) (79). Since $k_2 >> k_3$, the reaction is characterized by an initial burst (which is proportional to the free enzyme concentration) followed by a steady-state hydrolysis of the carbamoyl-enzyme. The kinetics of the reactions were shown to be in accordance with Scheme II, albeit with greatly reduced rates. The presteady-state treatment of the data permitted the evaluation of the kinetic parameters $K_s(k_{-1}/k_1)$, k_2 and k_3 (see appendix) (79).

The reaction of AcChase with esters of phosphoric acid have been shown to proceed through a reversible enzyme inhibitor complex (124). A phosphoryl enzyme analogous to acetyl enzyme is formed. But unlike the acetyl enzyme, the phosphoryl enzyme reacts with water very slowly. Better nucleophiles than H_2O, such as NH_2OH dephosphorylated the enzyme at faster

rates. Phosphorylation is blocked by reversible inhibitors such as tetramethylammonium or (3-hydroxyphenyl)-trimethyl ammonium ions (7, 125). Phosphorylation was also inhibited by F^- (118, 120).

The potential use of organophosphates as weapons of war has naturally sparked much interest, resulting in the development of very potent quaternary ammonium containing "active-site-directed" inhibitors (125). This in turn has led to the search for reactivators of the phosphoryl enzyme. Reactivation of the phosphoryl enzyme by choline has been reported (125). This was taken as an indication that the catalytic machinery of the enzyme was operative in the reactivation process. Choline is assumed to bind at the anionic site of the phosphorylated enzyme resulting in a precise geometry for the oxygen to attack the phosphorus atom. Potent reactivators such as pyridine-2-aldoxime methiodide (2-PAM) and related analogues were obtained by combining a good nucleophilic group with a suitably placed quaternary structure (126). 2-PAM has been shown to accelerate the AcChase catalyzed hydrolysis of acetic acid esters (127). The observed acceleration for MeOAc, EtOAc, n-PrOAc, n-BuOAc and AcCh was 3.09, 4.68, 2.16, 0.28 and 0 fold respectively. These observations demonstrate that the anionic site must not be blocked in order for acceleration to occur. Furthermore, 2-PAM induced conformational changes were again implicated in the reactivation of phosphoryl-AcChase and in the acceleration of acetic acid hydrolysis.

The catalytic properties displayed by AcChase such as

competitive inhibition; acceleration of the enzymic reaction by compounds that are not substrates; synergistic inhibition; ternary complex formation; widely different k_{cat} and K_{app} values displayed by substrates of similar size and structure; can all be explained by the equilibrium formulation of induced-fit (56, 114), as well as other models such as non-productive substrate binding or differential ligand binding to reversibly linked enzyme conformations (56, 128). However, some of these effects might also arise as a result of ligand-binding to peripheral anionic sites on the enzyme. This aspect is discussed further, below.

6) Peripheral Anionic Sites:

i) Kinetic evidence:

The earliest evidence for AcChase possessing more than one class of anionic sites came from inhibition studies using a series of bis- and mono-quaternary ammonium ligands (153). It was shown that inhibition by bis-quaternary ligands was maximized at 10 carbon atoms separating the two charged head groups. The bis-quaternary compounds give competitive inhibition constants (K_{comp}) that were 30-fold lower than the corresponding mono-quaternary ligands (153). Changeux (128) was the first to suggest that these "peripheral" anionic sites might be functional allosteric sites, the binding of ligands to which may result in conformational changes in the enzyme. It was found that pachycurares (compounds that prevent nerve depolarization) and leptocurares (compounds that cause depola-

rization of nerves) both inhibited AcChase, but the ethyl substituted pachycurares displayed non-competitive inhibition and were able to act as antagonists to leptocurare inhibition. It was further observed that inorganic cations (Na^{+}, Ca^{+2}, and Mg^{+2}) increased V_{max} and the K_{app} of the enzyme, whereas pachycurare drugs lowered V_{max} and K_{app}. These observations led Changeux to postulate that AcChase possessed at least two conformational states ($P \rightleftharpoons D$). The P state was thought to be stabilized by pachycurares, AcCh and by low ionic strength. The D state was stabilized by leptocurare drugs, mono- and divalent cations and by high ionic strength. Subsequently Kitz *et al*. (129) found that neuromuscular blocking agents (pachycurares) such as curare, dimethyl curare and gallamine accelerated the decarbamoylation of the carbamyl enzyme but had no effect on AcCh hydrolysis. Therefore it was assumed that these compounds exerted their effects by binding at a site other than the catalytic site. Taylor and Lappi (130) observed that the carbamoylation of the *Torpedo californica* enzyme with M7C resulted in curved reciprocal plots of the observed rates of carbamoylation (k_{obs}) vs M7C (at high) concentrations. The activation at high M7C concentrations could not be attributed to the appearance of a second class of catalytic sites, as the burst amplitude did not change. A suggestion was made that M7C binds at the peripheral sites and thereby activates carbamoylation. However, this second phase (activation) was not observed with *E. electricus* AcChase (64, 131). Belleau *et al*. (101) demonstrated leptocurare acceleration of the methane

sulphonation of AcChase. Since the acceleration was maximized at decamethonium (DMB) the distance between the active site and the peripheral sites was estimated to be 1.0-1.4 nm. Pachycurare drugs, on the other hand were found to protect AcChase from methane sulfonation, thus lending further support to the two state model of Changeux (128).

Antagonism between divalent inorganic cations and curare drugs or PCMB (132) led to the suggestion that inorganic cations also bind at the peripheral anionic sites. In a related study, Roufogalis and Quist (133) were able to show competitive antagonism between Ca^{+2} and DMB, as well as between d-tubocurarine and tetraethylammonium (TEA). The antagonism between DMB and gallamine was complex and non-competitive; Ca^{+2} and gallamine did not compete. These results were interpreted as follows: The peripheral site consists of a monovalent anionic site β, to which Ca^{+2} and DMB bind and a trivalent site γ to which gallamine binds. d-Tubocurarine is thought to occupy both β and γ sites. Since gallamine does not bind to the β anionic site, the antagonism between it and DMB was thought to be due to antagonism between β and γ allosteric sites (133). The inorganic cation dependent acceleration of hydrolysis rates were studied by Crone and his co-workers (134, 135). The acceleration has been shown to be dependent both on the ionic strength and on the nature of the cation.

Roufogalis et al. (136, 137) have reported modification of AcChase with water soluble carboxyl group specific reagents. The enzyme so modified, no longer displayed Ca^{+2} gallamine,

TEA, and hexamethonium dependent increase in maximum velocity; the inhibition constant (K_{comp}) for DMB was increased by 10-fold; non-linear double reciprocal plots were obtained in the presence of DMB. The observations were attributed to two conformational states of the enzyme being present; their interconversion was not possible due to non-functional peripheral sites.

Brodbeck and his co-workers (138) have observed curved Lineweaver-Burk plots, and biphasic inhibition with diisopropylfluorophosphate (iPr_2PF) (139), with unmodified, intact and fragmented E. electricus AcChase at low ionic strength. These observations led to the suggestion that there are two forms of the enzyme present in equilibrium at low ionic strength or that there are inter-subunit interactions in AcChase. Barnett and Rosenberry (77) failed to reproduce Brodbeck's (138, 139) results and concluded that there are no kinetic differences among the catalytic subunits of AcChase.

In summary, in addition to the anionic subsite of the active site, AcChase is thought to possess multiple peripheral anionic sites approximately 1.4 nm from the active site. Binding of specific ligands to these peripheral sites is thought to effect conformational changes which are reflected in the kinetic behaviour of the enzyme. The most recent schematic representation of the distribution of sites, based on the kinetic evidence presented above, was given by Rosenberry (56) (Fig. 3). In this model, the peripheral site is thought to be comprised of four anionic subsites. Site P_a (which is

Fig. 3. Diagrammatic model of the AcChase catalytic and peripheral sites. The enzyme-ligand complex with: (a) DMB; (b) Mg^{2+} or Ca^{2+}; (d) gallamine; and (c) d-tubocurarine.

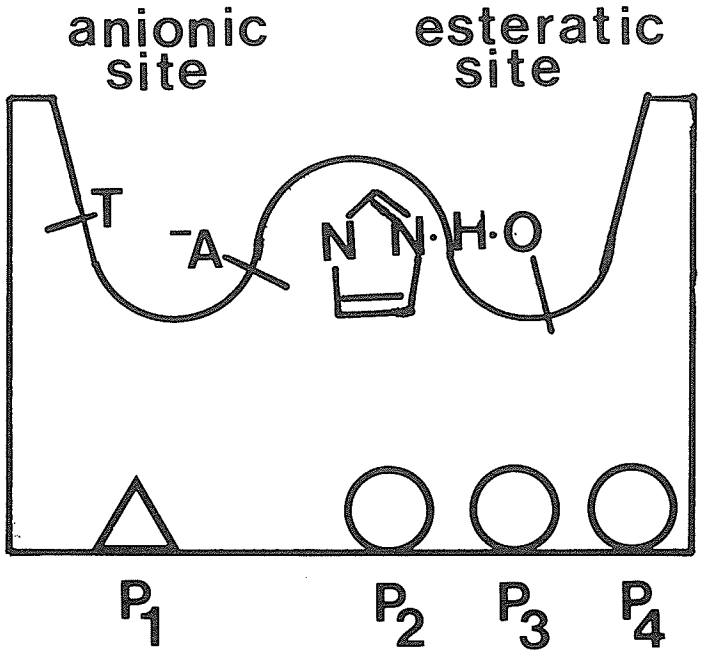
anionic site
esteratic site
T
-A
N
N·H·O
P1
P2
P3
P4

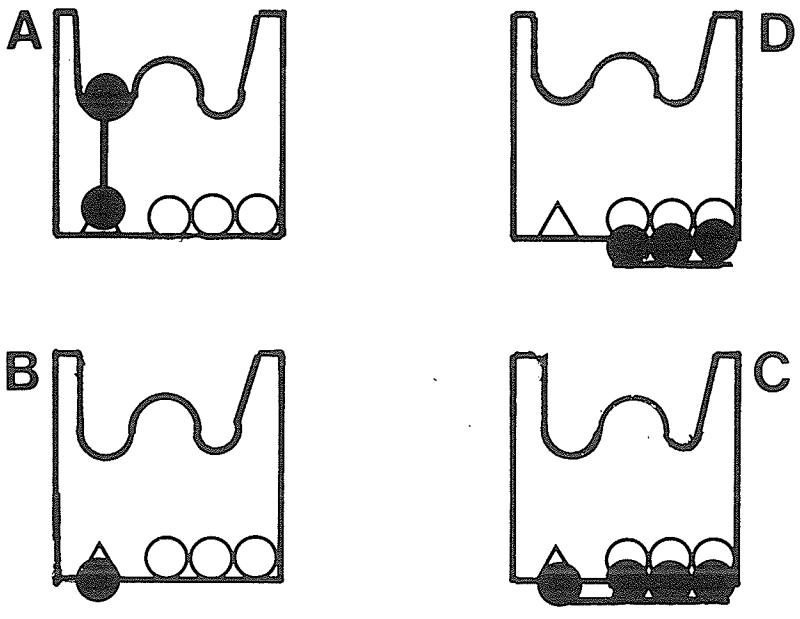
A
D
B
C

analogous to the subsite β in the model of Roufogalis and Quist (133)), is thought to be specific for DMB, Ca^{+2} and TEA. Sites P_2, P_3 and P_4 (which are analogous to subsite γ in Roufogalis and Quist's model (133)) are thought to be specific for trivalent cationic ligands such as gallamine. d-Tubocurarine is thought to occupy all of the peripheral anionic sites P_1 through P_4. The model of DMB, Ca^{2+}, gallamine and d-tubocurarine binding to the peripheral sites is illustrated in figure (3 a, b, c, d) respectively.

ii) Spectroscopic evidence:

Spectroscopic changes associated with ligand binding have been used as a direct, quantitative means of measuring reversible ligand associations with AcChase.

Taylor et al. (140) and Mooser et al. (131, 141, 142) have examined the effects of bis-(3-aminopyridinium)-1, 10-decane and 2,5-bis-(3-diethyl-o-chlorobenzylammonium-n-propylamino)benzoquinone on the intrinsic enzymic tryptophan fluorescence. The fluorescence was quenched by 50% at saturating ligand levels. Critical energy transfer distances of 2.42 nm and 1.89 nm were calculated for 2,5-bis(3-diethyl-o-chlorobenzylammonium-n-propylamino)benzoquinone and the bis-(3-aminopyridinium)-1, 10-decane respectively. The resultant Scatchard plots were linear and 4 ligand molecules were shown to bind per tetrameric (11s) AcChase molecular species. The linearity of the Scatchard plots suggested that the four ligand binding sites on AcChase were separated by at least twice the critical energy transfer distance. K_D's obtained either from

fluorescence titrations or from I_{50} (determined from the inhibition of AcCh hydrolysis) were in good agreement (140).

Propidium (3, 8-diamino-5,3'-diethylmethylamino-n-propyl-6-phenylphenanthridium) a peripheral site directed fluorescent probe, was first introduced by Taylor et al. (130, 143). Propidium fluorescence was shown to be enhanced by ten-fold upon binding to AcChase purified from T. californica (143). A binding constant of 3×10^{-7} M was obtained. The Scatchard plots were linear. Propidium was only displaced by peripheral site ligands, gallamine, d-tubocurarine and DMB. Binding constant for these ligands were determined by propidium displacement experiments. Active site directed ligands such as edrophonium and N-methylacridinium under saturating conditions had no effects on Scatchard plots of propidium binding. Also chemical modification of the active site with bulky sulphonates or phosphates (that inhibit bis-quaternary ligand binding) had no effect on propidium binding. Even though gallamine and propidium displaced one another from the peripheral sites Mg^{+2}, displaced gallamine rather than propidium when the displacement experiments were performed in the presence of constant gallamine and propidium concentrations (concentration of Mg^{+2} varied), suggesting that the gallamine and propidium sites do not exactly overlap (130, 143).

The kinetics of association of various fluorescent bis- and mono-quaternary ligands were determined from stopped flow measurements of fluorescence (144). Bis-quaternary ligands revealed a fast bimolecular step ($k_{obs} = 9.7 \times 10^{7}\ M^{-1}\ sec^{-1}$)

followed by a unimolecular slow step (k_{obs} = 44 sec^{-1}). Only the fast step was observed at low ligand concentrations. Propidium, on the other hand, displayed a fast bimolecular step (k_{obs} = 1.2 x 10^9 M^{-1} sec^{-1}) only. These data were interpreted on the basis of two preexisting conformations of the enzyme. Propidium would bind to either form, therefore it displayed only the fast step. Bis-quaternary ligands could only bind to one conformation, this was represented by the fast step, the slow step was thought to represent the rate of interconversion between enzyme conformations.

Following the demonstration by Pattison and Bernhard (145) that Zn^{+2} and d-tubocurarine were able to effect a slow transition of AcChase to an "unreactive" form, Epstein et al. (146) were able to detect Zn^{+2} and d-tubocurarine-induced slow conformational changes on AcChase that was covalently labelled at the active site by the fluorescent probe (dansylamido)pentyl methylphosphonofluoridate. The onset of Zn^{+2} and d-tubocurarine induced conformational changes was biphasic. The k_{obs} for the slow phase obtained from the perturbation of fluorescence (146) was in close agreement with those obtained kinetically by Pattison and Bernhard (145). No attempt was made to explain the biphasic behaviour. These results were explained in terms of a two state model, where the active and inactive forms of the enzyme are in slow equilibrium.

Berman et al. (147) have calculated the intersite distance between the anionic and peripheral sites, using steady-state

and time resolved fluorescence energy transfer measurements. The intersite distance obtained by these methods was 1.9-2.8 nm. These results are in contrast to the 1.4 nm intersite distance determined by bis-quaternary ligands and the mutually exclusive binding displayed by propidium and DMB. Two alternative explanations were offered to account for these discrepancies: DMB binds at the active site and at another site that indirectly closes down the peripheral sites; or DMB binding at the active site induces a conformational change that reduces the intersite distance to 1.4 nm (147).

As can be seen from the foregoing discussion, AcChase possesses a variety of peripheral anionic sites. Binding of ligands to these sites can affect the kinetic properties of the enzyme in a variety of ways, ranging from activation to total inactivation. The physiological significance, if any, of these phenomena remains to be established.

7) Inactivation of Acetylcholinesterase by Thiol Reagents:

Ever since the discovery of AcChase, various reports have demonstrated that the enzyme is inhibited by a variety of so-called "thiol specific reagents". Some of these earlier reports were summarized by Mounter and Whittaker (148) (Table IX). The involvement of essential enzymic thiol groups in the observed inactivations was discounted by Mounter and Whittaker (148) because the concentrations of the inactivating thiol reagents were too high and the rates of inactivation were too slow, when compared to typical thiol containing enzymes.

TABLE IX. The effect of thiol reagents on cholinesterase, summary of the earlier work (148).

Reagent	Enzyme Source	pI	Inhibition %	Reference
Arsenite	Horse serum	1.7	87	154
	Pigeon brain	4	52	155
Lewisite	Horse serum	2.4	30	156
	Serum?	4	85	157
	Pigeon brain	3	19	155
Phenyldichloro-arsine	Pigeon brain	3	57	155
3-amino-4-hydroxy-phenylarsenoxide	Electric organ?	4.2	57	158
Copper II	Torpedo	3.3	38	159
	Horse serum	2.7	87	156
Maleic acid	Torpedo	1.5	22	159
Iodoacetate	Torpedo	1.7	88	159
Iodoacetamide	Cat serum	-	Nil	160
Glutathione (oxidized)	Torpedo	2	24	159
Iodine	Torpedo	5.75	85	159
Alloxan	Torpedo	3.4	38	159
o-Iodosobenzene	Human plasma	-	Nil	161
Bromobenzyl cyanide	Horse serum	1.6	70	156
Chloropicrin	Horse serum	1.6	Nil	156
Bromoacetophenone	Horse serum	3	84	156

In addition, while most of the thiol reagents that were shown to inactivate AcChase were heavy metal cations, there was no evidence for the interaction of these metal ions with the AcChase catalytic site.

More recently Massoulié and Rieger (149) have reported that purified T. californica AcChase is inhibited by PCMB. The inactivation was very slow, the half-life of the reaction being approximately 90 minutes. Wins et al. (132) have demonstrated that the PCMB inactivation of AcChase can be reversed by Ca^{+2}, a peripheral-site-specific ligand, suggesting that PCMB combines with AcChase at or near the peripheral anionic sites. The effects of arsenite, another "thiol specific reagent" on T. californica AcChase were studied by Wilson and Silman (150). Arsenite was found to inhibit AcChase in a second order reaction with a rate constant of 10^{-2} M^{-1} sec^{-1}. Peripheral-site-specific ligands such as propidium and TEA were shown to block arsenite inhibition. 2-PAM on the other hand, accelerated the rate of arsenite inactivation by 220-fold. The arsenite inhibition was reversed by PCMB but not with DTNB or NEM, leading the authors to conclude that although the kinetic evidence is consistent with thioarsenate formation, the chemical evidence excludes the involvement of thiol groups.

In the opinion of this author the above evidence is not concrete enough to argue for or against the presence of thiol groups in AcChase. The rates of inactivation and the high concentration of thiol reagents required, can be explained by the inaccessibility of the thiol groups. The variance in the

reactivity of protein thiol groups, arising from the degree to which they are "buried" within the protein structure, has been well documented (151, 152).

In view of the peripheral-site-mediated inactivation of AcChase by Zn^{+2} and Cu^{+2}, two metal ions which can form extremely stable complexes with free thiols (151, 152), and the fact that data on the free thiol content of AcChase have yet to be published, it is very tempting to suggest that AcChase does possess free thiol groups and that these are involved in the binding of metal cations at the peripheral anionic sites.

Summary of objectives:

The aim of the present work is to clarify the role of the peripheral anionic sites in the catalytic function of AcChase. To this end, the specificity of ligands for the peripheral anionic sites was established through fluorescence equilibrium binding and displacement studies. These ligands were then used to determine the consequences of peripheral site occupation on catalysis. In these studies the pseudo-substrate M7C proved to be extremely useful, as the pre-steady-state kinetic treatment of its AcChase catalyzed hydrolysis enabled the evaluation of the kinetic parameters K_s, k_3 and k_2. As a result the effect of peripheral site occupation on the proposed catalytic mechanism was determined. Studies of the metal ion induced activation and inactivation, led to the proposal of a model for peripheral site-specific ligand induced kinetic states of AcChase. Several observations during the course of this study were

interpreted as an indirect indication of the presence of thiol groups at or near the peripheral anionic sites; this has led to a search for thiol groups in AcChase.

Whenever possible, the properties of AcChase from two different species, T. californica and E. electricus, were compared.

MATERIALS AND METHODS

i) Structures of some of the compounds used in this study:

Acetylthiocholine 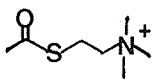

p-Nitrophenyl-acetate 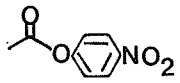

7-hydroxy-N-methylquinolinium 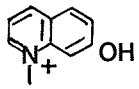

7-(dimethylcarbamoyloxy)-N-methyl quinolinium 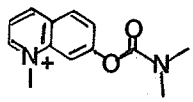

Gallamine 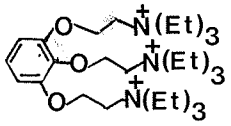

Decamethonium 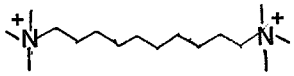

d-tubocurarine 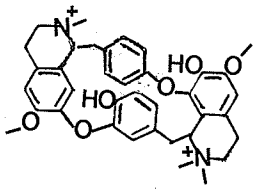

Edrophonium 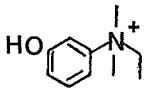

Propidium 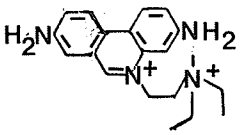

Pyridine-2-aldoxime methiodide

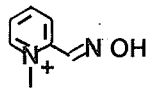

5,5'-Dithiobis-(2-nitrobenzoic acid)

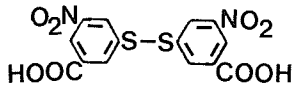

Diisopropylfluorophosphate

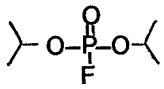

N-dansylaziridine

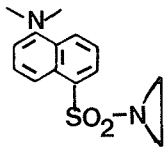

Dansyl-S-aminoethyl cysteine

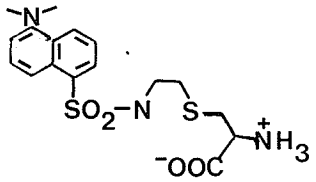

Affinity Ligands:

[(6'-aminocaproyl- 6 -aminocaproyl)-p-aminophenyl]trimethyl ammonium

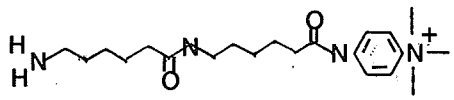

[6-aminocaproyl-p-aminophenyl]trimethyl ammonium

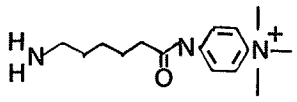

ii) Materials:

Materials	Supplier
T. californica electroplax	Pacific Bio-Marine Venice, California, USA

Materials	Supplier
crude lls *E. electricus* AcChase (Type VI-S) Acetylthiocholine 5,5'-Dithiobis-(2-nitrobenzoic acid) Tris hydroxymethyl aminomethane Decamethonium bromide Propidium iodide d-Tubocurarine iodide p-Nitrophenyl acetate Trypsin Soybean trypsin inhibitor N,N-p-phenylenediamine Cbz-ε-aminocaproic acid Triethylamine Isobutyl chloroformate Pyridine-2-aldoxime methiodide L-cysteine	Sigma Chemical Co. St. Louis, MO, USA
Cyanogen bromide Methyl iodide Diisopropylfluorophosphate Lanthanium chloride (gold label)	Aldrich Chemical Co. Milwaukee, Wisconsin, USA
$HgCl_2$ $CuSO_4$ $CdSO_4$ $MnSO_4$	J.T. Baker Chemical Co. Phillipsburg, New Jersey, USA
7-Quinol 7-(dimethylcarbamyloxy)-N-methylquinolinium iodide	Eastman Chemicals Rochester, New York, USA
$MgSO_4$ $ZnSO_4$	British Drug Houses London, England
Sepharose 4-B CM-Sephadex C-50	Pharmacia Fine Chemicals Upsala, Sweden
N-dansylaziridine	Pierce Chemical Co. Rockford, Il, USA
Amicon ultrafiltration Apparatus and membranes PMIO, microporous filter 0.45 μM	Amicon Canada Ltd. Oakville, Ontario, Canada

Materials	Supplier
TLC sheets 20 x 20 cm Silica gel	Fisher Scientific Co. Winnipeg, Manitoba, Canada
Beer (draft)	Aberdeen Hotel Winnipeg, Manitoba, Canada

iii) Syntheses:

a) Synthesis of the affinity ligand [(6-aminocaproyl-6'-aminocaproyl-p-aminophenyl)trimethyl ammonium]:

This procedure is essentially as described by Taylor et al. (64). Ten grams of p-N,N-dimethyl phenylenediamine hydrochloride was dissolved in 50 mL H_2O. The pH was adjusted to 9.0 by the addition of NaOH (3M). The free base so formed was extracted with ether (3 x 60 mL). The combined ether extracts were dried over anhydrous Na_2SO_4, filtered and evaporated to dryness on a rotary evaporator (Büchi). The resultant brown oil solidified upon cooling in the freezer (8.0 g of the free base were obtained).

Cbz-cap-PDA(6-carbobenzoxyaminocapropyl-p-N,N-dimethyl phenylene diamine):

9.6 g of carbobenzoxy-6-aminocaproic acid was dissolved in 120 mL ethyl acetate. This mixture was cooled to ∿10°C on an ice/salt bath, 5.1 mL of triethylamine was added followed by 5.1 mL of isobutyl chloroformate. A white precipitate was formed; this mixture was stirred for 20 minutes, then 5 g of the free base (dissolved in 50 mL of cold ethyl acetate was added slowly (∿1 mL/min). A grey precipitate replaced the white. This mixture was stirred for ∿3 hrs then

stood in the refrigerator overnight. The solid was filtered off and washed successively with 10 mL each of H_2O, ethyl acetate and finally petroleum ether (30-60°). 11.0 g of white solid resulted, and was re-crystallized from MeOH (hot) with activated charcoal, resulting in 9.0 g of Cbz-cap-PDA, m.p. 115-115.5°C (lit: 115-116°C (64)).

cap-PDA((6-aminocaproyl)-p-N,N-dimethylphenylene diamine):

To 75.0 mL of 33% HBr/acetic acid, 6.6 g of carbobenzoxy-6-aminocaproyl-p-N,N-phenylene diamine was added (dissolved in 30 mL of glacial acetic acid), stirred for 1 hr at room temperature, then approximately 200 mL of anhydrous ether was added. The resultant gummy solid was removed with a glass rod and dissolved in a minimum amount of isopropanol and added dropwise to ∿100 mL of ether. Upon contact with ether a flaky white solid was formed. The solid was filtered, washed with a further 3 x 30 mL of ether, then dissolved in, and crystallized from, hot methanol by the dropwise addition of anhydrous ether. 5.3 g of off-white (very hygroscopic) solid with a m.p. of 178-180°C was obtained (lit: 181-182°C (64)).

Z-dicap-PDA(6-carbobenzoxyaminocaproyl-6'-aminocaproyl)-p-N,N-dimethylphenylenediamine:

3.3 g of Cbz-6-aminocaproic acid was dissolved in 40 mL of ethyl acetate, cooled to -10°C in an ice/salt bath, then 1.8 mL triethylamine followed by 1.8 mL of isobutylchloroformate was added. The suspension was stirred for 20 minutes, then a mixture of cap-PDA (5.0 g) dissolved in 30-40 mL of

ethyl acetate containing 3.6 mL of triethylamine (cooled to <0°C) was added dropwise. This mixture was stirred at room temperature for 1 hr then stored in the refrigerator overnight. The resultant solid was filtered, washed sequentially with 100 mL each of H_2O, ethyl acetate and petroleum ether (30-60°). The product was recrystallized from hot methanol (with activated charcoal). 3.69 g of purplish crystals with a m.p. of 132-133°C (lit: 127-130°C (64)) were obtained.

Z-dicap-PDA([6-carbobenzoxyaminocaproyl-6'-aminocaproyl)-p-aminophenyl]trimethyl ammonium):

3.0 g of Z-dicap-PDA was dissolved in 4.0 mL of dimethyl formamide containing 4.0 mL CH_3I in a large screw-cap test tube (30 mL). This was placed in a beaker of boiling water in the fume hood (with hood closed) for 40 min, then cooled to 0°C. Ethyl acetate was added (∿0.5 mL), resulting in a cloudy solution, followed by a gummy oil, which settled to the bottom of the test tube. The oil was dissolved in hot absolute ethanol, crystals resulted upon cooling, m.p. 87-88°C (lit: 89-90°C (64)).

Dicap-PTA: ([6-aminocaproyl-6'-aminocaproyl)-p-aminophenyl trimethyl]ammonium:

500 mg of Z-dicap-PTA was added to 15 mL of 33% HBr/acetic acid, left at room temperature for ½ hr, then 100 mL of ether was added. The gummy solid was removed and treated as described above (cap-PDA). The solid was recrystallized resulting in 125 mg of extremely hygroscopic solid m.p. 176-178°(lit: 179-180°C (64)).

b) Coupling of the affinity ligand to Sepharose 4-B:

200 mL of packed Sepharose 4-B was washed with cold H_2O (1.0 L), then "activated" by the addition of 1.8 g of CNBr; the pH was maintained at 11.0±0.5 by the addition of NaOH (3N) and the temperature was maintained at 15°C±2 by the addition of ice. After 20 minutes the activated gel was washed with 2.0 L of cold $NaHCO_3$ (0.05 M; pH 9.8). The wet gel was transferred to a 600 mL beaker which contained 0.4 m moles of dicap-PTA dissolved in 200 mL of $NaHCO_3$ (pH 9.8). The mixture was stirred at low speed overnight at 5°C, washed with 1.0 L of $NaHCO_3$; 0.11 m moles of ligand were recovered in the wash (i.e. 0.29 m moles were bound). The gel was washed with 2.0 L of cold H_2O followed by 2.0 L of Torpedo preparation buffer (0.01 M $NaHCO_3$; 0.1 M NaCl; 0.04 M $MgSO_4 \cdot 7H_2O$; pH 7.4).

An identical procedure was followed for coupling cap-PTA and L-cysteine to Sepharose 4-B.

c) Synthesis of 1-methyl-7-hydroxy quinoline:

1.0 g of 7-quinol was dissolved in 90 mL of tetrahydrofuran, a small amount of insoluble material was filtered off and 1.0 mL of CH_3I was added. The reaction mixture was left at room temperature, in the dark for 5 days. The yellow solid that formed was filtered, dissolved in hot methanol (∿5.0 mL), cooled and applied to a (2 x 30 cm) column of silica gel (200-500 mesh) equilibrated with methanol. The yellow band was eluted, concentrated (to ∿5.0 mL), ether was then added (dropwise) until the solution became cloudy. On standing in the freezer crystals were obtained with a m.p. of 250-252°C. TLC

in methanol (using silica gel sheets) resulted in one single fluorescent spot.

d) Synthesis of S-(2-dansylaminoethyl)-cysteine (162):

N-dansylaziridine (279 mg) was dissolved in 20 mL ethanol. This solution was added dropwise with stirring to a solution of 135 mg cysteine in 30 mL water, adjusted to a pH of 8.6 with $NaHCO_3$. The solution was stirred overnight at 25°C. The solvent was removed by lyophilization, the resulting crude S-2-dansylaminoethyl cysteine was dissolved in a minimum volume of ethanol-water (1:1, v/v). To this hot butanol was added until the solution became slightly turbid. Hot ethanol was added to make the solution clear. The resulting crystals had m.p. 172-178 (lit: 178-180°C (162)). TLC in solvent systems 63, and 64 of Neiderweiser (164) resulted in a single fluorescent ninhydrin positive spot with an R_f = 0.91.

iv) Isolation and purification of AcChase:

a) Isolation of T. californica AcChase and subsequent purification by affinity chromatography:

The method used was that of Taylor et al. (64) with minor modifications. 50 g of frozen T. californica electric tissue was thawed, chopped into 1 cm^3 cubes; 40 mL of cold Torpedo preparation buffer (0.01 M $NaHCO_3$; 0.1 M NaCl; 0.04 M $MgSO_4$; pH 7.4) was added and the mixture was homogenized in a Virtis homogenizer for 30 seconds (at the low/medium setting). The homogenate was centrifuged at 30,000xg for 1 hr. The supernatant was discarded, 40 mL of Torpedo preparation buffer was added to the pellet and homogenized (at low speed) for 1

min. The homogenate (∿75 mL) was heated to 37°C in a water bath, 75 µL of trypsin (5 mg/mL) was added. The mixture was maintained at 37°C with stirring for 8 min, 75 µL of soybean trypsin inhibitor (10 mg/mL) was added. The mixture was cooled to 5°C and centrifuged at 30,000xg for 1 hr. The supernatant, containing ∿10,000 units of AcChase activity was applied to the affinity column (10 cm column containing 5.0 mL of Sepharose-4B-dicap-p-PTA), after application the column was washed with Torpedo preparation buffer until the absorbance of the eluate was <0.05. Upon elution with Torpedo preparation buffer containing 10 mM DMB, a sharp protein peak with ∿60% of the total applied AcChase activity was obtained. This fraction was applied to a 3 x 50 cm column of CM-Sephadex C-50 (equilibrated with Torpedo preparation buffer). The CM-Sephadex eluate was dialysed and concentrated on an AMICON ultrafiltration apparatus (using a PMIO membrane); the dialysis buffer was 1 mM Tris-Cl pH 8.0. After 2-3 L of buffer had passed through the ultrafiltration cell, the protein solution was concentrated to ∿20 mL, filtered through an AMICON microporous filter (0.45 µm) to remove insoluble material, divided into 1.0 mL lots and kept in the freezer (-20°C). For full details see Tables XI and XII.

b) Purification by affinity chromatography of crude *E. electricus* (11s) AcChase:

The method used was that of Dudai *et al*. (58) with minor modifications.

2.0 mL of equilibrating buffer (0.01 M phosphate; 0.1 M

NaCl; pH 7.4) was added to two vials (containing ∿10,000 units/vial) of crude lyophilized E. electricus AcChase (Sigma Type VI-S). The crude protein solution was applied to a 1 x 5 cm column containing 3.0 mL of affinity gel (Sepharose-4-B-cap-p-PTA). The column was washed with ∿75 mL of equilibrating buffer, then with 10 mM DMB in equilibriating buffer, this resulted in the elution of a sharp protein peak with ∿60% of the total AcChase activity. The DMB fraction was then pooled and applied to a CM-Sephadex-C-50 column. The eluate was dialysed and concentrated on an AMICON ultrafiltration apparatus, using 1 mM Tris-Cl pH 8.0. The dialysed protein was filtered through an AMICON microporous filter (0.45 μm) divided into 1.0 mL lots and stored in the freezer (-20°C).

Since the AcChase is eluted from the affinity column with a high concentration of DMB (10 mM), it is essential that all of this inhibitor be removed or the kinetic results obtained would be meaningless. A particular lot of purified enzyme was dialysed extensively; enough buffer being passed through the cell to ensure a decamethonium concentration of less than 10^{-12} M. The pre-steady-state parameter k_{obs} was determined over the entire M7C concentration range used (0.5 μM to 40 μM). These values were then used as a check for DMB contamination in subsequent purifications (Table X).

v) Kinetic studies:

Definition of a unit of AcChase activity: One unit of AcChase activity corresponds to 1 μ mole of AcSCh hydrolysed per minute under standard conditions (4.8×10^{-4} M AcSCh; 3.2

TABLE X. The pseudo-first order rates of carbamoylation with M7C; Affinity purified E. electricus AcChase.

[S] μM	k_{obs} sec^{-1}				Mean k_{obs}	$1/k_{obs}$	1/S x 10^{-5}
	1	2	3	4			
1.0	0.0351	0.0342	0.037	-	0.035	28.57	10
2.03	0.0474	0.0471	0.0457	0.041	0.045	22.27	4.93
3.38	0.0540	0.0571	0.0587	0.0557	0.056	17.86	2.96
5.07	0.0772	0.0712	0.0747	0.0631	0.072	13.89	1.97
6.75	0.0846	0.0820	0.0824	0.0790	0.082	12.2	1.48
8.06	0.0920	0.0881	0.0827	-	0.088	11.36	1.24
10.12	0.0951	0.0962	0.0994	0.1026	0.098	10.20	0.99
13.43	0.1086	0.1225	0.1207	0.1184	0.118	8.47	0.74
20.15	0.1518	0.1690	0.1596	0.1444	3 .156	6.41	0.50
33.09	0.1921	0.2114	0.2058	0.1958	0.200	5.00	0.30
40.29	0.2438	0.2364	0.2635	0.2557	0.250	4.00	0.25

x 10^{-3} M DTNB; in 0.1 M phosphate; pH 7.5 at 25°C).

a) Buffer media:

Two buffer media were routinely used in the kinetic studies of AcChase. A high (physiological) ionic strength buffer contained 1 mM Tris-Cl/0.1 M NaCl, pH 8.0. In some cases the Tris concentration was increased to 10 mM when a higher buffering capacity was required. The second buffer was low ionic strength medium consisting of 1 mM Tris-Cl, pH 8.0. In studies of the kinetics of inactivation of AcChase by iPr_2PF, the buffers used were 0.1 M and 1.0 mM phosphate, pH 7.0, respectively, in order to minimize the base catalyzed hydrolysis of substrate (NPA).

b) Ellman assay (73):

Routine assays of the enzyme activity were carried out by the method of Ellman et al. (73) using AcSCh as substrate. The production of the thionitrobenzoate anion generated by the reaction of DTNB with the hydrolysis product thiocholine was monitored at 412 nm ($\varepsilon_{M_{412}}$ = 13,600 M^{-1} cm^{-1}), on a BECKMAN model 25 spectrophotometer. Detailed studies of the steady-state kinetics of this reaction at either low or high ionic strength were carried out in a modified AMINCO-BOWMAN stopped-flow apparatus. The signal derived from the photomultiplier was collected on a Biomation 805 waveform recorder interfaced with a Heathkit H-11 computer and simultaneously displayed on an oscilloscope. The sensitivity of this instrument permitted the use of AcSCh concentrations as low as 1 μM. The apparatus

was operated under the control of a BASIC program developed by Dr. G. Tomlinson. Up to 2048 data points from each kinetic run were transferred from the waveform recorder to the computer where they were converted to absorbance values. Initial rates were determined by least-squares regression on points visually selected from the oscilloscope trace. The reactions at low ionic strength were carried out in the presence of 3.2 x 10^{-3} M DTNB and AcSCH concentrations of 1.0 to 100 µM. At high ionic strength the same DTNB concentration was used but the range of AcSCh used was from 10 to 300 µM (or 10 to 614 µM in the case of T. californica enzyme). The stopped-flow apparatus was equipped with two syringes. The enzyme ($\sim 10^{-10}$ N) was contained in one syringe, AcSCh, DTNB and inhibitor (when used) were contained in the other (with the exception of preincubation experiments where inhibitor was added to both syringes). The use of the stopped-flow apparatus enabled the determination of the steady-state rate of hydrolysis of AcSCh several milliseconds after the mixing of the reactants. In no case was the total change in AcCh concentration greater than 7.5 µM which was determined in separate experiments to produce no detectable change in the pH of the reaction mixture. The data were analysed according to the Henri-Michaelis-Menten (equation [6]) using Lineweaver-Burk plots. Complex inhibition patterns that resulted in non-linear Lineweaver-Burk plots were not analysed.

c) M7C assay:

The reaction of AcChase with the fluorogenic carbamoylating

agent M7C can be described by Scheme II, however owing to the decarbamoylation rate constant (k_3) being much smaller than the carbamoylation rate constant (k_2), the reaction is characterized by a pre-steady-state burst, the amplitude of which corresponds to the enzyme normality. The pseudo-first order approach to steady-state is related to the carbamoylation rate constant (k_2) and the steady-state hydrolysis rate (V_{ss}), can be related to the decarbamoylation rate constant (k_3). A full kinetic treatment is contained in the Appendix. The approach to the steady-state may be described in terms of the observed fluorescence due to the formation of the product M7H:

$$\ln (I_{ss} - I_{press}) = k_{obs}\, t + \ln I_{ss} \qquad [75a]$$

where $(I_{ss} - I_{press})$ is the difference in fluorescence intensities of a line extrapolated from the linear (steady-state) portion and the measured pre-steady-state (I_{press}) burst at any time t and k_{obs} is the pseudo-first order rate constant of carbamoylation. Therefore a plot of $\ln (I_{ss} - I_{press})$ versus t will yield a line with a slope k_{obs} and a vertical intercept (t = 0) of $\ln I_{ss}$ which is the amplitude of the burst phase. The dependence of k_{obs} upon M7C concentration under the experimental conditions used is given by:

$$k_{obs} = \frac{k_2\,[S_o]}{[S_o] + K_s} \qquad [78a]$$

or in reciprocal form

$$1/k_{obs} = 1/k_2 + \frac{K_s}{k_2\,[S_o]} \qquad [79a]$$

Therefore a plot of $1/k_{obs}$ vs. 1/M7C enables the evaluation of K_s as well as k_2 (165).

The decarbamoylation rate constant k_3 can also be evaluated from the steady-state velocity of M7H production, since:

$$V_{ss} = k_3 [E_o]. \qquad [81a]$$

and since E_o can be calculated from the burst amplitude then k_3 can be evaluated (165). The rate of M7H production in the presence or absence of effectors was measured on a Perkin-Elmer MPF-44 spectrofluorometer with a Hamamatsu HTVR 446 photomultiplier tube, operated in the energy mode. The absorption and emission maxima were 405 nm and 505 nm respectively. The M7H fluorescence was not quenched by dissolved O_2 as identical M7H fluorescence intensities were obtained whether or not the M7H solutions were saturated with N_2.

The carbamoylation amplitude was related to the enzyme normality by comparison of fluorescence intensities with those of an M7H standard curve.

The M7C concentration range used, both under conditions of low and high ionic strength, was 0.5 to 40 μM. Under these conditions carbamoylation rates were slow enough to enable both the pre-steady-state and steady-state portions of the reaction to be easily examined. Enzyme active site concentration employed in these studies was usually in the range 1-4 x 10^{-8} M.

vi) Fluorescence titrations:

Free propidium exhibits an absorbance maximum at 494 nm with a fluorescence maximum at 596 nm. Upon interacting

with AcChase its spectral properties are altered markedly. The absorbance maximum is shifted to 535 nm and the fluorescence emission to 630 nm. The titrations were carried out by the addition of successive (5 μL) aliquots of propidium solution (2×10^{-5} or 2×10^{-4} M) to the solution of enzyme ($1\text{-}5 \times 10^{-6}$ N) in 2.0 mL buffer in 3.0 mL (1 cm path length) cells. The total volume of solution did not increase by more than 10% during the titration. The observed fluorescence intensity was corrected for a small contribution from the enzyme. A blank titration in the absence of enzyme was carried out simultaneously as a linearity and a stability check. The intensity coefficient of free propidium under the experimental conditions was obtained from the slope of a plot of fluorescence intensity vs. propidium concentration in the absence of the enzyme. The intensity coefficient of bound propidium was determined by titration of the enzyme under conditions of stoichiometric binding. The concentration of free and bound propidium during the course of the titration were calculated using eq. [9a], [2a] (see appendix).

$$[P_f] = I_t - \frac{\gamma\,[P_o]}{\gamma - \gamma'} \qquad [9a]$$

$$[P_b] = [P_o] - [P_f] \qquad [2a]$$

Where $[P_f]$ and $[P_b]$ are the concentrations of free and bound propidium respectively, $[P_o]$ is the total propidium concentration, I_t is the observed fluorescence intensity and γ and γ' are the intensity coefficients of free and bound propidium respectively, under given experimental conditions. Binding

data were further analyzed by means of Scatchard plots according to:

$$[P_b/P_f] = K_D^{-1} ([E_o] - [P_b])$$

where E_o is the enzyme normality determined by M7C titrations and K_D is the dissociation constant for the binding of propidium to the enzyme.

The ability of edrophonium, gallamine, Zn^{2+} and Mg^{2+} to displace propidium from the enzyme was determined by the addition of successive 5 µL aliquots of displacing ligand solution to a solution containing both enzyme and propidium in 300 µL (0.3 cm^2) microcells. The initial conditions were chosen such that most of the propidium present was in the bound form. A decrease in the observed fluorescence intensity (after corrections for dilution) was taken to indicate displacement of bound propidium. Analysis of competitive binding data was carried out by the method of Taylor et al. (130).

$$[ED]/[EP] = (f_o - f)/(f - f_D) \cdot ([D]/[P] \cdot K_P/K_D) \quad [28a]$$

where [ED], [EP], [D] and [P] are the concentrations of enzyme-displacing ligand complex, enzyme-propidium complex, free displacing ligand and propidium respectively; f_p is the fluorescence of fully bound propidium, f_D is the fluorescence observed when all the enzyme is present as ED, and f_o is the observed fluorescence. K_p and K_D are the dissociation constants of EP and ED respectively (see appendix).

vii) Inactivation profiles:

The inactivation profiles of metal ions were obtained by preincubation of the enzyme for 10 minutes with the inactivating metal ion, then measuring either the steady-state velocity or the carbamoylation amplitude after the addition of either AcSCh, NPA or M7C.

viii) Kinetics of inactivation of AcChase by metal ions:

The inactivation process was followed by two methods. In a continuous assay the loss of enzyme activity was followed by monitoring the absorbance at 400 nm due to the enzyme catalyzed formation of p-nitrophenol. p-Nitrophenol-acetate was dissolved in MeOH and this solution was made daily. The NPA concentration was 2×10^{-4} M. This is ∿10-fold lower than the K_{app} for NPA displayed by AcChase. Under these conditions less than 20% of the total substrate was hydrolyzed in the time course of the inactivation thus ensuring steady-state conditions. The linearity of the reaction under these conditions was determined in separate experiments without inhibitor. The enzyme concentration used was $\sim 10^{-10}$ N. A second discontinuous method involved periodic measurements of the carbamoylation amplitude after addition of M7C to samples of the metal ion enzyme mixtures. This second method is less accurate in the early points since the pre-steady-state carbamoylation of the enzyme is rather slow (requiring 15-25 seconds to attain steady-state).

Most of the metal salts used were sulphates; as a result the pH of the stock solutions were checked and re-adjusted to 8.0 where necessary.

La^{3+} solutions were unstable and a precipitate formed upon storage. This was attributed to $La_3(CO_3)_2$ which is extremely unstable. This problem was overcome by boiling the H_2O prior to preparation of the La^{3+} solutions, and flushing the cuvettes with N_2 during the course of the experiment.

ix) Kinetics of inactivation of AcChase by iPr_2PF:

The inactivation of AcChase by iPr_2PF was followed by two methods. In a continuous assay the loss of enzyme activity was followed by monitoring the absorbance at 400 nm, due to the enzyme catalyzed formation of p-nitrophenol (as in viii above). A second discontinuous method, similar to the "rapid sampling" method of Gentinetta and Brodbeck (139), involved, the removal of (20 µL) aliquots from a iPr_2PF/enzyme mixture, at various time intervals, and subsequent assay using NPA.

x) Modification of AcChase with DTNB and N-Dansylaziridine:

a) DTNB:

To 2.0 mL enzyme ($\sim 5 \times 10^{-7}$ M), 200 µL Tris-Cl (1 mM; pH 8.0), 200 µL SDS (10% in 1 M Tris-Cl; pH 8.0), and 200 µL DTNB (10^{-2} M in 0.1 M Tris-Cl; pH 8.0) was added. The reaction was followed by monitoring the absorbance at 412 nm due to the formation of thionitrobenzoate anion (resulting from the reaction of DTNB with free protein thiol groups). A duplicate sample without enzyme served as the blank. The extinction coefficient used for the thionitrobenzoate anion was $\varepsilon_{M_{412}} = 13{,}600\ M^{-1}\ cm^{-1}$.

b) N-Dansylaziridine:

2 mg of N-DAZ was dissolved in 1 mL absolute ethanol (7×10^{-3} M). 20 µL of this solution was added to 2.0 mL of enzyme solution ($1\text{-}5 \times 10^{-7}$ M), and to 2.0 mL of buffer (as a control). The reaction was monitored by spectral changes in the emission spectrum of N-DAZ: Upon reacting with protein thiol groups the apparent emission maximum is blue shifted by ∿10 nm and the fluorescence is enhanced. The excitation maximum of N-DAZ is 347 nm with an emission maximum of 565 nm.

The excess N-DAZ was removed by two different methods: 1) The protein/N-DAZ (/effector) mixture was dialysed on an AMICON ultrafiltration apparatus. 2) The protein/N-DAZ (/effector) mixture was chromatographed on a Sepharose 4-B column to which L-cysteine was covalently attached. The elution rate was very slow (0.5 mL/hr).

Protein hydrolysis: The modified protein was hydrolyzed in 6.0 N HCl in sealed evacuated tubes for 4 hr at 110°C. The HCl was removed by placing tubes in a desiccator containing NaOH.

2-Dimensional TLC: The protein hydrolysate was extracted with methanol and applied to 20 x 20 cm TLC sheets (silica gel). The solvent system used in the first direction was benzene: pyridine:acetic acid (80:20:5 v/v) (solvent system #63 of Neidweiser (164)). In the second direction toluene:2-chloroethanol:NH_4OH (25%) (80:20:5 v/v) was used as the solvent system (#64 of Neiderweiser (164)). The spots were identified by a wide range UV lamp and/or with a ninhydrin spray (1% in ethanol).

RESULTS

1) Isolation and purification of AcChase:

The isolation of AcChase from the electroplax of *T. californica* and the purification of the crude protein extracts of AcChase from *T. californica* and *E. electricus* by affinity chromatography are summarized in Tables XI and XII.

2) Stability of AcChase:

AcChase isolated from *E. electricus* or *T. californica* (in 1 mM Tris-Cl pH 8.0) was incubated at 25°C. Aliquots (80 µL) were removed and assayed using the fluorogenic carbamoylating agent M7C. The observed pseudo-first order rate constant as well as the carbamoylation amplitude, which is proportional to the amount of active enzyme was unchanged (within experimental error) after incubation for up to 11 hrs (Fig. 4).

3) Experiments with *E. electricus* AcChase:

A) Fluorescence titrations:

An apparent dissociation constant for the propidium-AcChase complex of around 10^{-8}M was estimated from pre-steady state and steady-state kinetic experiments (see results Section 3B and C).

Accurate determinations of this dissociation constant using equilibrium binding techniques require that the enzyme concentration also be around this value in order for the concentration of free and bound ligand to be significant. However,

TABLE XI. Isolation of AcChase from the electroplax of *T. californica*.

Step	Total Protein (mg)[a]	Total Units (u)	Specific Activity $U \cdot mg^{-1}$
1) Crude homogenate	350	22,000	63
2) Supernatant after 8'Trypsinization	108	17,600	163

[a] Determined from A_{280} using an $E_{1\ mg\ \%} = 17.6$.

TABLE XII. Purification of AcChase by Affinity Chromatography.

Step	*E. electricus*			*T. californica*		
	Total Protein (mg)	Units	Specific Activity	Total Protein (mg)	Units	Specific Activity
Crude protein	13.4	8,900	664	108	17,600	163
AFFINITY CHROMATOGRAPHY						
Equilibrating buffer wash	11.4	490	42.9	69	3,200	46
DMB/Equilibrating buffer wash	.76	2,400[a]	3,150[a]	2.0[a]	3,000[a]	1,500[a]
1 M NaCl/Equilibrating buffer wash	1.0	1,230	1,230	12.0	2,180	182
C-50 Chromatography eluate	0.7	4,340	6,200	1.8	9,000	5,000
Amicon dialysis	0.7	5,180	7,400	1.7	10,000	5,800
% YIELD		58			56	

[a] Not a true reflection as assay contained DMB.

Fig. 4. Effect of prolonged incubation of AcChase at 25°C on the carbamoylation amplitude and the observed pseudo-first order rate constant of carbamoylation. The buffer was 1.0 mM-Tris-Cl, pH 8.0. A) T. californica AcChase, assayed: (○) immediately; and after: (●) 15 min; (◆) 2 hr; (■) 6 hr 20 min; (△) 7 hr 5 min; (◇) 10 hr 50 min of incubation by the addition of 4.72 μM M7C. B) E. electricus AcChase assayed: (○) immediately; and after: (●) 2 hr 5 min; (▼) 5 hr; (□) 6 hr 30 min; (◆) 10 hr 30 min; (△) 11 hr 30 min; of incubation by the addition of 4.72 μM M7C.

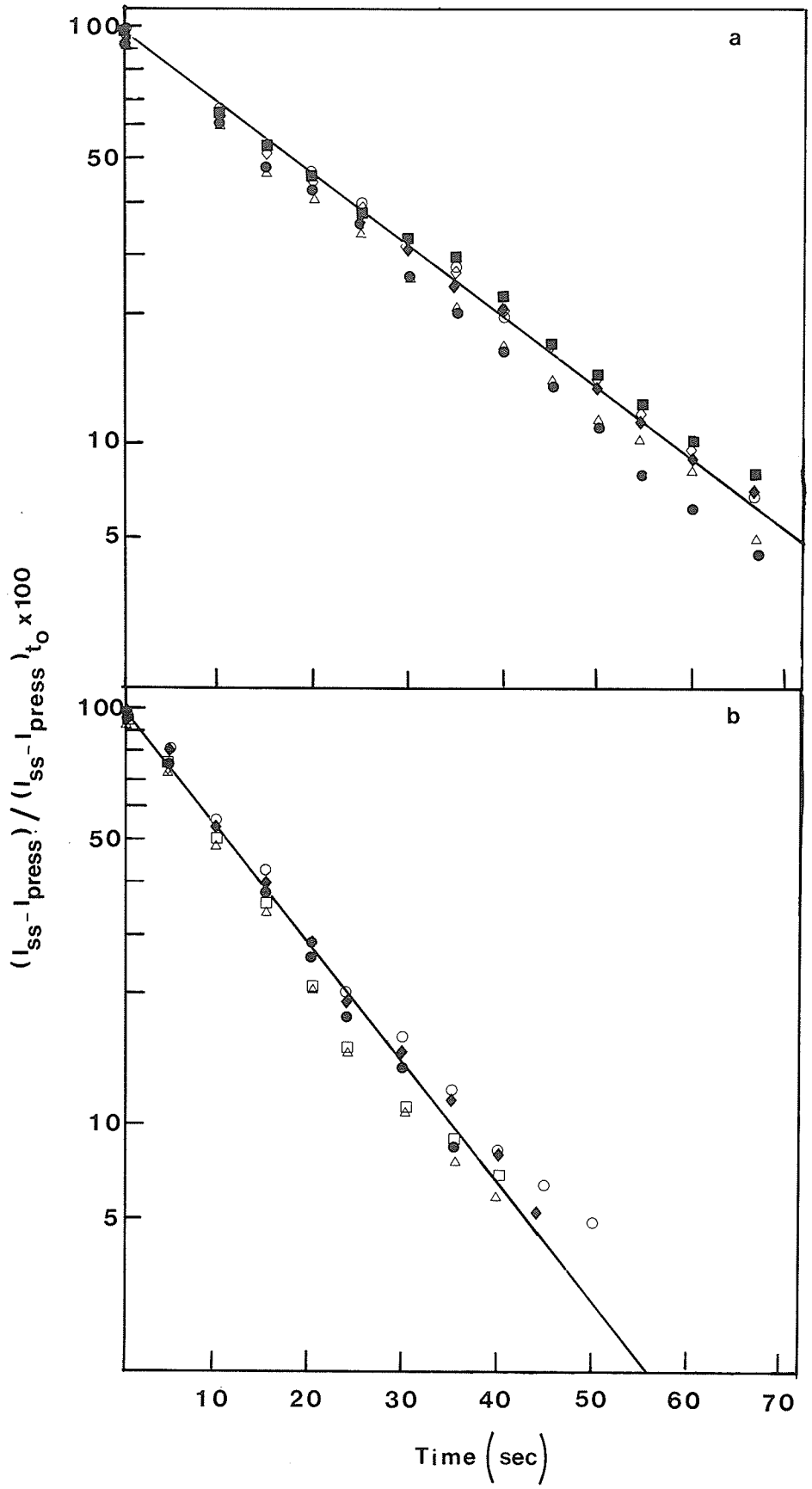
100
50
10
5
a
b
$(I_{ss}-I_{press})/(I_{ss}-I_{press})_{t_o} \times 100$
10
20
30
40
50
60
70
Time (sec)

Fig. 5. Fluorescence titration of AcChase with propidium. (●) observed fluorescence in the presence of 3.82×10^{-6} N AcChase, (○) blank titration in the absence of the enzyme. Titrations were carried out at 25°C in 1.0 cm^2 cells in 1.0 mM Tris-Cl, pH 8.0. Excitation wavelength = 395 nm Emission wavelength = 565 nm

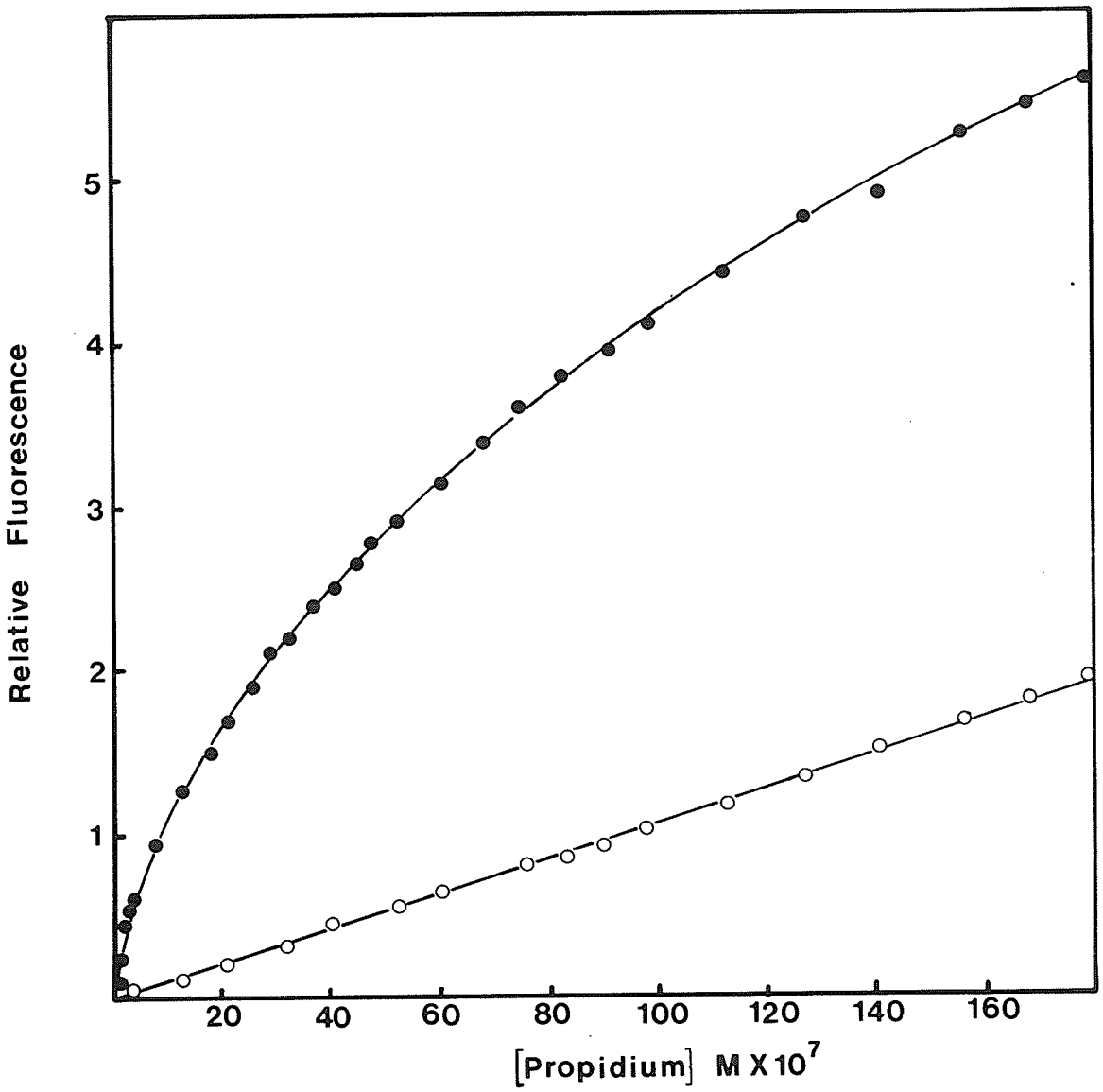
Relative Fluorescence
1
2
3
4
5
20
40
60
80
100
120
140
160
[Propidium] M X 10^7

the fluorescence intensity of propidium is such that accurate measurements could be made only at propidium concentrations of 10^{-7} M or higher. It was therefore expected that, owing to the high enzyme concentration required to observe propidium binding, the equilibrium region of the titration curve would be lost to stoichiometric binding. However, even with enzyme concentrations as high as 5×10^{-6} M, there was a considerable equilibrium region in the titration curve (Fig. 5). Analysis of the data by means of a Scatchard plot revealed the presence of at least two classes of propidium binding sites, one class with a K_D of less than 10^{-7} M and a second class with a K_D of 4×10^{-6} M (Fig. 6), suggesting possible heterogeneity in propidium binding sites or in the enzyme population.

The ability of gallamine, propidium, edrophonium, Mg^{2+} and Zn^{2+} to compete for the peripheral sites is illustrated in Fig. 7. Addition of a large excess of edrophonium had virtually no effect. Mg^{2+} displaced $\sim$30% of the bound propidium at a concentration of 1 mM. Zn^{2+} displaced approximately 50% of the bound propidium at its ($Zn(OH)_2$) solubility limit. Gallamine was the most effective ligand for the displacement of propidium, $\sim$80% of the bound propidium being displaced at 3.2×10^{-4} M gallamine. Analysis of the gallamine displacement data according to the logarithmic form of eq. 28a (see appendix) allowed an estimation of the dissociation constant for the gallamine enzyme complex. The value of the K_D was 8.9×10^{-8} M based on an enzyme site concentration of 1.71×10^{-6} M and an enzyme-propidium K_D of 2×10^{-8} M. This is in reasonable agree-

Fig. 6. Scatchard plot of data derived from Fig. 5.

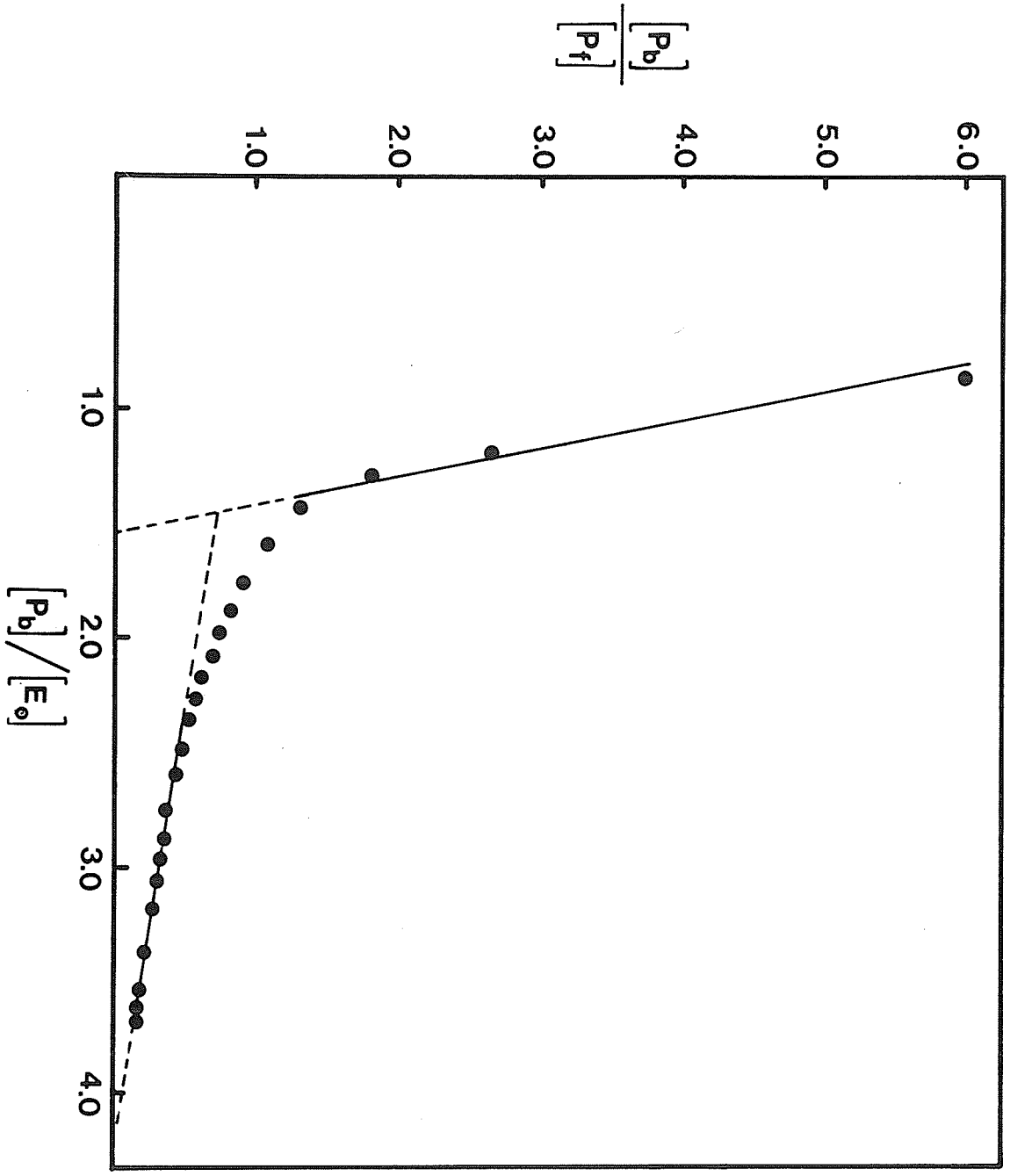
[Pb]/[Pf]
1.0
2.0
3.0
4.0
5.0
6.0
[Pb]/[Eo]
1.0
2.0
3.0
4.0

Fig. 7. Displacement of bound propidium. The enzyme (3.42×10^{-6} N) was first titrated with propidium until about 2 mol of propidium per tetrameric enzyme were bound. Aliquots of displacing ligand were then added and the fluorescence intensity due to bound propidium were recorded. Titrations were carried out in 0.3 cm^3 cells . (●) edrophonium; (▽) Mg^{2+}; (▲) Zn^{2+}; (■) gallamine.

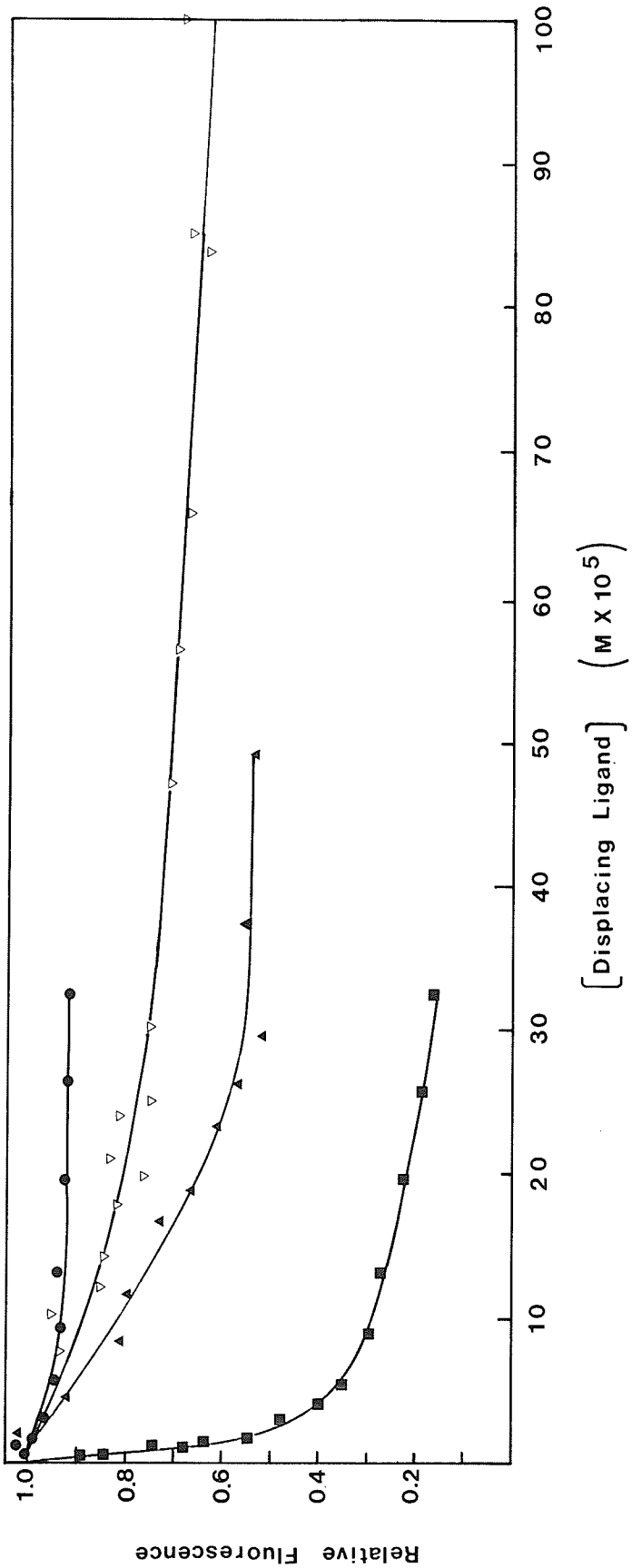
Relative Fluorescence
1.0
0.8
0.6
0.4
0.2
10
20
30
40
50
60
70
80
90
100
[Displacing Ligand] (M X 10^5)

ment with the kinetic data (Results Section 3B and 3C).

B) Steady-state kinetics:

The kinetics of the AcChase-catalyzed hydrolysis of AcSCh under steady-state conditions were performed at low (1 mM Tris-Cl pH 8.0), high (1 mM Tris-Cl; 0.1 M NaCl) and at an intermediate ionic strength (1 mM Tris-Cl; 0.025 M NaCl). The kinetics at low and high ionic strength obeyed Henri-Michaelis-Menten behaviour (Fig. 8). The steady-state kinetic parameters K_{app} and k_c were calculated to be: low ionic strength K_{app} = $4.3 \pm .2 \times 10^{-6}$ M, $k_c = 3.5 \pm 0.5 \times 10^{5}$ min^{-1}; high ionic strength $K_{app} = 5.6 \times 10^{-5}$ M, $k_c = 9.0 \times 10^{5}$ min^{-1}. At intermediate ionic strength the double reciprocal plots exhibited downward curvature, suggesting the presence of at least two forms of the enzyme. Above 0.1 M, NaCl displayed competitive inhibition patterns (Fig. 8).

The cationic ligands edrophonium, gallamine and propidium were found to be potent inhibitors of the enzyme (Fig. 9). However, only edrophonium displayed classical competitive inhibition ($K_c = 1.8 \times 10^{-8}$ M). Gallamine and propidium resulted in curved double reciprocal plots suggesting that these ligands exert their effects on the enzyme in a manner different from or in addition to direct competition with substrate for the active sites. Note that these results were obtained from initial rate measurements made within the first 1-2 seconds after the mixing of the enzyme with ligand-containing substrate solution. Incubation of the enzyme with the inhibitors (propidium, gallamine) prior to the introduction of the substrate, resulted

Fig. 8. Kinetics of acetylthiocholine hydrolysis at various ionic strengths. Initial velocities were determined using the stop-flow apparatus as described in the Materials and Methods section. Each point represents the average of five determinations. (■) 1.0 mM Tris-Cl, pH 8.0; (▲) 1.0 mM Tris-Cl/0.025 M-NaCl, pH 8.0; (●) 1.0 mM-Tris-Cl/0.10 NaCl, pH 8.0; (○) 1.0 mM-Tris-Cl/1.0 M-NaCl, pH 8.0.

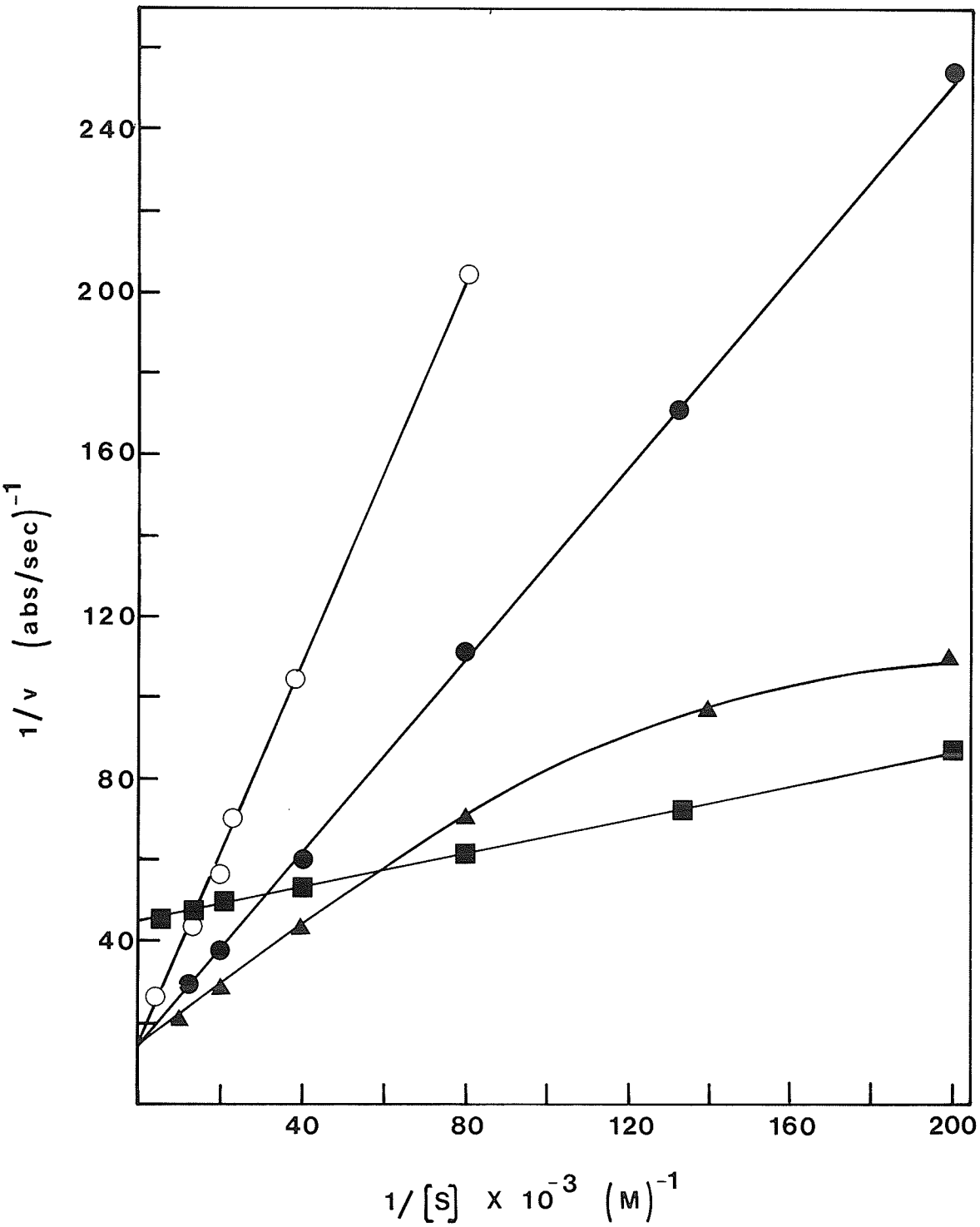
240
200
160
120
80
40
1/v (abs/sec)$^{-1}$
40
80
120
160
200
1/[S] X 10^{-3} (M)$^{-1}$

Fig. 9. Inhibition of acetylthiocholine hydrolysis by edrophonium, gallamine and propidium. The buffer was 1.0 mM Tris-Cl, pH 8.0, 25°C. Acethylthiocholine concentrations were in the range 1.43-49.8 μM. Uninhibited runs are indicated by open circles. Edrophonium: (●) 3.9×10^{-8} M; (▲) 7.75×10^{-8} M; (■) 1.55×10^{-7} M; (△) 3.1×10^{-7} M. Gallamine: (●) 6.45×10^{-8} M; (■) 1.6×10^{-7} M; (△) 3.2×10^{-7} M. Propidium: (●) 8.0×10^{-8} M; (■) 1.6×10^{-7} M; (△) 3.2×10^{-7} M.

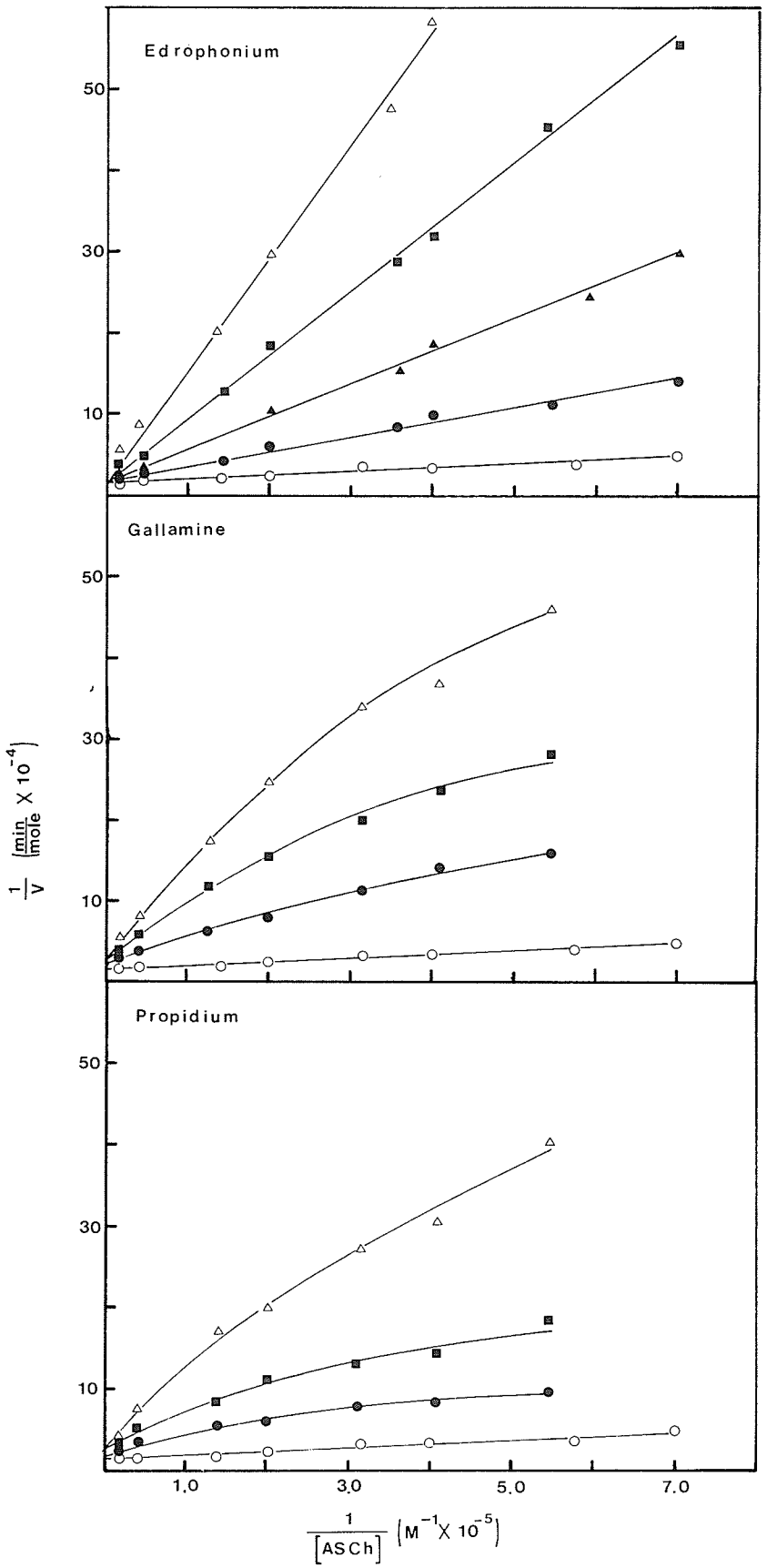
Edrophonium
Gallamine
Propidium
50
30
10
1.0
3.0
5.0
7.0
$\frac{1}{V}$ $\left(\frac{min}{mole} \times 10^{-4}\right)$
$\frac{1}{[ASCh]}$ $\left(M^{-1} \times 10^{-5}\right)$

in linear Lineweaver-Burk plots, and the rates were enhanced (relative to the non-preincubated case). This was observed over most of the substrate concentration range used as illustrated in the case of gallamine (Fig. 10). The activation was directly observed in a stopped-flow spectrophotometer, with very low enzyme concentration, to ensure that less than 20% of the substrate was hydrolyzed during the time course of the activation (Fig. 11). Under these conditions the rate of thionitrobenzoate production is enhanced 1.36 fold in comparison to the rate observed in the first few seconds following the mixing of the reactants. In the absence of propidium, production of thionitrobenzoate was linear with time.

The inhibition pattern after preincubation with either propidium or gallamine appeared to be of the competitive type. No activation upon preincubation was observed with d-tubocurarine. However, the inhibition pattern became more uncompetitive upon incubation with this ligand (Fig. 12).

The metal ions Mg^{2+}, Mn^{2+}, Ca^{2+} and Na^{+} were all found to enhance the steady-state rate of hydrolysis of AcSCh under conditions of near-saturation with substrate (Fig. 13). The maximal effect was observed at an ionic strength of 0.07 to 0.1 and was independent of the metal ion used. However, the divalent metal ion-induced activation was observable at an ionic strength more than ten fold lower than that observed with monovalent sodium. Also the concentrations of divalent cation required to induce 50% of the total activation (a rough estimate of the dissociation constant of the metal ion-AcChase

Fig. 10. Effect of preincubation of AcChase with 5 x 10^{-7} M propidium on the rate of acetylthiocholine hydrolysis (1 x 10^{-10} N AcChase). (■) No propidium; (▲) + propidium, no preincubation; (△) + propidium, 10 min preincubation.

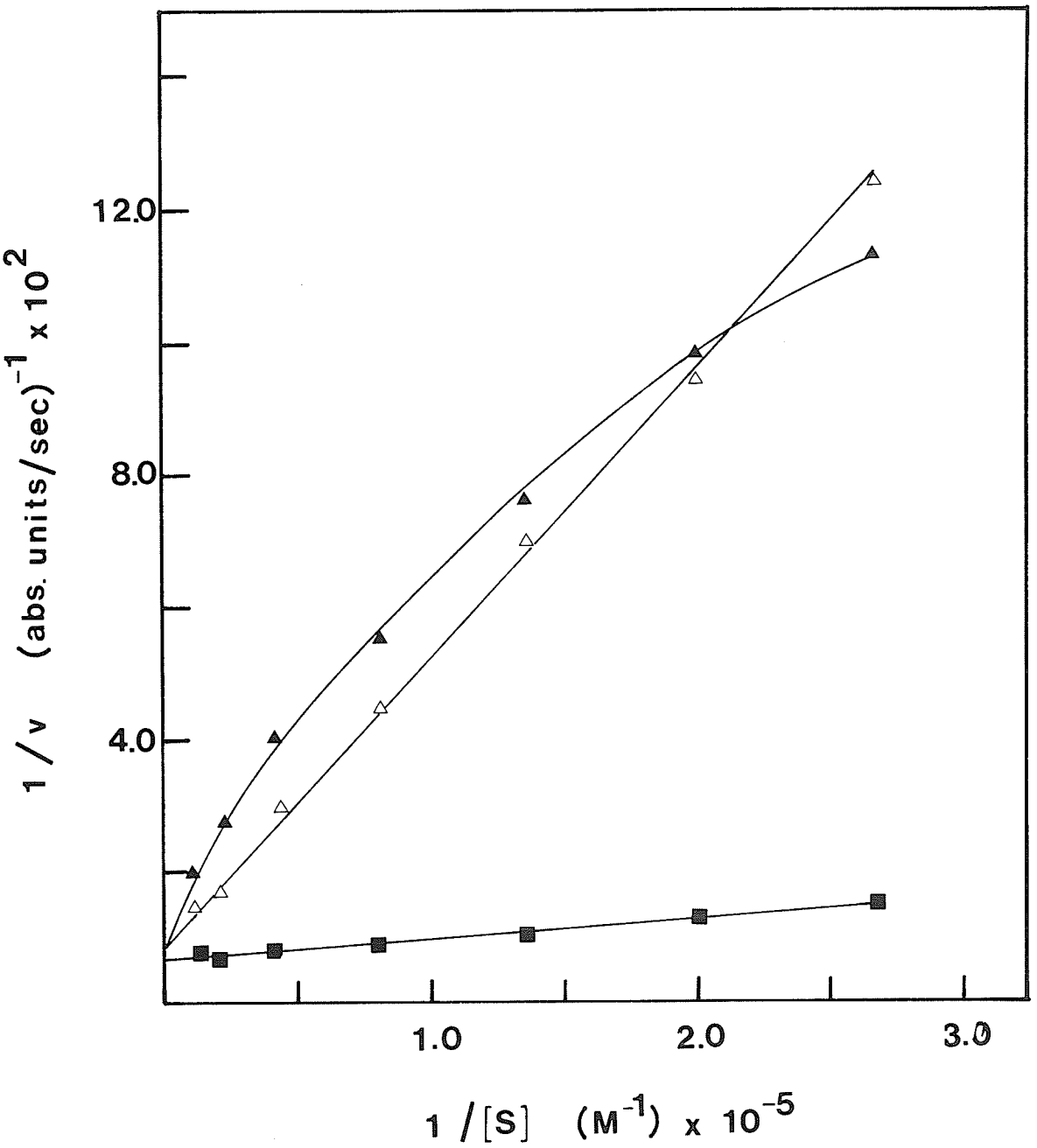
12.0
8.0
4.0
1 / v (abs. units/sec)$^{-1}$ x 10^{2}
1.0
2.0
3.0
1 /[S] (M^{-1}) x 10^{-5}

Fig. 11. Activation of AcChase by 5×10^{-7} M propidium. Enzyme solution was mixed in the stopped-flow apparatus with an equal volume of a solution containing either substrate + DTNB or substrate + DTNB + propidium. The increase in absorbance at 412 nm was monitored immediately thereafter (final concentration: 2.5×10^{-5} M AcSCh; 3.14×10^{-2} M DTNB; 9.3×10^{-12} N AcChase. (●) No propidium; (◆) + propidium.

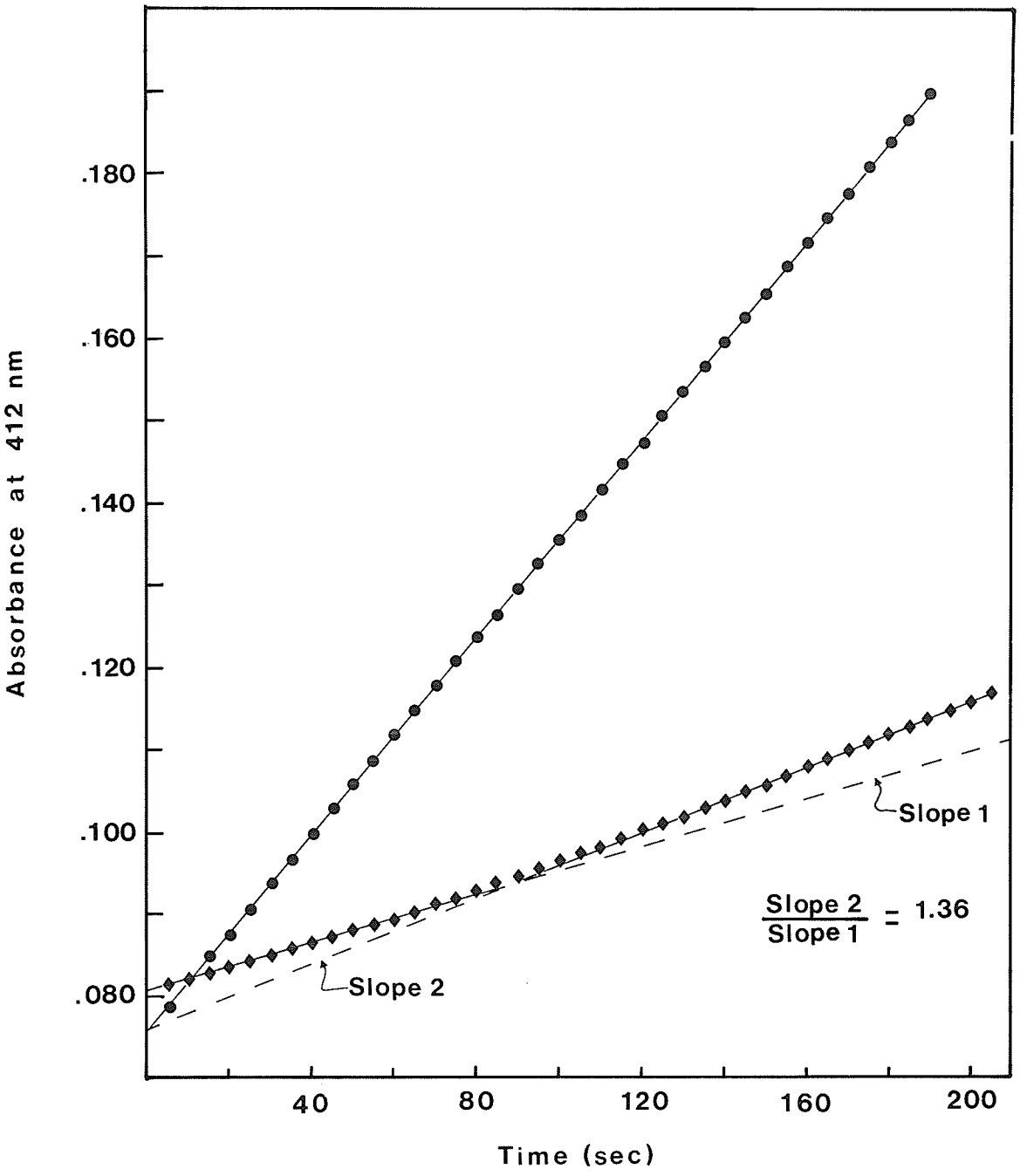
Absorbance at 412 nm
.180
.160
.140
.120
.100
.080
40
80
120
160
200
Time (sec)
Slope 1
Slope 2
Slope 2 / Slope 1 = 1.36

Fig. 12. Inhibition of AcSCh hydrolysis by gallamine and d-tubocurarine following 10 min preincubation with effector. (a) Gallamine: (□) none; (●) 3.9×10^{-7} M; (○) 9.7×10^{-7} M; (■) 1.9×10^{-8} M. (b) d-Tubocurarine: (□) none; (●) 2.0×10^{-6} M; (○) 8.0×10^{-6} M; (■) 2.0×10^{-5} M.

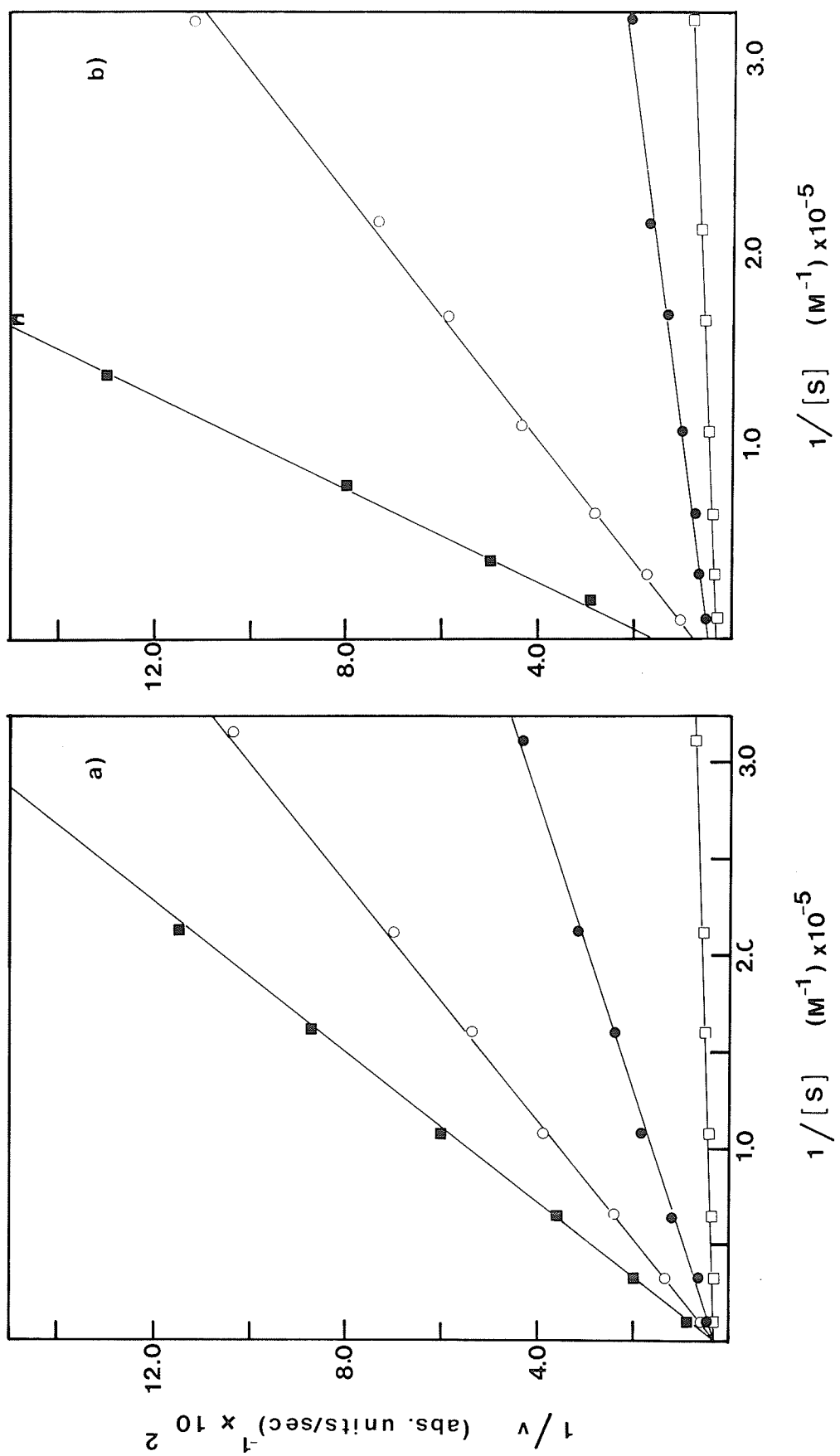
a)
b)
12.0
8.0
4.0
1.0
2.0
3.0
1/[S] (M⁻¹) x10⁻⁵
1/v (abs. units/sec)⁻¹ x 10²

Fig. 13. Activation of AcChase by metal ions. Initial velocities of the reaction of AcChase with AcSCh (1×10^{-4} M) were measured in the presence (V) and absence (V_o) of metal salts by the method of Ellman et al. (see Materials and Methods section for details). The buffer was 1.0 mM-Tris, pH 8.0. (□) $MnSO_4$; (▲) $CaCl_2$; (○) $MgSO_4$; (◆) NaCl.

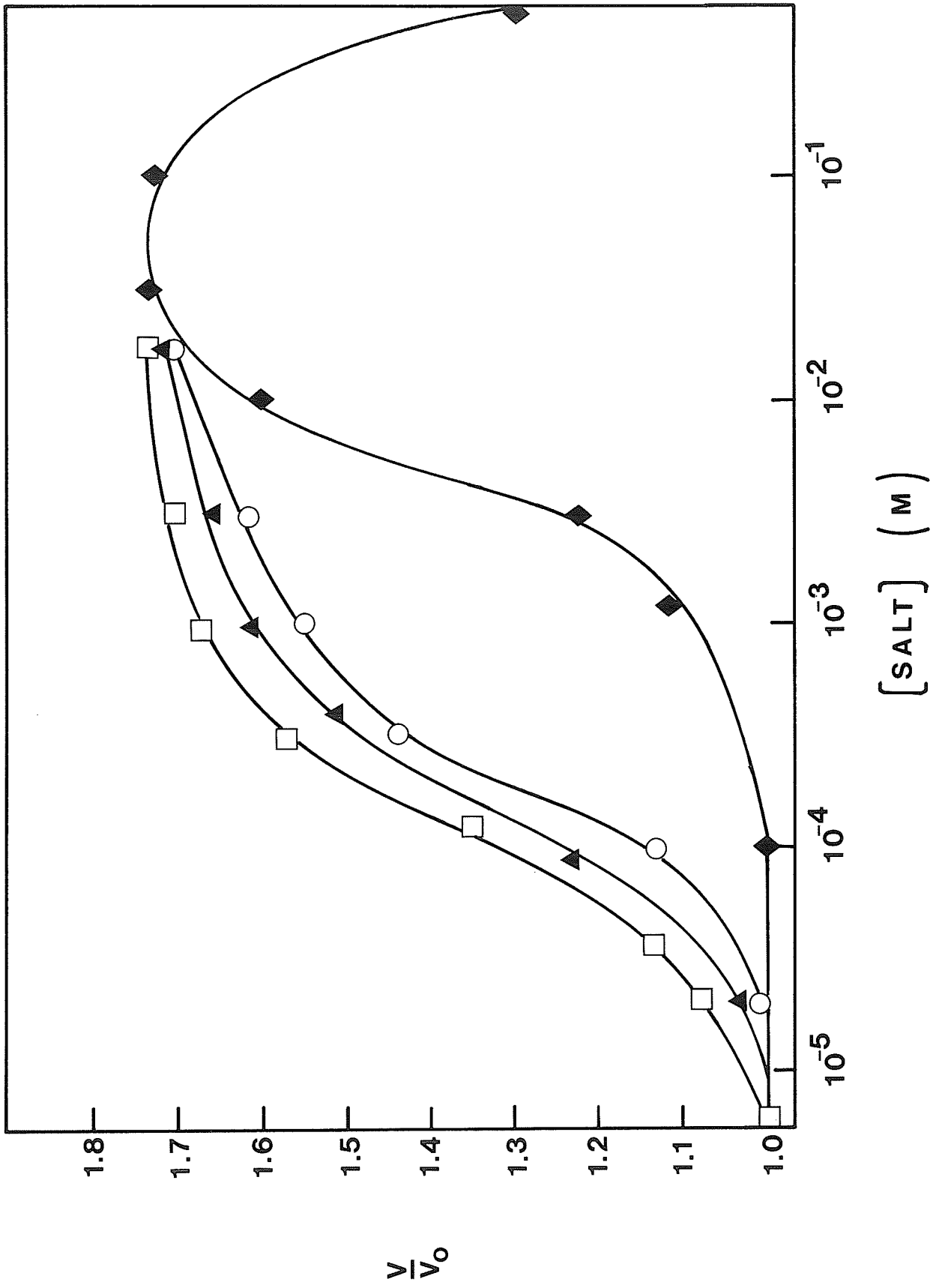
1.8
1.7
1.6
1.5
1.4
1.3
1.2
1.1
1.0
V/Vo
10-5
10-4
10-3
10-2
10-1
[SALT] (M)

complex) were 25-30 fold lower than that observed with sodium ion, suggesting that metal ion activation is dependent both on the ionic strength of the assay medium as well as on the nature of the cation used. The measured velocities of AcSCh hydrolysis in the presence of saturating salt concentrations were independent of the order of mixing (manual or rapid mixing techniques) suggesting that the rate of metal-induced activation of AcChase is very high. This is in contrast to the results obtained with organic activators of the enzyme such as propidium, which were shown to activate AcChase relatively slowly (Fig. 11).

The effect of the divalent cations Zn^{2+} and Cu^{2+} was a slow inhibition of the AcSCh hydrolysis rates, the maximum inhibition being observed after a ten minute preincubation of the enzyme with either cation (Fig. 14). The instantaneous effects of Zn^{2+} and La^{3+} on the steady-state kinetic hydrolysis of AcSCh were tested using a stopped-flow spectrophotometer which allows the determination of hydrolysis rates $\sim$10 msec after mixing of the reagents. Under these conditions Zn^{2+} and La^{3+} were found to inhibit hydrolysis rates below 8 μM AcSCh, but activated the rates by as much as 1.7-fold and 1.4-fold, respectively at 100 μM AcSCh (Fig. 15). The instantaneous activation of hydrolysis rates by Zn^{2+} (and La^{3+}) suggests that a) the slow inactivation observed in the presence of these metal cations is not due to simple competitive inhibition and b) these metal ions have a dual effect on the enzyme which may arise from their binding to separate classes of peripheral sites.

Fig. 14. Effect of Zn^{2+} on the rate of AcSCh hydrolysis. ([AcSCh] = 50.0 μM); $CuSO_4$ shows similar behaviour. The buffer was 1.0 mM Tris-Cl, pH 8.0.

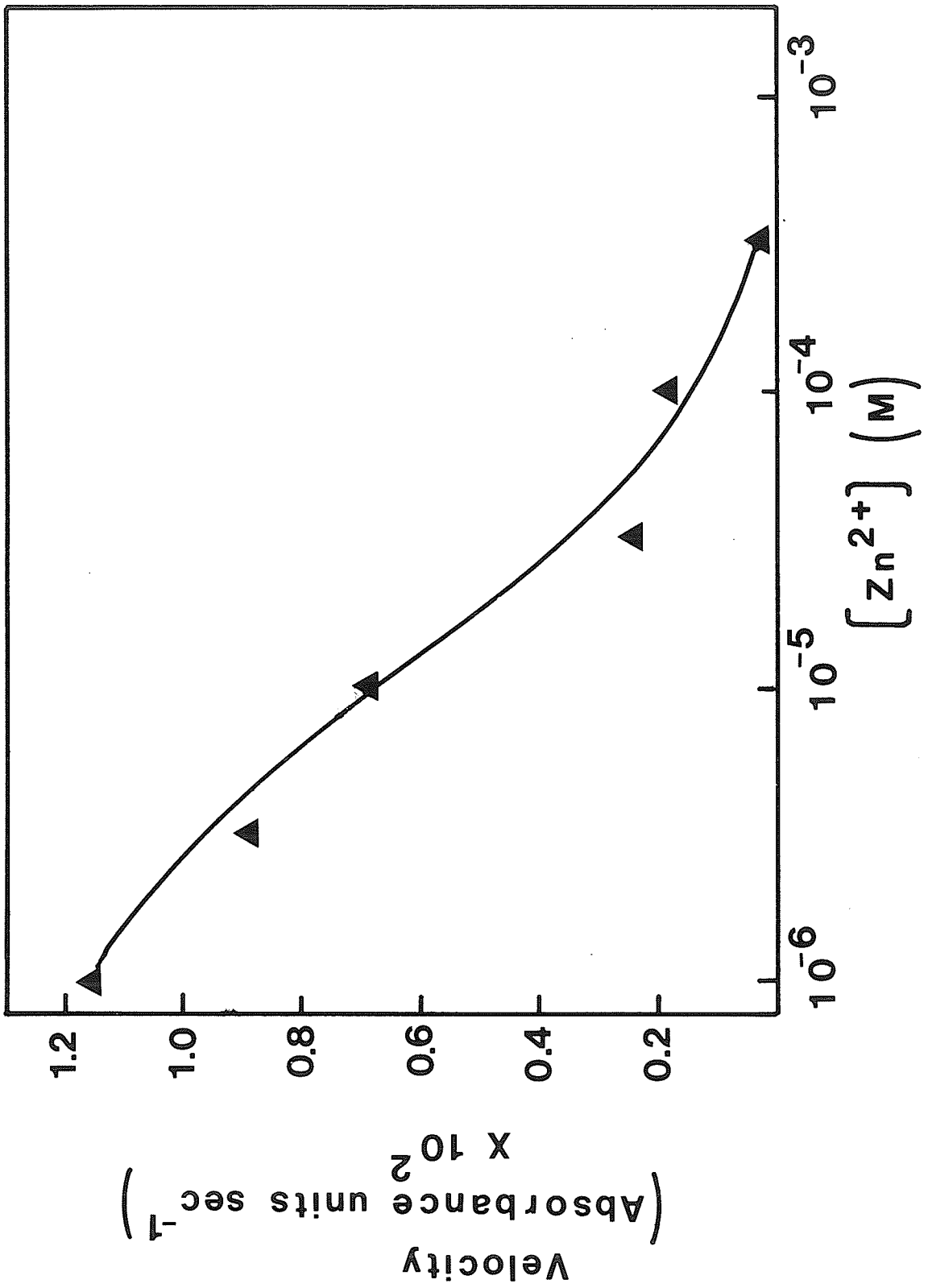
Velocity
(Absorbance units sec^{-1})
X 10^2
1.2
1.0
0.8
0.6
0.4
0.2
10^{-6}
10^{-5}
10^{-4}
10^{-3}
$[Zn^{2+}]$ (M)

Fig. 15. The effect of Zn^{2+} on the steady-state hydrolysis of AcSCh. Initial velocities were determined using the stop-flow apparatus as described in the Materials and Methods section. The buffer was 1 mM Tris-Cl, pH 8.0. AcSCh concentrations were in the range 4.5 to 100 μM. Runs without Zn^{2+} are indicated by open circles. Zn^{2+}: (▽) 7.5×10^{-5} M; (△) 1.94×10^{-4} M; (●) 5.8×10^{-4} M. The concentration of enzyme was 2.69×10^{-11} N.

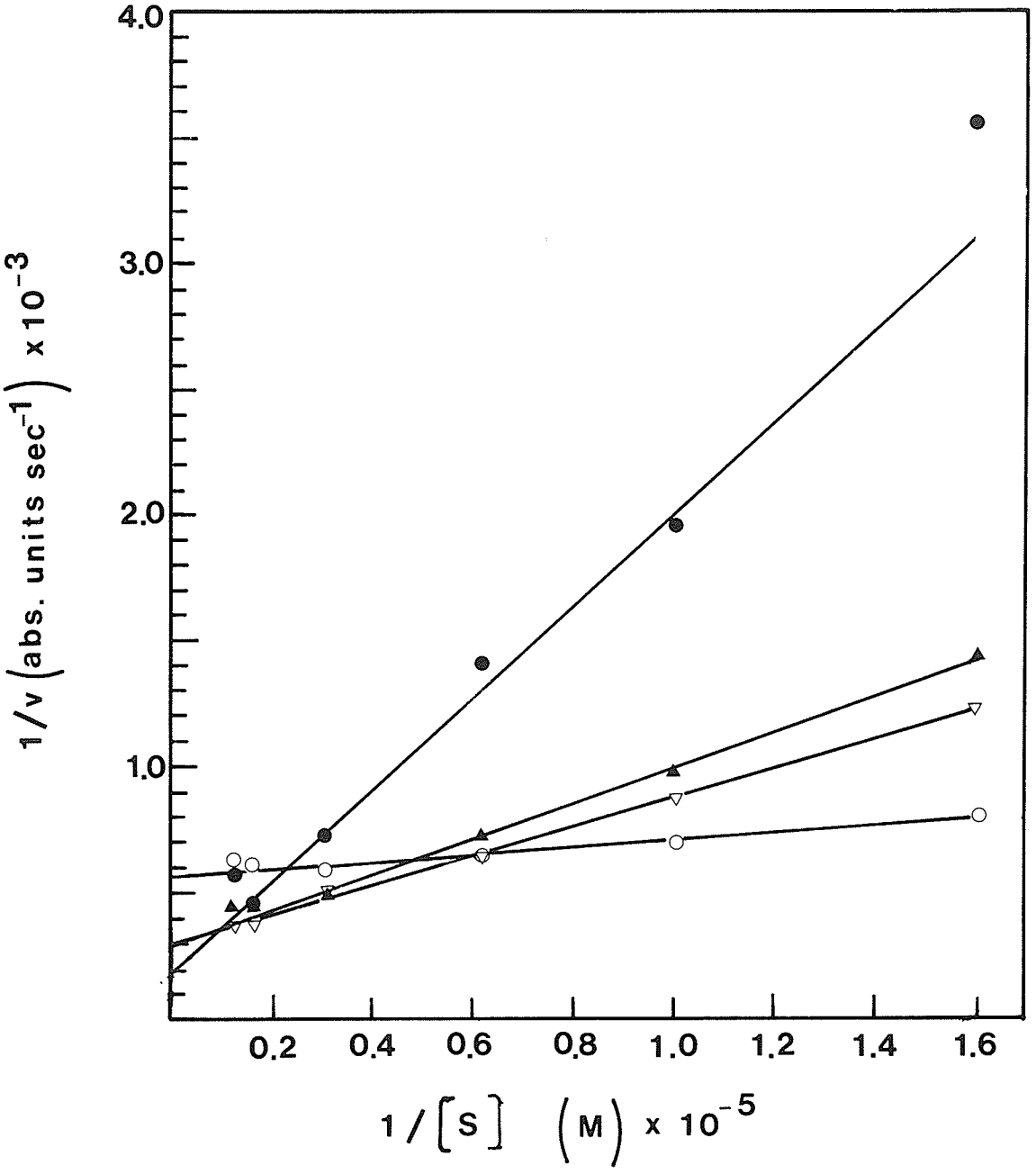
4.0
3.0
2.0
1.0
1/v (abs. units sec^{-1}) x 10^{-3}
0.2
0.4
0.6
0.8
1.0
1.2
1.4
1.6
1/[S] (M) x 10^{-5}

C) Pre-steady-state kinetics:

In the substrate concentration range 0.5 to 10 μM, the dependence of the pseudo-first order rate constant of carbamoylation of AcChase upon the substrate (M7C) concentration, was in close correspondance with the behaviour predicted by eq. [79a] (see appendix).

The values of k_2 and K_s were calculated to be 0.09 sec^{-1} and 1.27 x 10^{-6} M, respectively. The inhibition pattern produced in the presence of edrophonium was competitive (Fig. 16), with a calculated K_{comp} of 2.1 x 10^{-8} M.

Gallamine and propidium produced a downward displacement of the extrapolated vertical intercept, the slopes of the lines did not increase linearly with increasing inhibitor concentrations, and appeared to approach a maximum value (Fig. 17). Inaccuracies in the rate measurements at high inhibitor concentrations prevented a detailed study of this saturation phenomenon. Similar observations (activation of AcSCh hydrolysis rates) with gallamine and propidium in the steady-state kinetics lead to the suggestion that these two compounds may interact with the enzyme at the peripheral anionic sites.

i) Activation:

At M7C concentrations of 10 μM or above substrate activation was observed; pseudo-first order rate constants of carbamoylation were increased from an extrapolated value of 0.08 sec^{-1} (obtained from the substrate concentration range 1 to 10 μM), to a maximum of 0.23 sec^{-1} from the high substrate concentration data (Fig. 18). The increased carbamoylation

Fig. 16. Inhibition of the carbamoylation reaction of AcChase with M7C by edrophonium. The buffer was 1.0 mM Tris-Cl, pH 8.0. Enzyme concentration = 1.0×10^{-8} N. (●) no edrophonium; (○) 1.32×10^{-8} M edrophonium; (■) 5.24×10^{-8} M; (□) 1.05×10^{-7} M edrophonium.

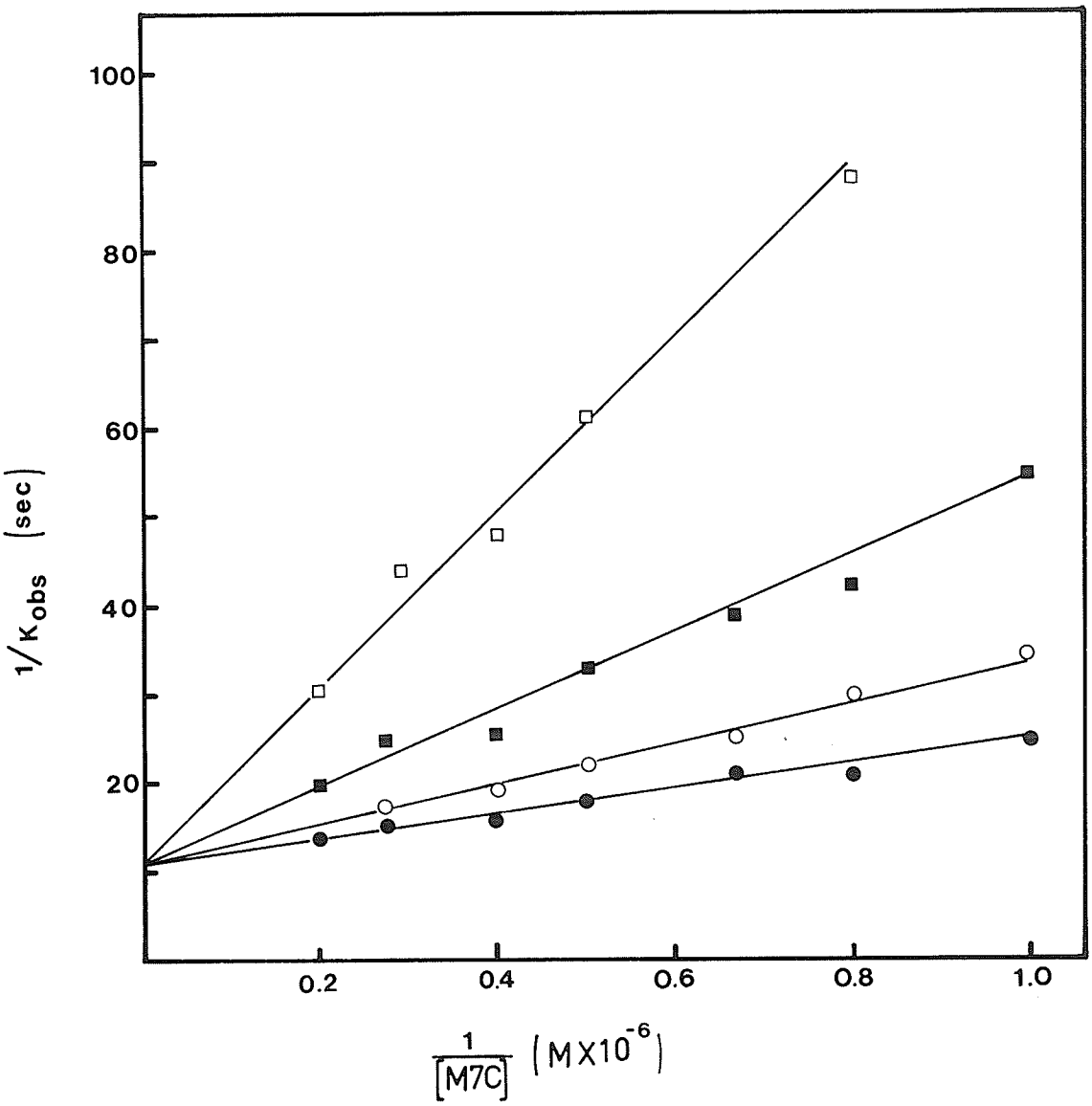
100
80
60
40
20
1/K obs (sec)
0.2
0.4
0.6
0.8
1.0
1/[M7C] (MX10^-6)

Fig. 17. Inhibition of the carbamoylation reaction of AcChase with M7C by gallamine and propidium. The buffer was 1.0 mM Tris-Cl, pH 8.0. Enzyme concentration was 1 x 10^{-8} N. Left-hand plot: (○) no gallamine; (●) 5.4 x 10^{-8} M gallamine; (■) 1.08 x 10^{-7} M gallamine; (□) 2.7 x 10^{-7} M gallamine; (△) 5.4 x 10^{-7} M gallamine. Right-hand plot: (○) no propidium; (●) 1.26 x 10^{-8} M propidium; (■) 2.52 x 10^{-8} M propidium; (□) 6.34 x 10^{-8} M propidium; (△) 1.27 x 10^{-7} M propidium.

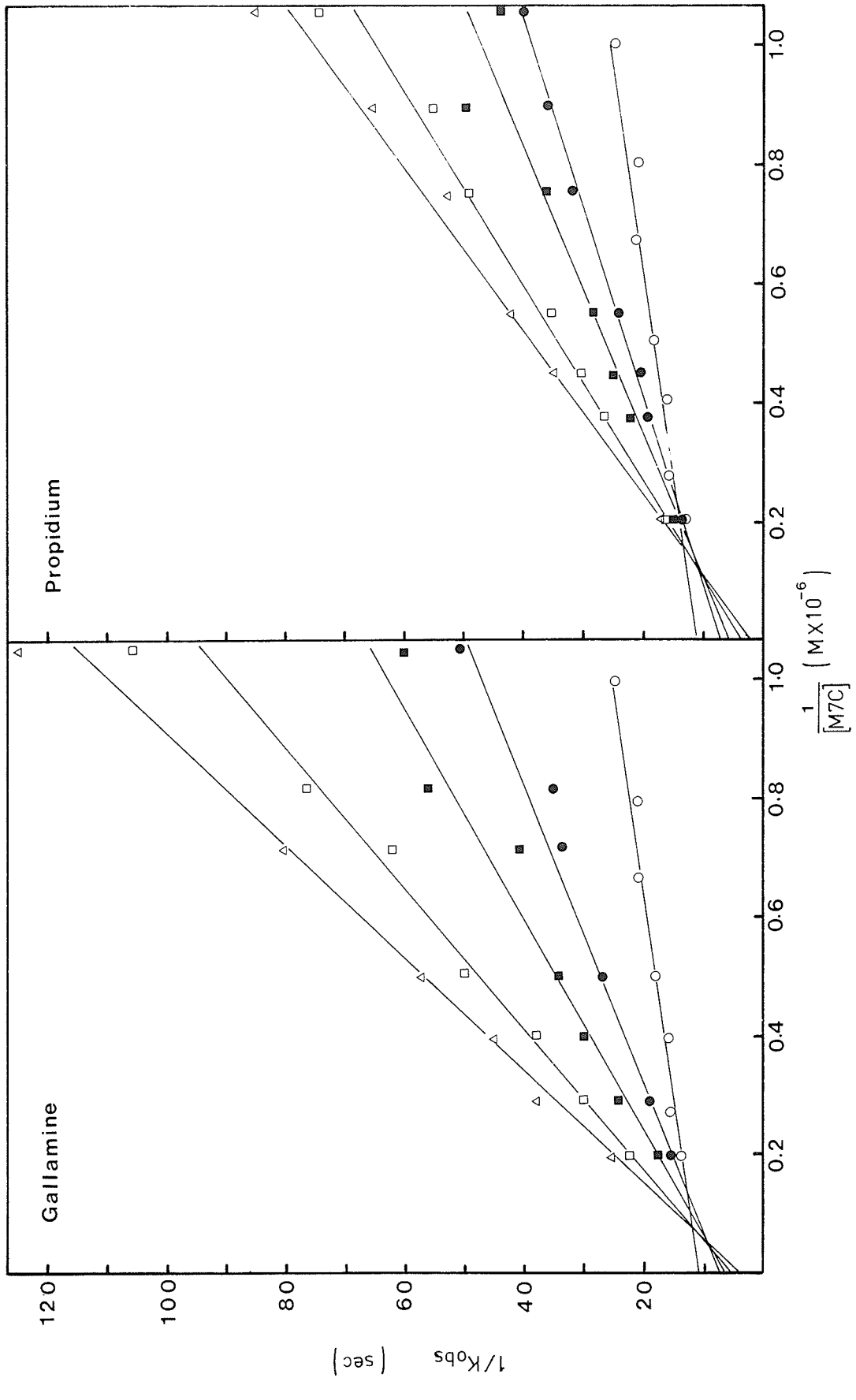
Gallamine
Propidium
120
100
80
60
40
20
0.2
0.4
0.6
0.8
1.0
1/Kobs (sec)
1/[M7C] (MX10⁻⁶)

Fig. 18. Kinetics of carbamoylation of AcChase by M7C and subsequent decarbamoylation of the dimethylcarbamoyl enzyme. (a) Double reciprocal plot of the pseudo-first-order rate constant as a function of M7C concentration. (b) Variation in k_3 with M7C concentration.

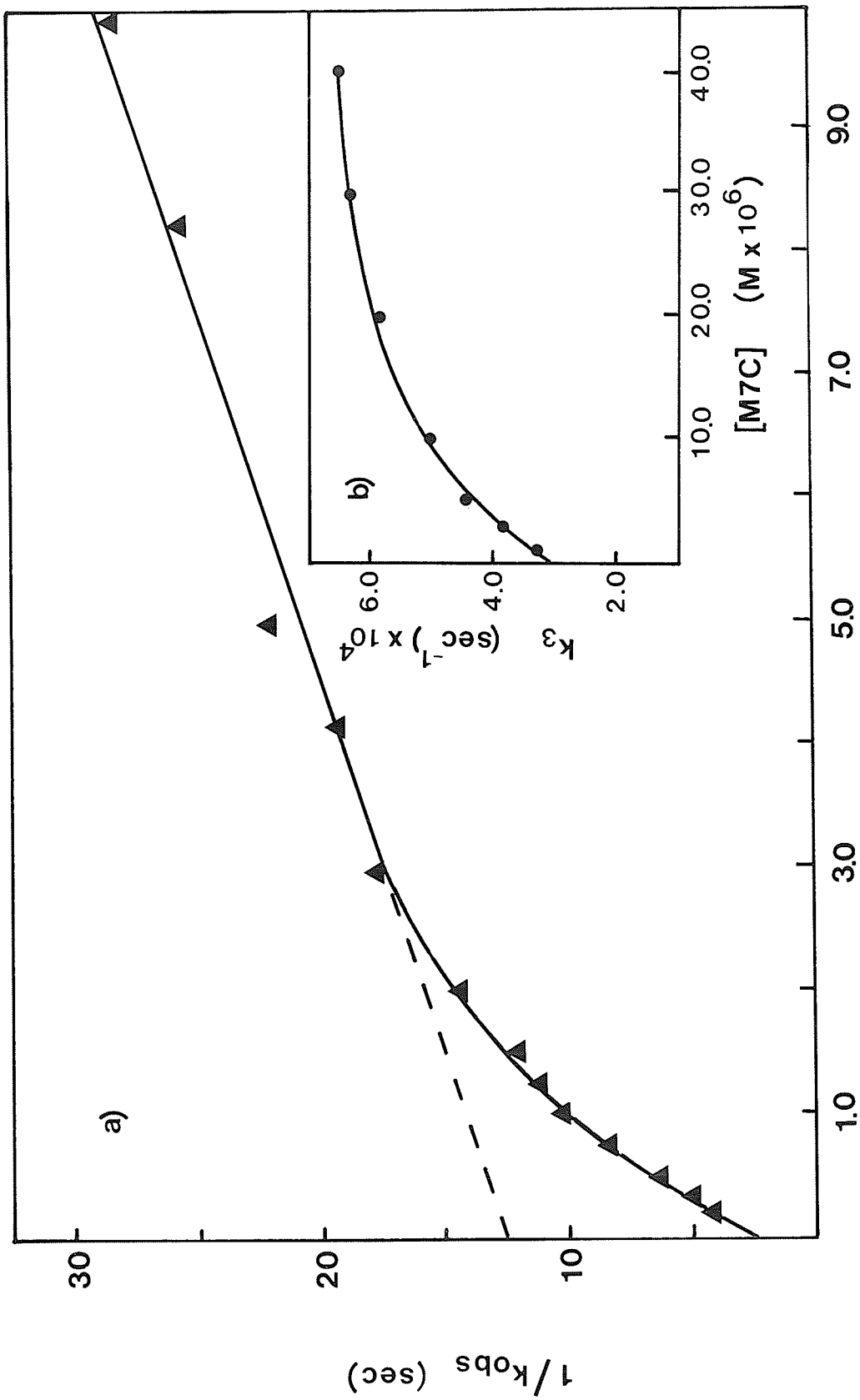
a)
b)
1/kobs (sec)
1 / [M7C] (M⁻¹) x10⁻⁵
[M7C] (M x10⁶)
k3 (sec⁻¹) x 10⁴
30
20
10
1.0
3.0
5.0
7.0
9.0
10.0
20.0
30.0
40.0
6.0
4.0
2.0

rates were not accompanied by any changes in the amplitude of the carbamoylation reaction. The rate of decarbamoylation (k_3) of the dimethylcarbamoyl enzyme was also found to be substrate concentration-dependent; with k_3 increasing from 3.3 x 10^{-4} sec^{-1} at 1 μM M7C to 6.5 x 10^{-4} sec^{-1} at 38 μM M7C (Fig. 18, Table XIII).

In the presence of gallamine, propidium or d-tubocurarine, the carbamoylation rate was found to be inhibited in the substrate range 0.5 to 5 μM. At higher substrate concentrations these ligands appeared to have little influence on the carbamoylation rate (Fig. 19). Again no change in the carbamoylation amplitude was observed at all substrate and peripheral site ligand concentrations with the exception of very high concentrations (∿1 mM) of d-tubocurarine. Na^+, Ca^{2+}, and Mg^{2+} likewise were found not to have an effect on the carbamoylation rate or amplitude (Fig. 20). In all cases, the linear portion of the curves extrapolated to a common intercept, indicating that these species have no effect on the carbamoylation rate constant. The principal effect of metal ion activators was on the decarbamoylation rate constant. It was observed that the effects of Ca^{2+} and M7C on the decarbamoylation rate constant (k_3) were additive and that the carbamoylation rate constant was enhanced by substrate even at high ionic strength (Fig. 20, Table XIII), suggesting that there are distinct binding sites for organic and inorganic activators at the peripheral anionic sites.

TABLE XIII. Influence of effectors on the decarbamoylation rate constant, k_3 following reaction of AcChase with M7C.

Effector	[M7C] μM	k_3 (S^{-1} x 10^4)
None	1.2	3.3
None	24.0	6.2
None	38.3	6.5
$CaCl_2$ (1 mM)	1.2	5.8
$CaCl_2$ (1 mM)	24.0	9.9
$MgSO_4$ (1 mM)	1.2	5.3
$MgSO_4$ (1 mM)	24.0	10.5
Gallamine (5 μM)	1.2	6.6
Gallamine (5 μM)	24.0	6.8
Propidium (5 μM)	1.2	4.4
Propidium (5 μM)	38.3	5.9

Fig. 19. Inhibition of the carbamoylation of AcChase with M7C by propidium and d-tubocurarine. (a) Propidium: (□) none; (●) 1.3×10^{-8} M; (▲) 1.3×10^{-7} M; (■) 1.3×10^{-6} M. (b) d-Tubocurarine; (○) none; (●) 4.0×10^{-5} M; (▲) 2.0×10^{-5} M; (■) 4×10^{-4} M.

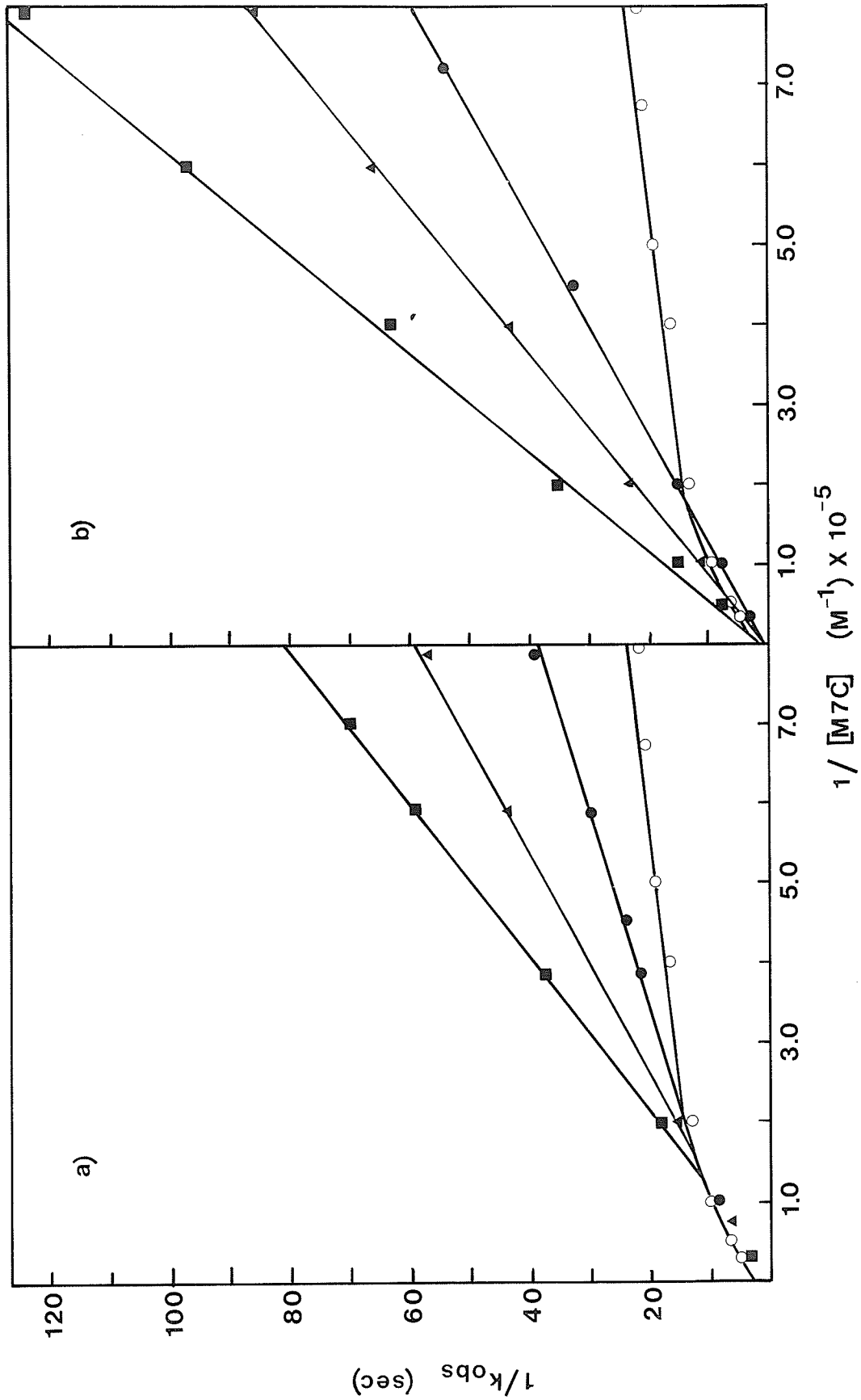
a)
b)
1/kobs (sec)
120
100
80
60
40
20
1.0
3.0
5.0
7.0
1/ [M7C] (M-1) X 10-5

Fig. 20. Kinetics of carbamoylation of AcChase by M7C and subsequent decarbamoylation of the dimethylcarbamoyl enzyme. Double-reciprocal plots of the pseudo-first order rate constant of carbamoylation as a function of M7C concentration. (▲) in 1.0 mM-Tris-Cl, pH 8.0; (●) in 1.0 mM-Tris-Cl/1.0 mM-$CaCl_2$, pH 8.0; (■) in 10 mM-Tris-Cl/0.1 M NaCl, pH 8.0. Inset variation of the decarbamoylation rate constant (k_3) with M7C concentration. (●) in 1.0 mM Tris-Cl, pH 8.0; (■) in 1.0 mM Tris-Cl/1.0 mM $CaCl_2$, pH 8.0.

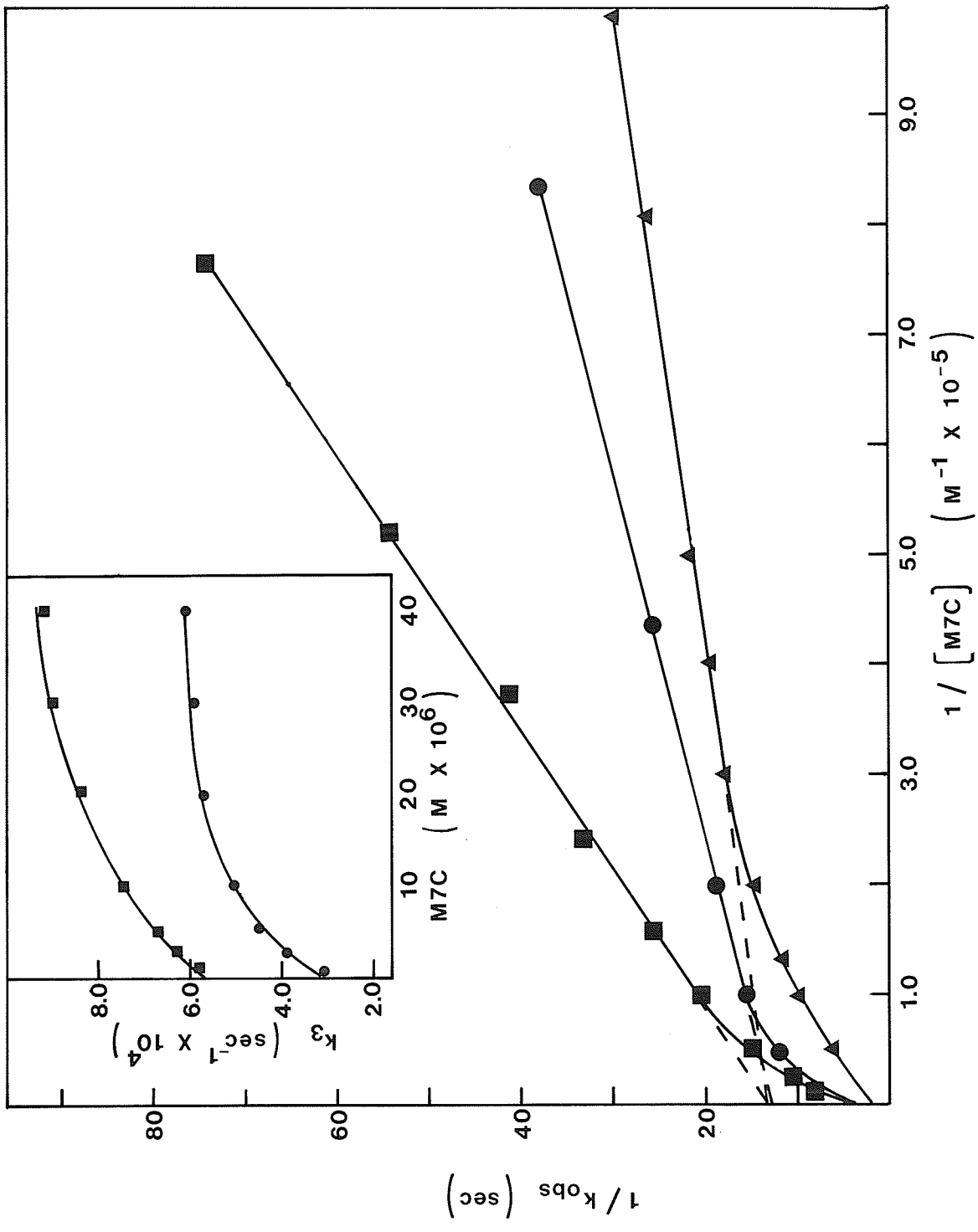
1 / kobs (sec)
20
40
60
80
1.0
3.0
5.0
7.0
9.0
1 / [M7C] (M-1 x 10-5)
k3 (sec-1 x 10^4)
2.0
4.0
6.0
8.0
10
20
30
40
M7C (M x 10^6)

ii) Amplitude effects:

The amplitude of the carbamoylation phase and the rate constant of the decarbamoylation (k_3) were progressively decreased with increasing d-tubocurarine concentrations. This was most readily observed if the enzyme was pre-incubated with the effector for about ten minutes and is apparent even at high M7C concentrations where d-tubocurarine concentrations as high as 1 mM were shown not to have any effect on the carbamoylation rates (Fig. 19). The amplitude decreased in an approximately hyperbolic fashion as the d-tubocurarine concentration was increased and approached a final value which corresponds to about 50% of the initial amplitude at M7C concentrations from 0.5 to 5 μM. However, in the M7C concentration region where activation of k_2 and k_3 are observed (10 to 40 μM), the corresponding d-tubocurarine dependent amplitude decrease is smaller (Fig. 21), thus suggesting a competition between d-tubocurarine and M7C for the peripheral anionic sites.

The decrease in the carbamoylation amplitude was also brought about by incubating the enzyme with the divalent cations Cd^{2+}, Hg^{2+}, Zn^{2+} and Cu^{2+}. The carbamoylation amplitude decreased in an hyperbolic manner with increasing metal ion concentration, and unlike d-tubocurarine the metal ion inactivators were capable of abolishing all of the carbamoylation amplitude. This effect was seen both at low and high ionic strength (Fig. 21).

Apparent K_D values were obtained from the data (Fig. 22):

Fig. 21. Effect of d-tubocurarine on the amplitude of the carbamoylation reaction. Measured by the decrease in the carbamoylation amplitude after reaction with M7C. Concentration of M7C: (●) 1.23×10^{-6} M; (○) 4.91×10^{-6} M; (◆) 9.84×10^{-6} M; (●) 2.46×10^{-5} M. Enzyme concentration 2×10^{-8} N.

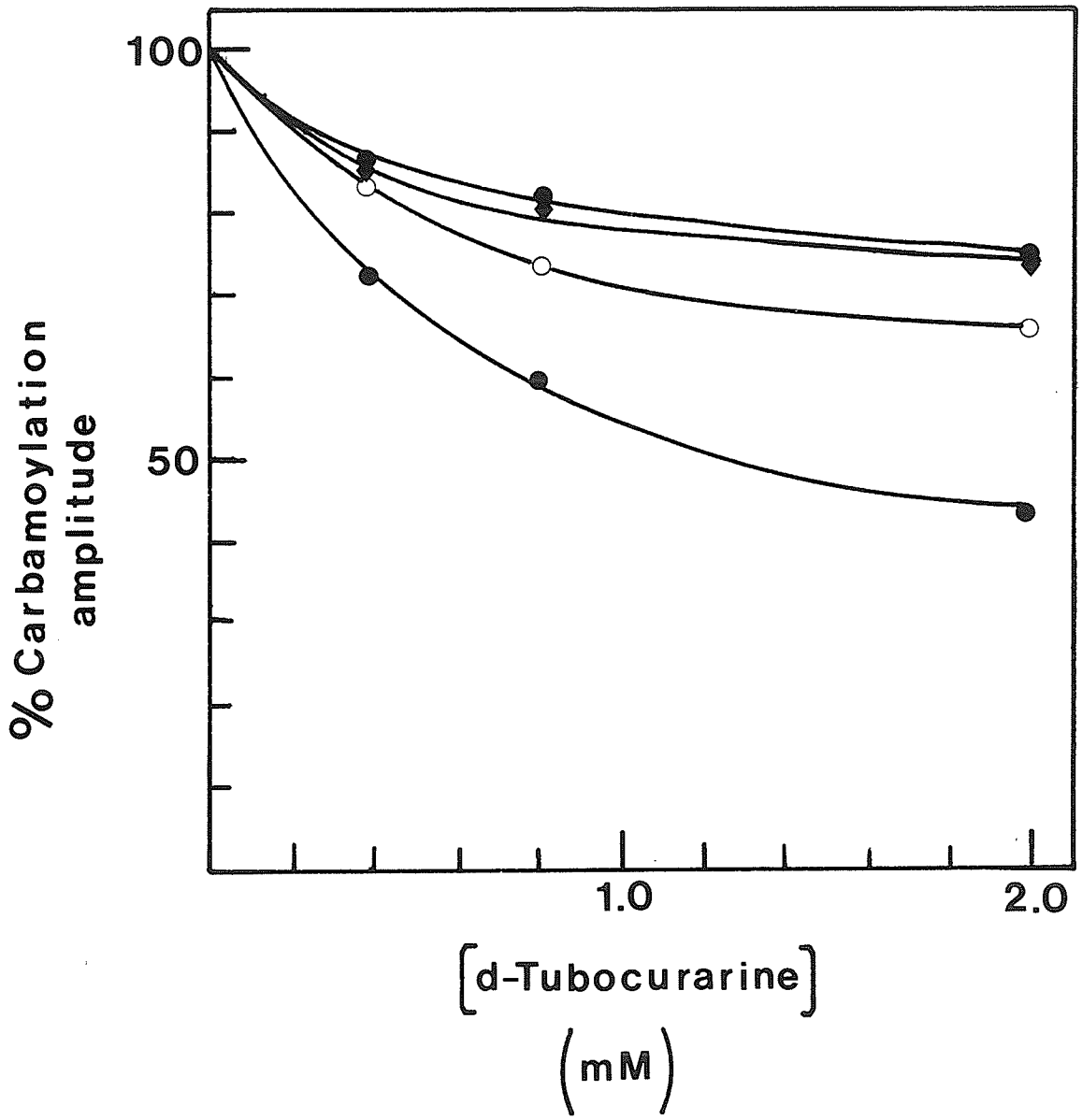
100
50
% Carbamoylation amplitude
1.0
2.0
[d-Tubocurarine]
(mM)

Fig. 22. Inactivation of AcChase by metal ions at low and high ionic strength. Inactivation was determined by three criteria as described in the Materials and Methods section. Selected examples: A & B loss of activity towards hydrolysis of AcSCh (1 x 10^{-4} M), (▲) $ZnSO_4$; (■) $CdCl_2$. C & D, loss of activity towards NPA (9.8 x 10^{-4} M), (▲) $HgCl_2$; (■) $CuSO_4$. E & F decrease in the carbamoylation amplitude after reaction with M7C (1.2 x 10^{-5} M), (▲) $HgCl_2$; (■) $CdSO_4$. Low ionic strength buffer was 1.0 mM-Tris-Cl, pH 8.0; high ionic strength buffer was 10.0 mM-Tris-Cl, pH 8.0. All measurements were made after a 10 min preincubation period in the presence of the inactivators.

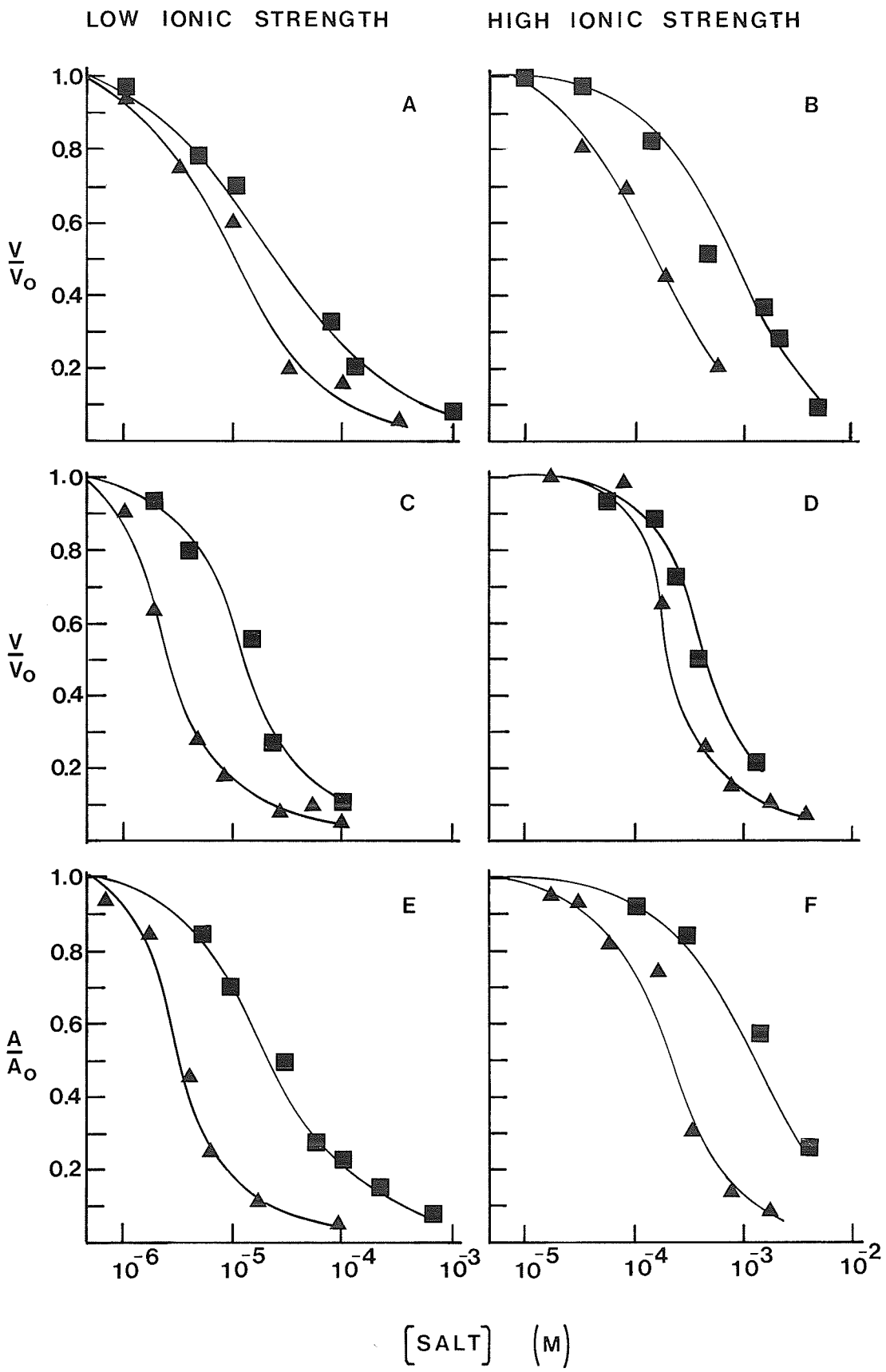
LOW IONIC STRENGTH
HIGH IONIC STRENGTH
A
B
C
D
E
F
V/Vo
A/Ao
1.0
0.8
0.6
0.4
0.2
10-6
10-5
10-4
10-3
10-2
[SALT] (M)

Hg^{2+} appeared to be the most potent inactivator with an apparent K_D at low ionic strength of 5×10^{-6} M and 5×10^{-3} M at high ionic strength. Cd^{2+}, Zn^{2+} and Cu^{2+} appeared to have apparent K_D's at low ionic strength of 3×10^{-5} M, 5×10^{-5} M and 8×10^{-5} M, respectively. Cu^{2+} at high ionic strength had an apparent K_D of 7×10^{-4} M. The effect of Zn^{2+} on carbamoylation amplitude could not be fully tested under conditions of high ionic strength because of the low solubility of its hydroxide.

The effects of inactivating ligands Hg^{2+}, Zn^{2+} was reversed by EDTA. However all of the original activity could not be recovered. This prompted a study of the effects of prolonged incubation of the enzyme with a given inactivator. Prolonged contact of the enzyme with the inactivator resulted in a time-dependent decrease in the amount of recoverable activity (Fig. 23b). If the experiment was repeated under O_2 saturating conditions the irreversible inactivation was more rapid (Fig. 23c), but under saturating N_2, the irreversible inactivation was slower (Fig. 23a).

iii) Lanthanum:

Incubation of La^{3+} with the enzyme resulted in decreased carbamoylation amplitudes both at low and high ionic strength (Fig. 24). Unlike the other inactivating metal ions tested, the concentration range of La^{3+} required for the abolition of all of the carbamoylation amplitude at low ionic strength covered four orders of magnitude (Fig. 24). This anomalous behaviour did not extend to the high ionic strength conditions

Fig. 23. Slow denaturation of AcChase by $ZnSO_4$. Enzyme was incubated with $ZnSO_4$ (8×10^{-5} M) for various time intervals. EDTA (2×10^{-3} M) was then added and the carbamoylation amplitude measured after a further 6 min recovery period. The buffer was 1 mM-Tris-Cl, pH 8.0. Reaction conditions: ( ) N_2-saturation; ( ) air-saturation; ( ) O_2-saturation.

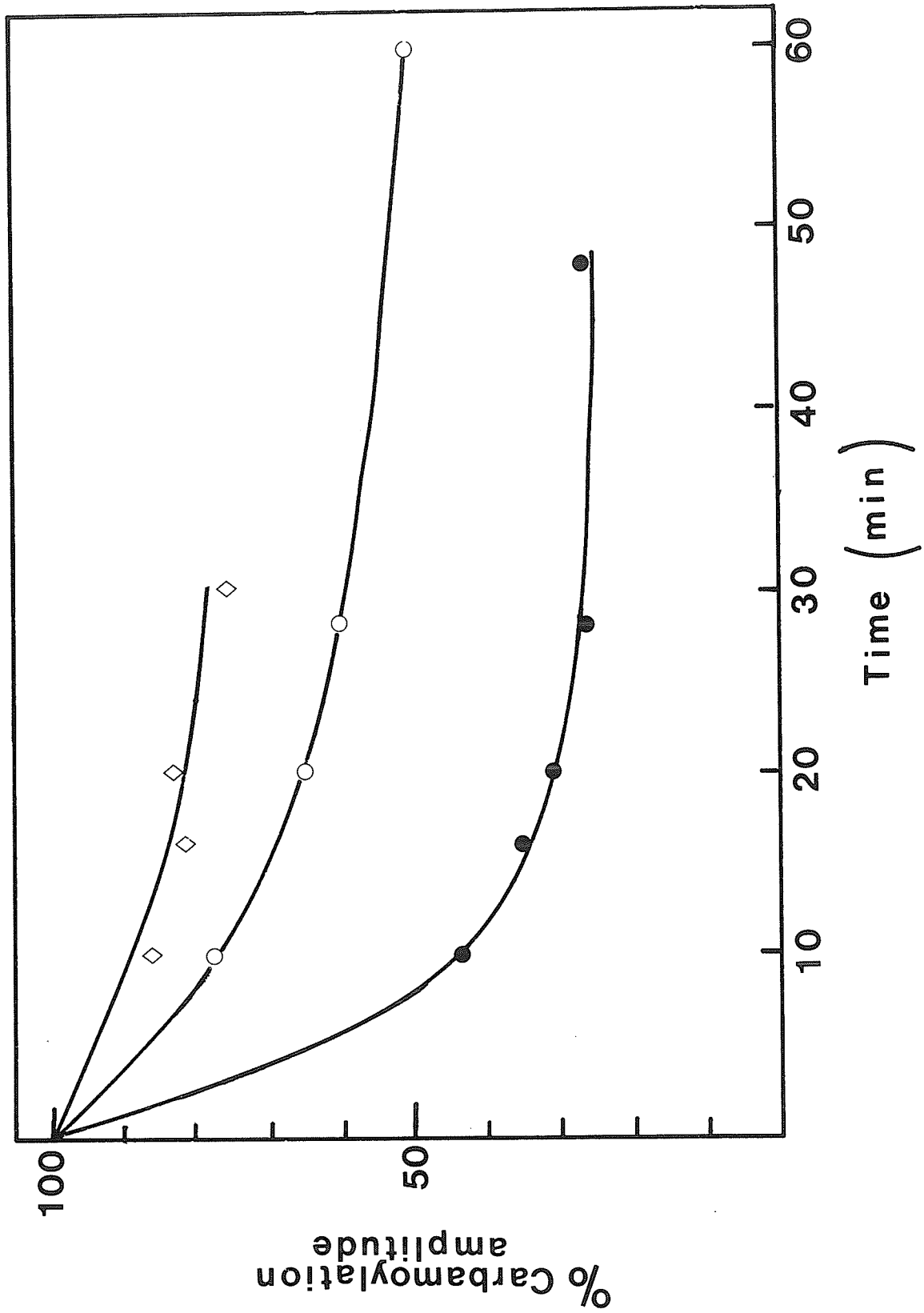
% Carbamoylation amplitude
100
50
10
20
30
40
50
60
Time (min)

Fig. 24. Inactivation of AcChase by La^{3+} at low and high ionic strength. The inactivation was determined by decrease in the carbamoylation amplitude after reaction with M7C (2.5×10^{-5} M). Low ionic strength (●); high ionic strength (○).

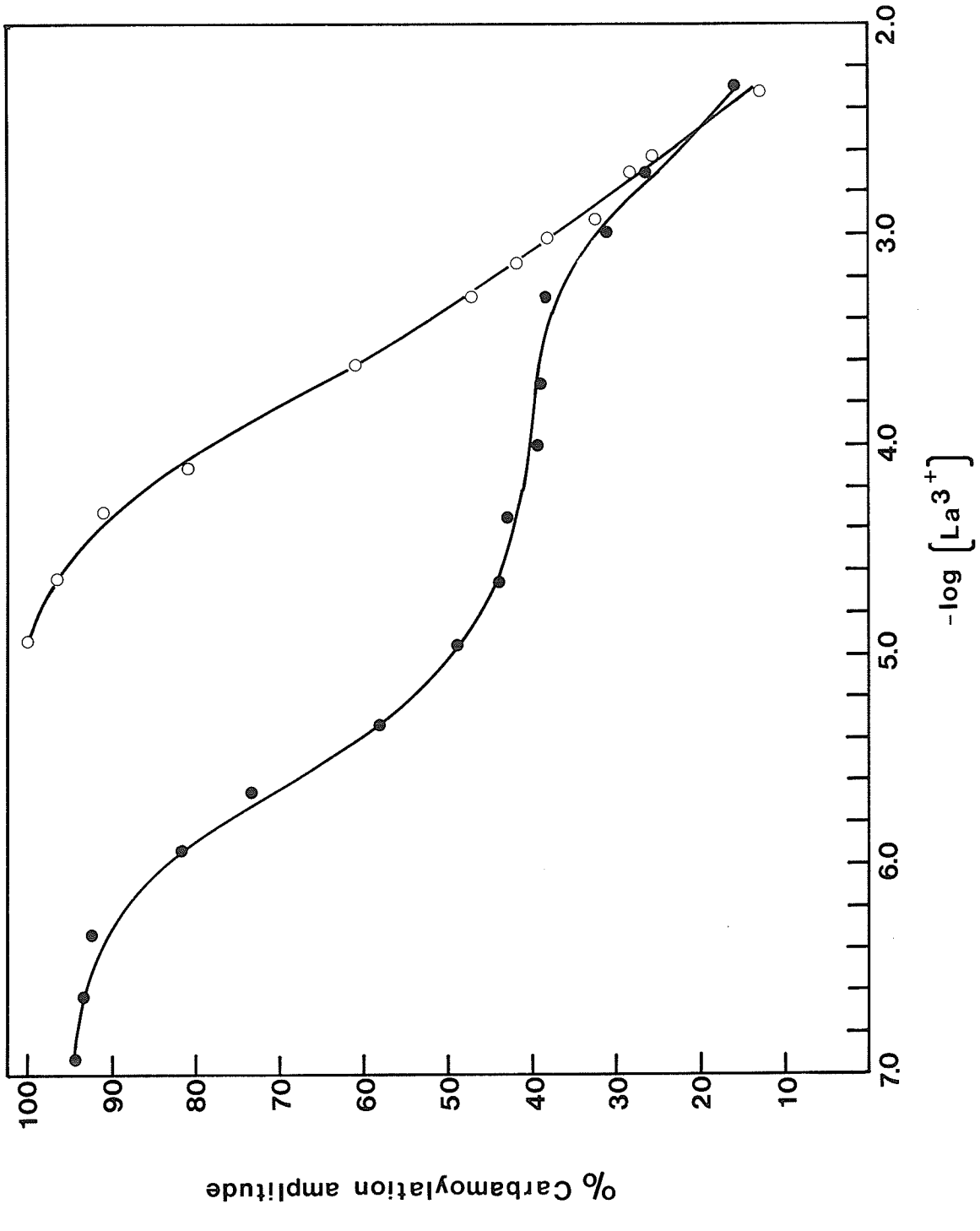
% Carbamoylation amplitude
100
90
80
70
60
50
40
30
20
10
7.0
6.0
5.0
4.0
3.0
2.0
-log [La3+]

where La^{3+} behaved similarly to the other inactivating metal ions. The inactivation was complete within two orders of magnitude (Fig. 24). The apparent K_D of La^{3+} for E. electricus AcChase was 5×10^{-3} M at high ionic strength. One possible explanation for La^{3+} behaving differently from the other divalent inactivating metal ions is that La^{3+} is trivalent and therefore makes a larger contribution to the ionic strength of the solution. This postulate was tested: Hg^{2+} was made equivalent to La^{3+} in ionic strength by the addition of appropriate amounts of NaCl. However, this made no difference to the Hg^{2+} inactivation profile (Fig. 25). Hg^{2+} was still able to "shut off" AcChase within two orders of magnitude of Hg^{2+} concentration and the apparent K_D for Hg^{2+} was unchanged (Fig. 25).

D) Kinetics of conversion to unreactive species:

The inactivation process was studied by two methods. In the first continuous assay, the loss of enzyme activity was followed by monitoring the absorbance at 400 nm due to the enzyme-catalyzed formation of p-nitrophenol. A second discontinuous method involved periodic measurements of the carbamoylation amplitude after addition of M7C to samples of inactivating metal ion-enzyme mixtures. Hg^{2+} proved the best inactivator for these studies since it binds most tightly to the enzyme and allows the inactivation experiment to be carried out under conditions of saturating metal ion concentration, at both low and high ionic strength.

The results obtained with Hg^{2+} are shown in Fig. 26. At

Fig. 25. The effect of ionic strength on Hg^{2+}-induced inactivation of AcChase. Measured by the decrease in the carbamoylation amplitude after a 10 min preincubation with, (●) Hg^{2+}; (○) Hg^{2+} + NaCl (made equivalent in ionic strength to La^{3+}). The buffer was 1.0 mM Tris-Cl, pH 8.0.

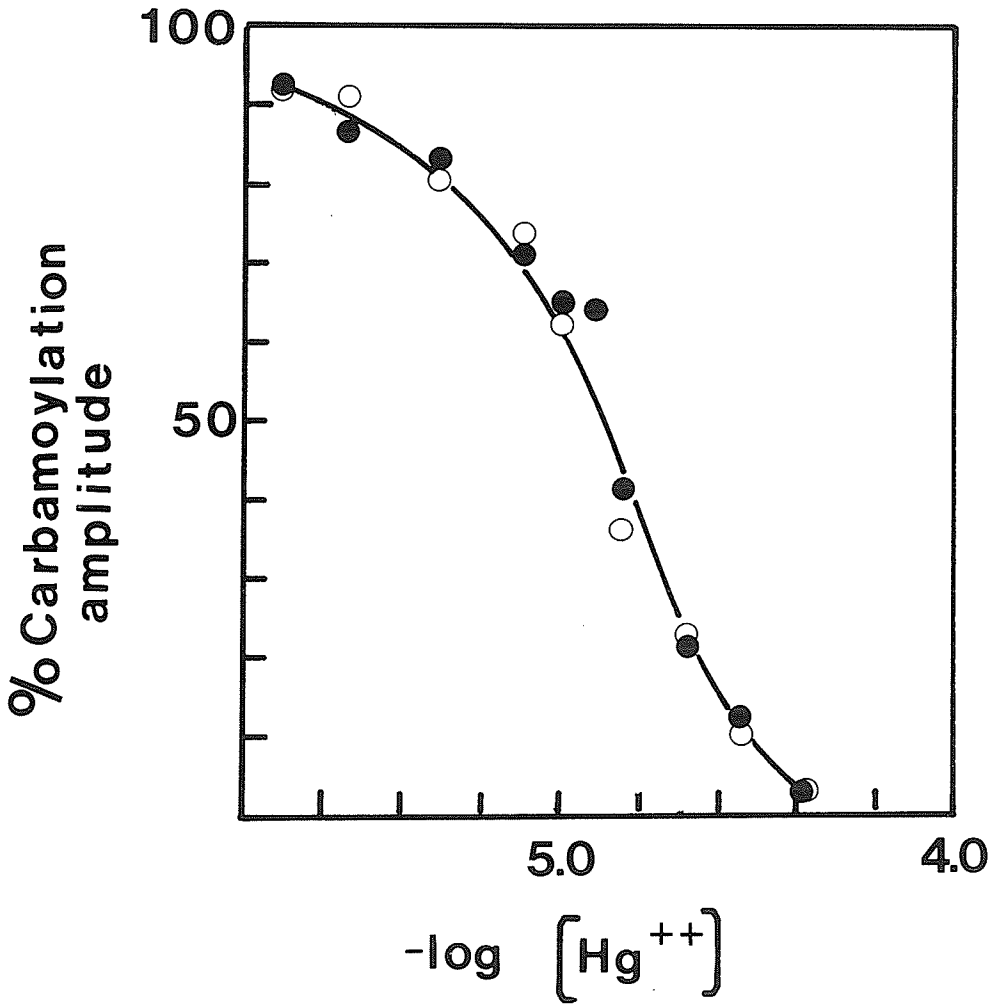
100
50
% Carbamoylation amplitude
5.0
4.0
-log [Hg++]

Fig. 26. Kinetics of inactivation of acetylcholinesterase by $HgCl_2$. A) As measured by loss of activity towards hydrolysis of NPA (2×10^{-4} M), continuous assay; B) As measured by the decrease in carbamoylation amplitude after reaction with M7C (5×10^{-5} M), discontinuous assay. See text for experimental details. In both A & B the symbols represent the following conditions: (●) biphasic time course at low ionic strength (1.0 mM-Tris-Cl/3×10^{-5} M-$HgCl_2$); (○) fast process extracted from the biphasic time course at low ionic strength; (■) monophasic time course at high ionic strength (1.0 mM Tris-Cl/0.1 M-NaCl/1.0 mM-$HgCl_2$). The measured pH of the reaction mixtures was 7.9. The inactivation rates at high ionic strength were too rapid for accurate measurement by method B. Average rate constants (6 determinations) were k_{fast} = $5.2(\pm 1.7) \times 10^{-2}$ s^{-1}; k_{slow} = $4.4(\pm 1.2) \times 10^{-3}$ s^{-1}.

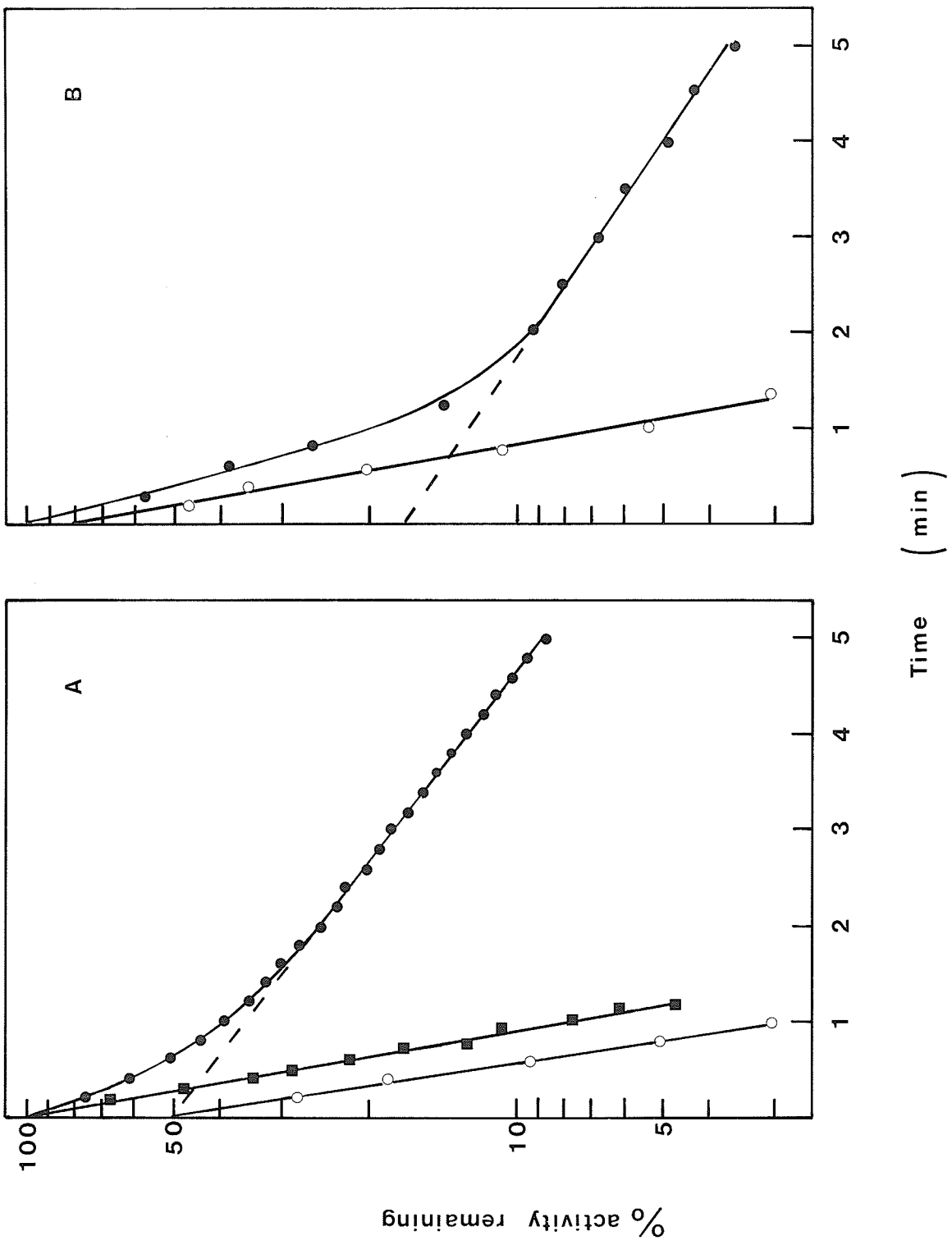
A
B
100
50
10
5
% activity remaining
1
2
3
4
5
Time (min)

low ionic strength the kinetics of inactivation can be resolved into two first order processes characterized by rate constants of 5.2×10^{-2} sec^{-1} and 4.4×10^{-3} sec^{-1}, respectively. The relative amplitudes of the slow and fast phases appear to differ according to the method of assay but the rate constants extracted from the biphasic time courses are virtually identical for either method.

The discontinuous method likely exaggerates the biphasicity somewhat owing to the finite time required for the measurement of the carbamoylation amplitude, thus introducing a considerable degree of uncertainty into the measurements which is most critical for the earliest points on the curve. The points shown have been arbitrarily corrected by adding 10 seconds to the incubation time. At high ionic strength, the inactivation becomes monophasic with a rate constant similar to that of the faster component observed at low ionic strength.

Zn^{2+} and Cd^{2+} resulted in similar biphasic rates of inactivation at low ionic strength. The relative amplitudes of the two components varied according to the metal ion used but the extracted rate constants were independent of the nature of the inactivating ligand.

At high ionic strength, with Zn^{2+} and Cd^{2+}, monophasic kinetics were obtained, but the rate constants were smaller than found with Hg^{2+}, owing to incomplete saturation of the enzyme with these metal ions.

In summary, although the binding characteristics of these metal ions to the enzyme differ, each is capable of inducing

a conformational change in AcChase that results in a kinetically unreactive species.

E) Effect of activators on metal ion inactivation:

The rate of the Zn^{2+}-induced inactivation as measured by the time course of the decrease in the carbamoylation amplitude, was inhibited in the presence of organic and inorganic activators (Mg^{2+}, propidium and gallamine) of AcChase (Fig. 27). These experiments were performed at high M7C concentrations, where peripheral site activators have been shown to have no effect on either the carbamoylation rate or amplitude (Fig. 19).

The inhibition of the Zn^{2+}-induced inactivation rates suggests either a possible overlap of the activator and inactivator sites or that activators can bind at inactivator sites and vice versa. However, these same activating ligands failed to reactivate enzyme which was incubated with Zn^{2+} for 10 minutes prior to the addition of activating ligands, in up to 500 fold excess over the Zn^{2+} concentration (Table XIV). One possible explanation of this result could be a lowering of the affinity for activating ligands, and/or an increase in the affinity for inactivating ligands, of the peripheral anionic sites in the inactivator-induced unreactive conformational state.

4) Experiments with AcChase from the electroplax of T. californica:

A) Pre-steady-state kinetics:

The enzyme isolated and purified from tissue lot #1,

Fig. 27. The effect of propidium and gallamine on the kinetics of Zn^{2+}-induced inactivation of AcChase. As measured by the decrease in the carbamoylation amplitude after reaction with M7C (2.43×10^{-5} M), discontinuous assay, see text for details. Propidium or gallamine added to enzyme ($\sim 2 \times 10^{-8}$ N) in low ionic strength buffer (1 mM Tris-Cl; pH 8.0), prior to the addition of $ZnCl_2$ (8×10^{-5} M). A) Propidium: (◆) none; (○) 9.95×10^{-5} M; (▼) 4.77×10^{-7} M; (△) 9.55×10^{-8} M; (■) 4.77×10^{-8} M. B) Gallamine: (◇) none; (○) 9.5×10^{-6} M; (▲) 9.5×10^{-7} M; (▽) 9.5×10^{-8} M; (△) 4.26×10^{-9} M.

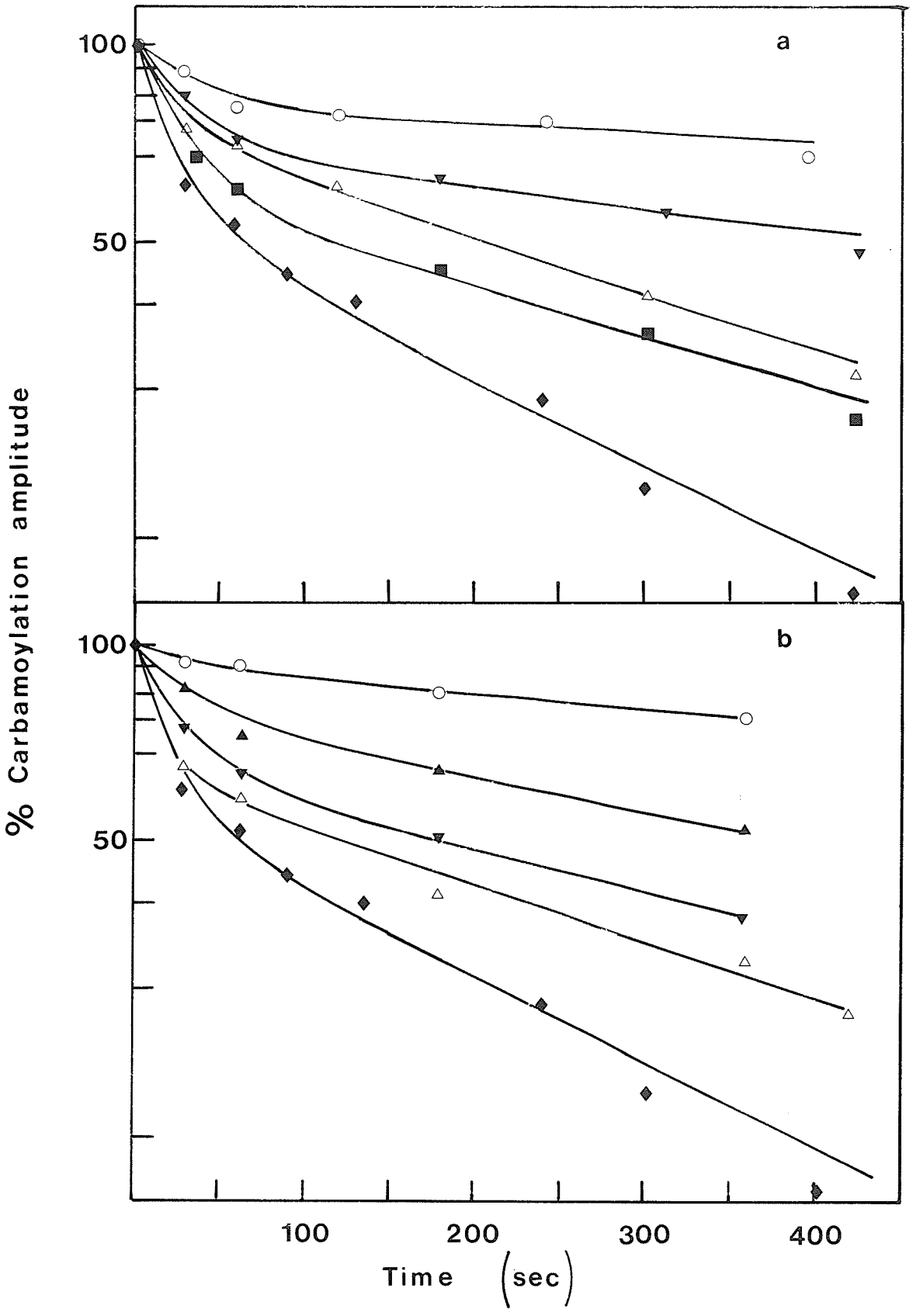
a
b
100
50
100
50
% Carbamoylation amplitude
100
200
300
400
Time (sec)

TABLE XIV. Effect of Mg^{2+} on Zn^{2+} induced decrease in carbamoylation amplitude of E. electricus AcChase.

Experimental Conditions	Relative % carbamoylation amplitude			
	1	2	3	Mean
Enzyme + M7C	100	100	100	100
Enzyme + Mg^{+2} incubated for 10 min; Zn^{+2} added incubated for a further 10 min; then M7C added	93	89	95	92
Enzyme + Zn^{2+} incubated for 10 min; then M7C added	54	62	55	57
Enzyme + Zn^{2+} incubated for 10 min; Mg^{+2} added incubated for a further 10 min; then M7C added	60	69	59	63

$[E] = 2.4 \times 10^{-8}$ N
$[M7C] = 4.7 \times 10^{-6}$ M
$[Mg^{+2}] = 4.82 \times 10^{-3}$ M
$[Zn^{+2}] = 2.41 \times 10^{-5}$ M

displayed biphasic carbamoylation rates at low ionic strength, with the pseudo-substrate M7C; both the observed fast and slow pseudo-first order rates of carbamoylation increased with increasing M7C concentrations (Fig. 28). The fast and the slow rates were extracted from the biphasic time courses. The dependence of the fast pseudo-first order rates of carbamoylation on the M7C concentration was hyperbolic in the substrate concentration range used (0.5 to 10 μM) (Fig. 29), permitting the evaluation of the pre-steady-state kinetic parameters. The values of K_s, k_2 and k_3 were 3.1×10^{-6} M, 0.148 sec^{-1}, 1.4×10^{-4} sec^{-1} (average of three determinations), respectively. The fast carbamoylation amplitude increased as the slow amplitude decreased with increasing M7C concentrations (Table XV). The total (slow and fast) amplitude was constant, suggesting a conversion of the slow enzyme to the fast form with increasing M7C concentrations. The dependance of the slow carbamoylation rates on the M7C concentration was also hyperbolic (Fig. 29). The values of K_s and k_2 obtained from the slow rates were 1.67×10^{-7} M and 5 x 10 sec^{-1}, respectively. The peripheral site activators, propidium or Mg^{2+}, did not effect the fast carbamoylation rate (although propidium inhibited at concentrations > 5×10^{-5} M) but increased the slow carbamoylation rate (Fig. 30) and the fast carbamoylation amplitude, as observed with M7C.

Under high ionic strength conditions the carbamoylation rates appeared to be monophasic and the dependence of the pseudo-first order rate of carbamoylation on the concentration

Fig. 28. Effect of M7C concentration on the kinetics of carbamoylation of "biphasic" T. californica AcChase. The buffer was 1 mM-Tris-Cl, pH 8.0. M7C concentrations: (○) 4.87×10^{-7} M; (▲) 1.21×10^{-6} M; (●) 1.94×10^{-6} M; (▼) 2.43×10^{-6} M; (△) 4.84×10^{-6} M; (◆) 9.71×10^{-6} M.

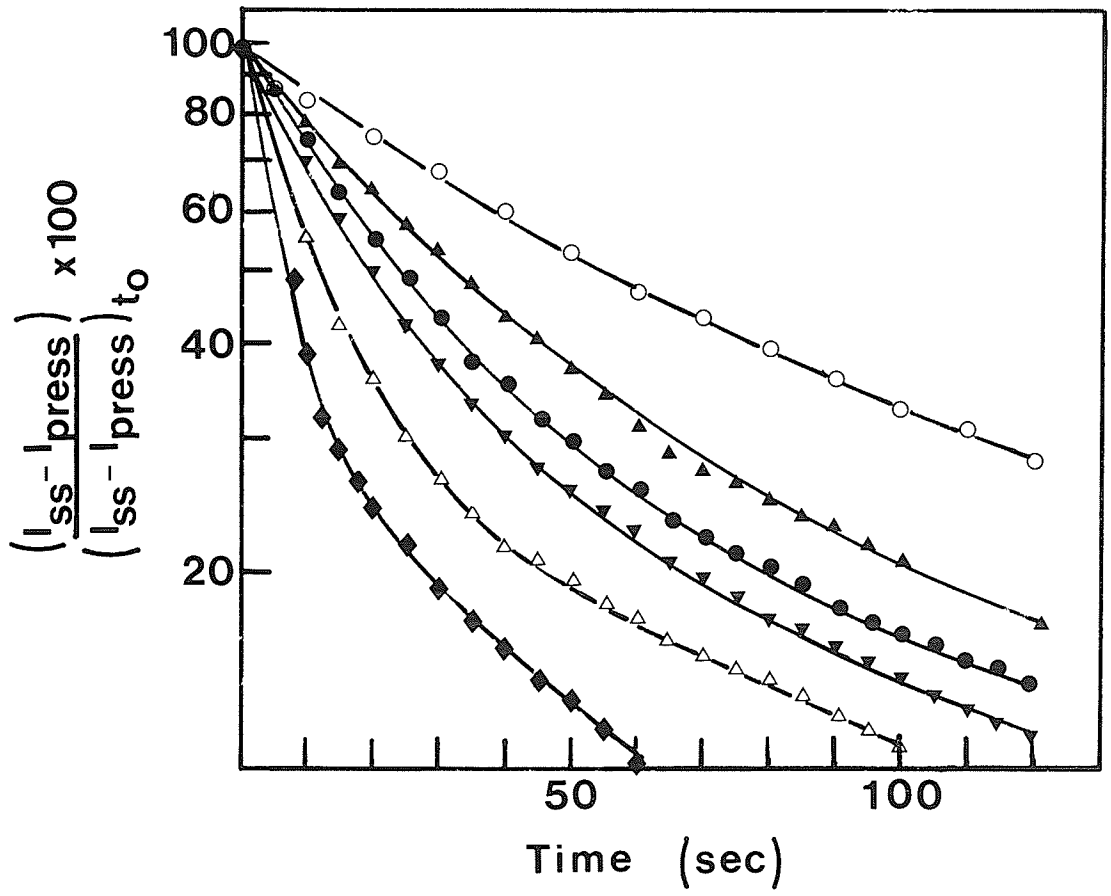
100
80
60
40
20
50
100
Time (sec)
$\left(\frac{I_{ss}-I_{press}}{I_{ss}-I_{press}}\right)_{t_o} \times 100$

TABLE XV. The effect of M7C concentration on the relative slow and fast carbamoylation amplitudes of biphasic *T. californica* AcChase.

[M7C] μM	% Apparent Fast amplitude	% Apparent Slow amplitude
0.487	36	64
1.21	48	52
1.94	62	38
2.43	60	40
4.84	68	32
9.71	70	30

$[E]_0 = 2 \times 10^{-8}$ N

Fig. 29. Kinetics of carbamoylation of "biphasic" *T. californica* by M7C. Double reciprocal plots of the pseudo-first order rate constant of carbamoylation (k_{obs}) as a function of M7C concentration. The buffer was 1 mM Tris-Cl, pH 8.0. (●) the extracted slow rate; (○) the extracted fast rate.

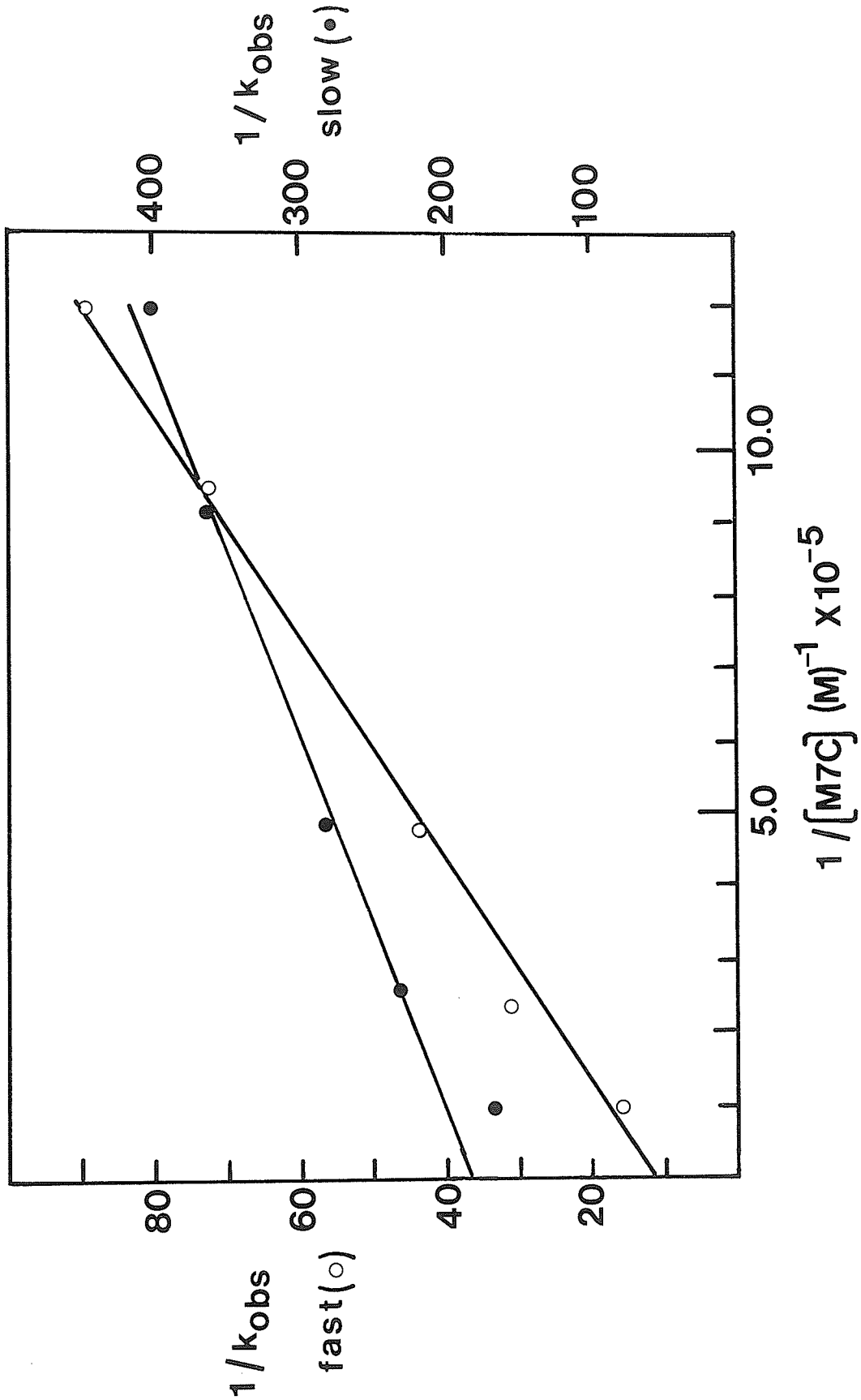
1 / k_{obs} slow (•)
400
300
200
100
80
60
40
20
1 / k_{obs} fast (○)
5.0
10.0
1 / [M7C] $(M)^{-1}$ x 10^{-5}

Fig. 30. The effect of propidium on the biphasic rates of carbamoylation of T. californica AcChase. Pseudo-first order rate constants of carbamoylation with M7C (5.23 x 10^{-6} M) at various concentrations of propidium: (●) 3.6 x 10^{-7} M; (○) 7.2 x 10^{-7} M; (■) 1.79 x 10^{-6} M; (△) 3.6 x 10^{-6} M. The buffer was 1 mM-Tris-Cl, pH 8.0.

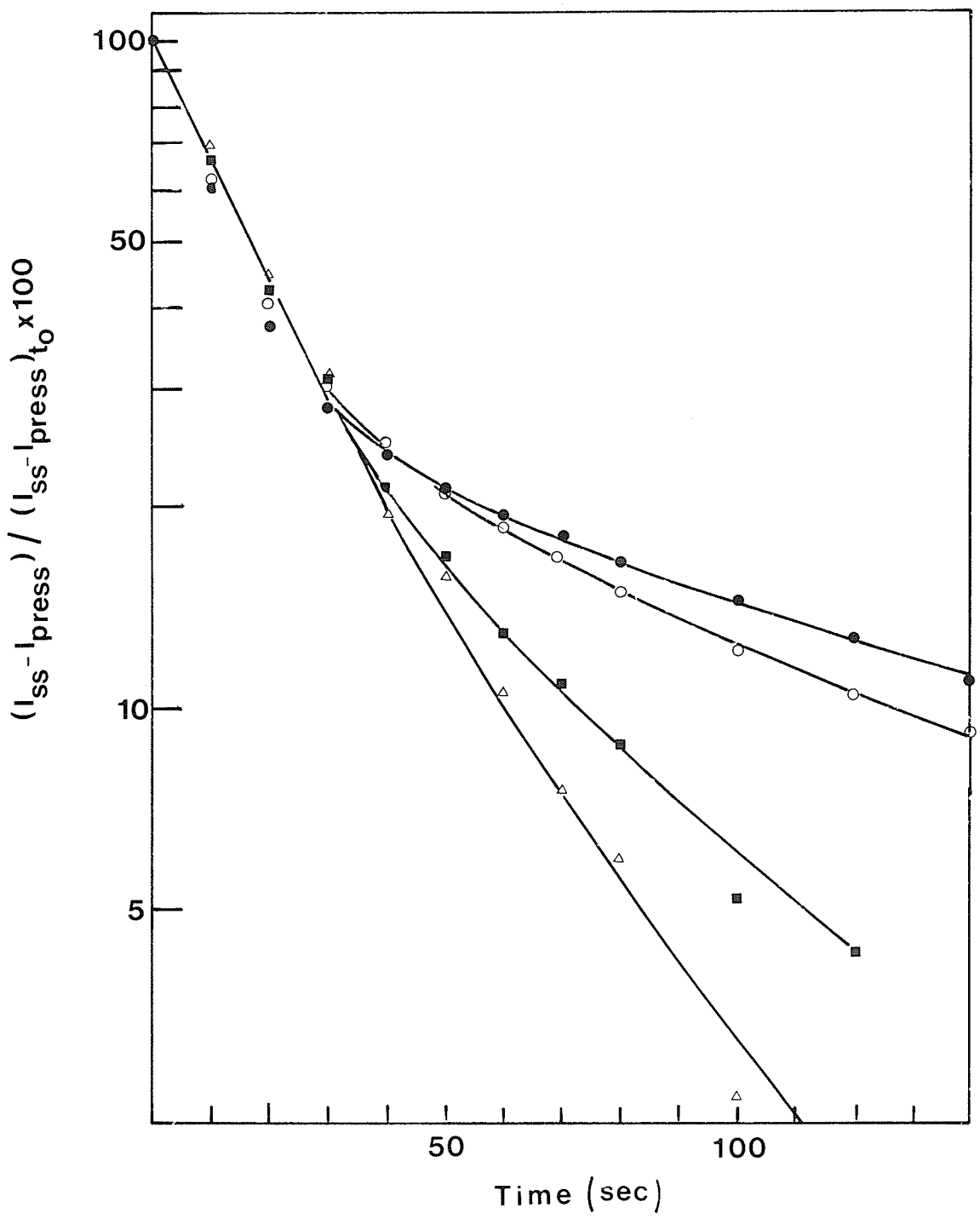
100
50
10
5
50
100
Time (sec)
$(I_{ss}-I_{press}) / (I_{ss}-I_{press})_{t_o} \times 100$

of M7C was hyperbolic and was inhibited by propidium (Fig. 31). The values of K_s, k_2 and k_3 obtained were 35.1 x 10^{-6} M, 0.23 sec^{-1} and 3.2 x 10^{-4} sec^{-1}, respectively and were in very close correspondence with previously published values (130).

The effect of Zn^{2+} and d-tubocurarine on the carbamoylation amplitude was studied. Both Zn^{2+} and d-tubocurarine were shown to decrease the carbamoylation amplitude in a hyperbolic manner upon 10 minutes preincubation with the enzyme. Both ligands abolished all of the carbamoylation amplitude and the inactivation profile for Zn^{2+} (concentration of Zn^{2+} vs % carbamoylation amplitude) was independent of ionic strength, suggesting that in T. californica AcChase the peripheral anionic inactivator sites are not altered by ionic strength-dependent conformational changes in the enzyme (Fig. 32).

i) Monophasic enzyme:

Subsequent isolation and purification of AcChase from tissue lots #2 and #3 resulted in an enzyme preparation that no longer displayed biphasic carbamoylation rates at low ionic strength. In view of these results attempts were made to "induce" biphasicity in the carbamoylation rates by controlling isolation and reaction conditions.

A summary of the various experiments that were attempted is given in Table XVI . Although no biphasicity could be induced to the carbamoylation rates, an interesting observation was that the incubation of AcChase with DTNB for 11 hrs resulted in a 30% loss in the carbamoylation amplitude, suggesting the possible modification of AcChase by this thiol-specific reagent.

Fig. 31. Kinetics of carbamoylation of "biphasic" *T. californica* AcChase by M7C at high ionic strength. Double reciprocal plots of the pseudo-first order rate constant of carbamoylation (k_{obs}) as a function of M7C concentration. (○) in 1.0 mM-Tris-Cl/0.1 M-NaCl, pH 8.0; (●) in 1.0 mM-Tris-Cl/0.1 M-NaCl/1.0 x 10^{-6} M propidium, pH 8.0.

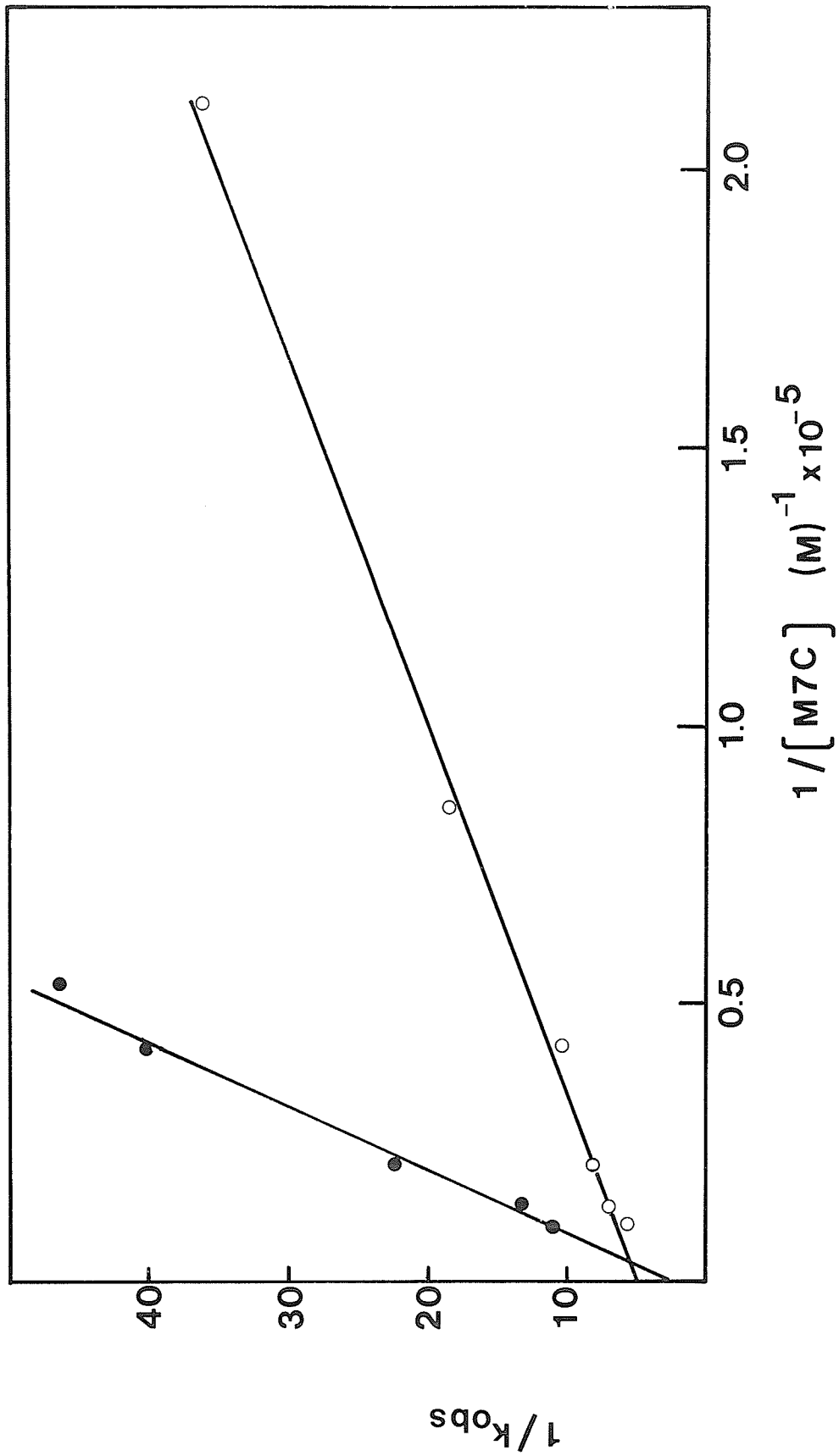
40
30
20
10
1/kobs
0.5
1.0
1.5
2.0
1/[M7C] (M)$^{-1}$ x10^{-5}

Fig. 32. Inactivation of "biphasic" T. californica AcChase by $ZnCl_2$ at low and high ionic strength. Measured by the decrease in the carbamoylation amplitude after reaction with M7C (2.53×10^{-5} M). (○) low ionic strength (1 mM-Tris-Cl, pH 8.0); (●) high ionic strength (1 mM-Tris-Cl/0.1 M-NaCl, pH 8.0).

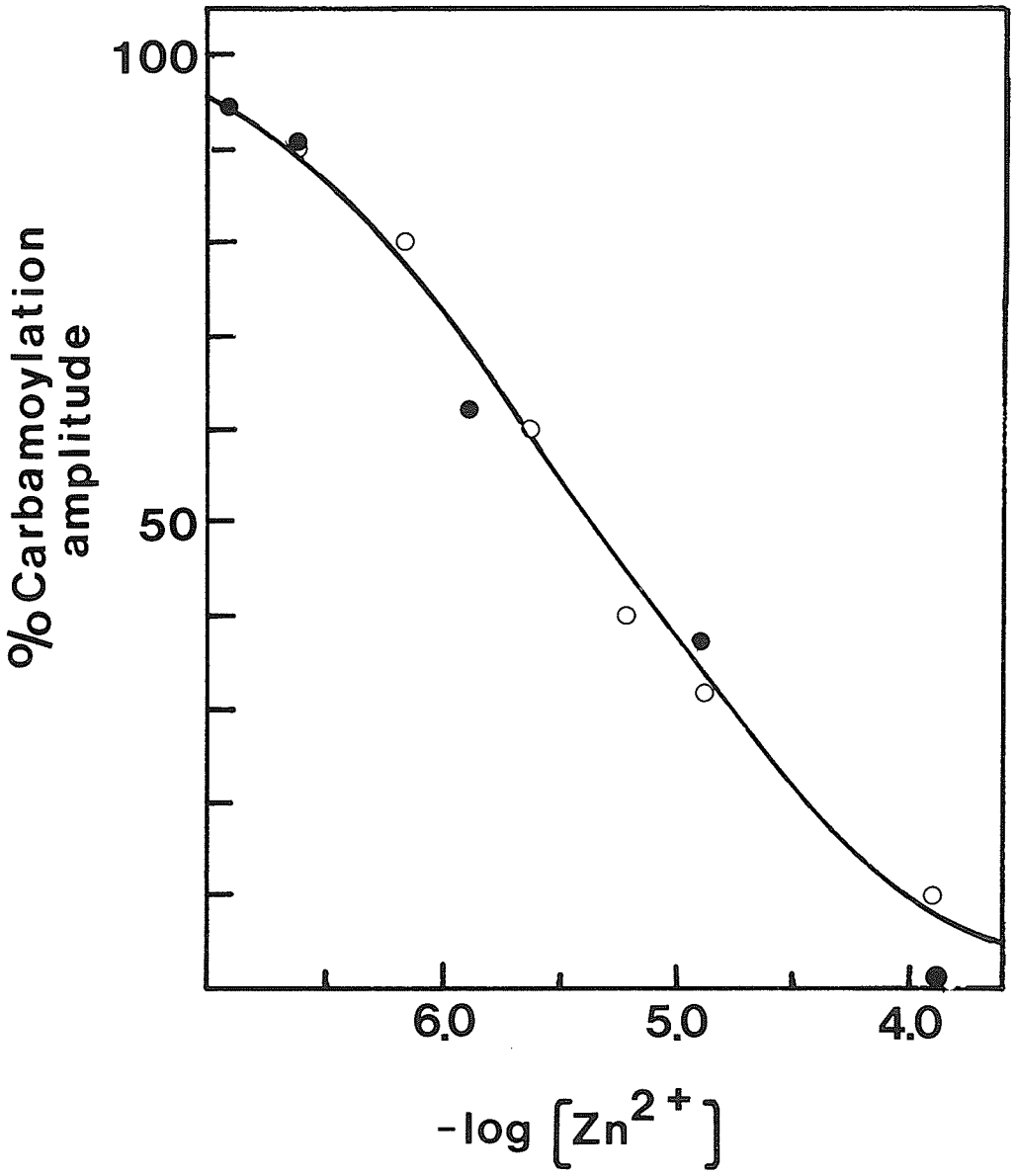
100
50
% Carbamoylation amplitude
6.0
5.0
4.0
-log [Zn2+]

TABLE XVI. Experiments to induce biphasicity to monophasic T. californica AcChase.

Experiment	Conditions	Results	Comments
[a]Enzyme + SDS	SDS (1.6×10^{-4} M) incubated with enzyme for 4 hrs.	∿25% of carbamoylation amplitude lost, but no biphasicity in carbamoylation.	Partial denaturation does not induce biphasicity.
Enzyme + Trypsin	Trypsin (4×10^{-7} M) incubated with the enzyme at 25°C aliquots removed and assayed at various time intervals.	Progressive decrease in carbamoylation amplitude but no biphasicity apparent in carbamoylation rates.	Proteolysis under these conditions does not induce biphasicity.
Enzyme + DTNB	DTNB (10^{-3} M) incubated	30% of the carbamoylation lost after 10 hrs; no apparent biphasicity in the carbamoylation rates.	Possible modification of the enzyme with DTNB.
Enzyme + DMB	DMB concentrations used 2.5×10^{-8} M; 4.82×10^{-8} M; 1×10^{-7} M.	Carbamoylation rates inhibited but no biphasicity.	Biphasicity cannot be due to possible DMB contamination.
Enzyme + DTT	DTT (6.5×10^{-2} M) incubated with enzyme aliquots removed at various time intervals.	Gradual decrease in the carbamoylation amplitude; 35% in 12 hrs no biphasicity.	
Enzyme left at 25°C	Aliquots removed at different time intervals and assayed.	Carbamoylation amplitude unchanged upon 12 hr incubation at 25°C.	

[a] $[E] = 5.35 \times 10^{-7}$ M stock solution; ∿2×10^{-8} M in assay.

B) Steady-state kinetics (monophasic enzyme):

The concentration of T. californica AcChase used in the steady-state kinetic studies was approximately 10^{-11} M. At this concentration the enzyme was found to be unstable, and ∿15% of the activity was lost within 30 minutes (Fig. 33). To minimize the denaturation at low enzyme concentrations, stock enzyme (2×10^{-7} M), which has been shown to be very stable (Fig. 4), was freshly diluted for each substrate concentration used. As a result there was no detectable decrease in the initial rate values within the time required to obtain quadruplicate determinations at a particular substrate concentration. Incubation of the enzyme (10^{-11} M) with DTNB was observed to increase the time-dependent inactivation; at the end of 30 minutes the rate was decreased by 37% (Fig. 33) in comparison to the control experiment which only lost ∿15% of the initial activity (Fig. 33).

The kinetics of the hydrolysis of AcSCh (1 to 50 μM) at low ionic strength displayed Henri-Michaelis-Menten behaviour. The values of K_{app} and k_c obtained from the linear portion of the double reciprocal plots (Fig. 34) were 1.18×10^{-5} M and 3.14×10^{4} min^{-1}, respectively. Above 50 μM the double reciprocal plots displayed downward curvature, this result being reminiscent of E. electricus steady-state kinetics obtained at an intermediate ionic strength (0.025 M, Fig. 8). It might be explained by either two pre-existent kinetic forms of the enzyme, (low K_{app} and high K_{app} forms, the latter becoming activated at high substrate concentrations) or by substrate

Fig. 33. Time-dependant loss of activity of "monophasic" T. californica AcChase. (△) enzyme (1.0×10^{-11} N) incubated for various time intervals in low ionic strength buffer, 25°C (1 mM-Tris-Cl, pH 8.0); (▲) enzyme (1.0×10^{-11} N) incubated for various time intervals in low ionic strength buffer + DTNB (1.0 mM-Tris-Cl/6.45×10^{-4} M DTNB, pH 8.0). Initial velocities were determined by the addition of AcSCh (1×10^{-4} M).

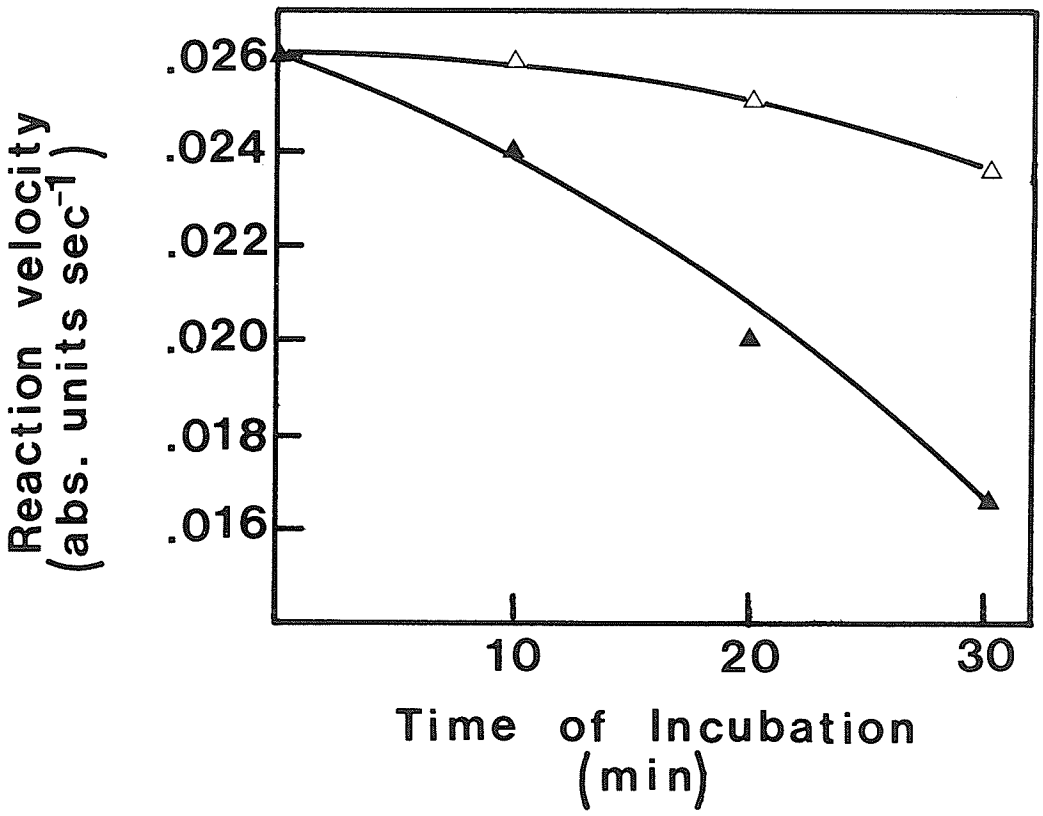
Reaction velocity
(abs. units sec^{-1})
.026
.024
.022
.020
.018
.016
10
20
30
Time of Incubation
(min)

Fig. 34. Kinetics of acetylcholine hydrolysis of "monophasic" T. californica AcChase at low and high ionic strength. Initial velocities were determined using the stopped-flow apparatus as described in the Materials and Methods Section. (●) low ionic strength (1.0 mM-Tris-Cl, pH 8.0); (○) high ionic strength (1.0 mM-Tris-Cl/0.1 M-NaCl, pH 8.0). The concentration of the enzyme was 3.56×10^{-10} N.

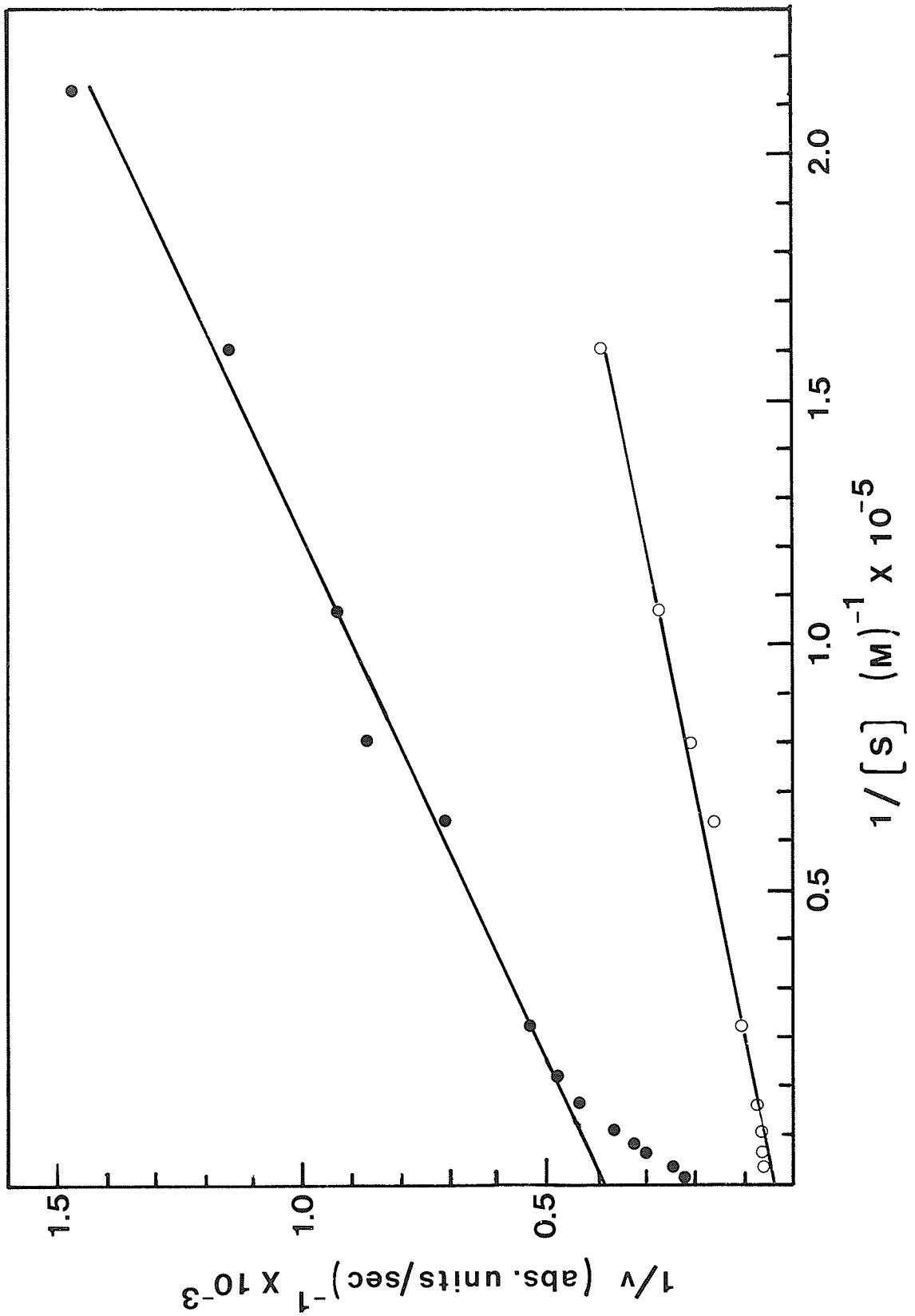
1.5
1.0
0.5
1/v (abs. units/sec)$^{-1}$ X 10^{-3}
0.5
1.0
1.5
2.0
1/[S] (M)$^{-1}$ X 10^{-5}

activation. However under steady-state conditions it is not possible to distinguish between these two possibilities.

5) The kinetics of iPr_2PF inactivation of AcChase:

The inactivation kinetics were studied by two methods. A continuous assay where the loss in enzyme activity was followed by monitoring the absorbance at 400 nm due to enzyme-catalyzed hydrolysis of NPA to form p-nitrophenol. A second discontinuous method involved the measurement of enzyme activity after addition of NPA to samples of iPr_2PF-enzyme mixtures.

The inactivation by iPr_2PF followed by either method of assay produced linear pseudo-first order inactivation plots in the case of the E. electricus and monophasic T. californica AcChases (Fig. 35). However, the biphasic T. californica AcChase that displayed biphasic carbamoylation rates, produced non-linear iPr_2PF inactivation profiles. The second order rate constants of iPr_2PF inactivation of E. electricus AcChase under a variety of conditions are summarized in Table XVII . The second order rate constant was ($\sim$1.45 fold) higher at high ionic strength than at low, in accord with the general trend observed in hydrolysis rates (AcSCh, M7C) and in the rates of inhibition (Zn^{2+}, Cu^{2+}, Hg^{2+}, etc.). Mg^{2+}, at low ionic strength, did not effect the iPr_2PF inactivation rates, however, very low concentrations of propidium (3.71×10^{-8} M) lowered the rates by approximately 1.5 fold.

Fig. 35. Kinetics of [iPr_2PF] inactivation of AcChase. Measured by the discontinuous method see Materials and Methods for details. (a) "biphasic" T. californica AcChase, [iPr_2PF] = 2.87×10^{-4} M; (b) "monophasic" T. californica AcChase, [iPr_2PF] = 1.02×10^{-2} M; (c) E. electricus AcChase [iPr_2PF] = 9.64×10^{-5} M. The enzyme concentration was $\sim 8 \times 10^{-9}$ N.

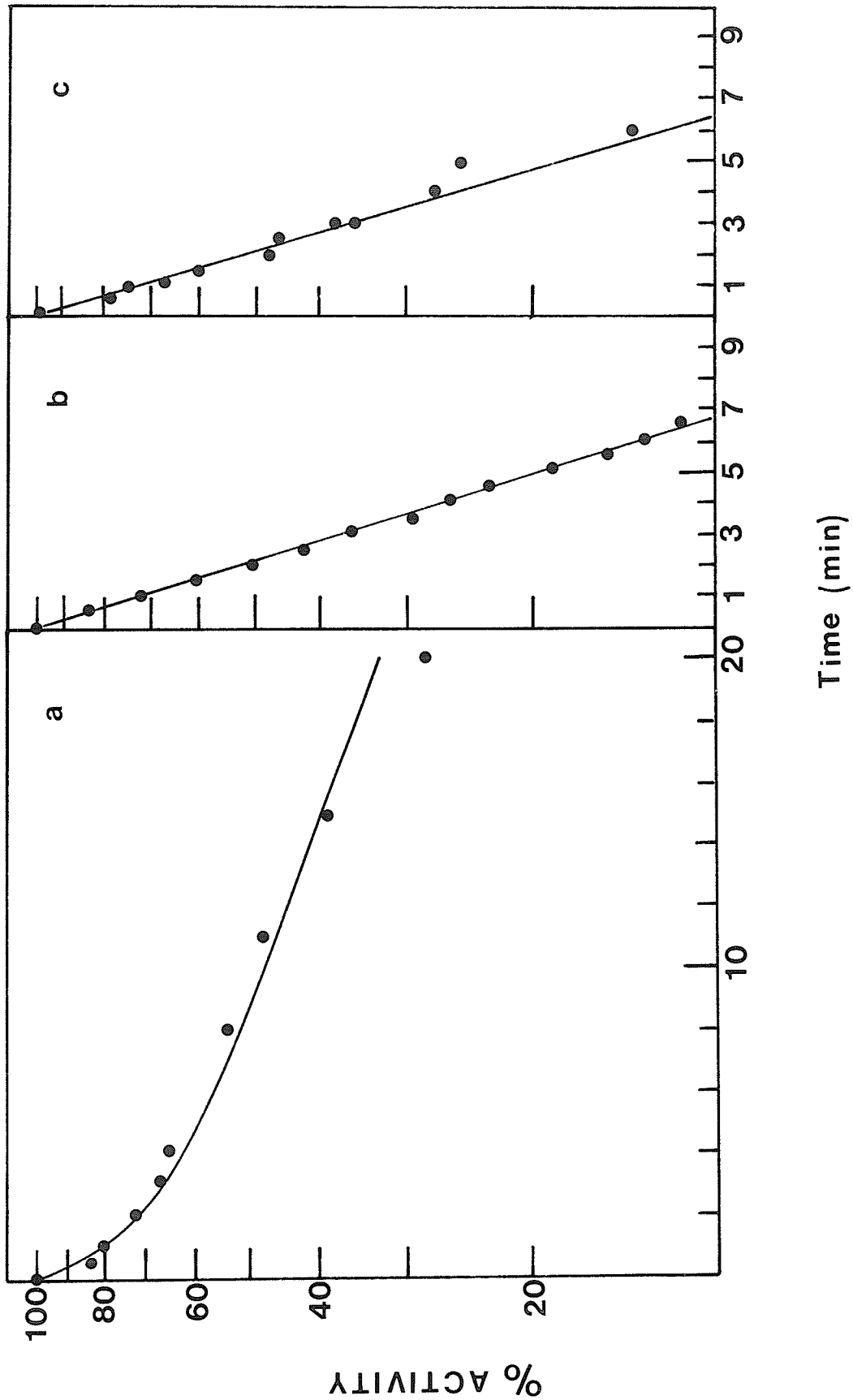
% ACTIVITY
100
80
60
40
20
a
10
b
20
1
3
5
7
9
c
1
3
5
7
9
Time (min)

TABLE XVII. Rate constants of the iPr_2PF inactivation of *E. electricus* AcChase.

Method[b]	$[iPr_2PF]$ M x 10^{-5}	k (M^{-1} sec^{-1} x 10^{-2})[a]
HIGH IONIC STRENGTH (Tris-Cl (10 mM/0.1 m NaCl) pH 8.0)		
Rapid sampling	3.75	2.21 ± .48
Continuous	7.08	1.74 ± .06
LOW IONIC STRENGTH (Tris-Cl (1 mM) pH 8.0)		
Rapid sampling	3.75	1.20 ± .30
Continuous	4.62	1.22 ± .17
Continuous + Propidium (3.71×10^{-8} M)	4.62	0.81 ± .02
Continuous + Mg^{2+} (3.3×10^{-4} M)	4.62	1.11 ± .17

[a] Average of 4 runs.
[b] p-nitrophenyl acetate was used as the substrate. [NPA] = 2×10^{-4} M. [E] = 10^{-10} N.

6) Chemical modification of Acetylcholinesterase:

A) DTNB:

Attempts were made to determine the free thiol content of AcChase from T. californica and E. electricus, using DTNB. The reaction with DTNB was performed under denaturating conditions (1% SDS; 0.1 M Tris-Cl; pH 8.0) with enzyme concentrations of 1-2 x 10^{-6} N. Both T. californica and E. electricus AcChases were reactive towards DTNB under these conditions, although the amount of thionitrobenzoate anion (equal to the free thiol concentration) was quite variable (Table XVIII). This is thought to arise from inaccuracies in measuring small absorbance values (.02-.05), and the autooxidation of the enzymic thiol groups (prior to the addition of DTNB) and/or the thionitrobenzoate anion. In view of these results, a more sensitive assay of thiol content was sought.

B) N-Dansylaziridine:

The fluorescent, thiol-specific reagent N-dansylaziridine (N-DAZ) was first introduced by Scouten et al. (162). N-DAZ has an excitation maximum of 345 nm and an emission maximum of 565 nm. Upon reacting with free protein-thiol groups the apparent emission maximum is blue shifted by approximately 10-15 nm and the fluorescence intensity is enhanced. The free thiol groups in the protein are thought to react with the aziridinyl portion of N-DAZ to yield dansyl-S-aminoethylcysteinyl-protein. The covalently linked dansyl moiety has an excitation maximum of 345 nm with an emission maximum of 495 nm (162).

TABLE XVIII. Titration of free thiol groups in AcChase under denaturating conditions.[a]

	Moles of NBS^- [b]	mol SH/mol enzyme
T. californica (4.45×10^{-7} M)		
Trial 1	1.86×10^{-6}	4.78
Trial 2	1.25×10^{-6}	2.81
E. electricus (2.87×10^{-7} M)		
Trial 1	2.2×10^{-6}	7.6
Trial 2	1.2×10^{-6}	4.2

[a] 1% SDS in 0.1M Tris-Cl pH 8.0.
[b] $\varepsilon_{M(412)} = 13600$.

i) T. californica AcChase (monophasic):

Introduction of N-dansylaziridine to enzyme (2.5×10^{-7} M; in low ionic strength; pH 8.0) resulted in a time dependant shift and enhancement of the N-DAZ emission maximum (Fig. 36). The reaction was extremely slow, requiring ∿17 hrs for completion (at 25°C). The enzyme so modified retained ∿90% of its activity (as measured by the carbamoylation amplitude resulting from the pre-steady-state "burst" upon addition of M7C).

Subsequently, the modification with N-DAZ was performed under a variety of conditions (Fig. 37): The fluorescence spectrum of the reagent (N-DAZ) in the absence of enzyme remained unchanged over a period of 17 hrs (at 25°C), in the presence or absence of a variety of peripheral-site ligands (Fig. 37B). The reaction of N-DAZ with AcChase appeared to be inhibited in the presence of Mg^{2+} or at high ionic strength (Fig. 37C) but was enhanced in the presence of Zn^{2+} (Fig. 37D, with 1.6-fold higher fluorescence intensity at 500 nm than with AcChase + N-DAZ alone; Fig. 37C). Only 30% of the original activity remained when the enzyme was modified in the presence of Zn^{2+}.

The excess N-DAZ (and peripheral-site ligands) were removed, either by extensive dialysis on an AMICON ultrafiltration apparatus or by chromatography on a column of Sepharose 4B which had L-cysteine covalently attached to it. The protein samples so treated had an intense new fluorescent peak at 495 nm with an excitation maximum at 345 nm (Fig. 38). Upon removal of the excess N-DAZ the partially modified enzyme (N-DAZ plus

Fig. 36. Reaction of T. californica AcChase with N-dansylaziridine. Monitored by changes in the emission spectrum of N-DAZ. The scan of emission spectrum (400-600 nm) at various time intervals after the addition of N-DAZ (3×10^{-5} M) to AcChase (2.57×10^{-7} M): (1) t=0; (2) 5 min; (3) 15 min; (4) 35 min; (5) 1 hr 15 min; (6) 2 hr; (7) 3 hr 4 min; (8) 5 hr 20 min; (9) 9 hr 23 min. The excitation wavelength was 345 nm. 0.3 mL fluorescence cells were used.

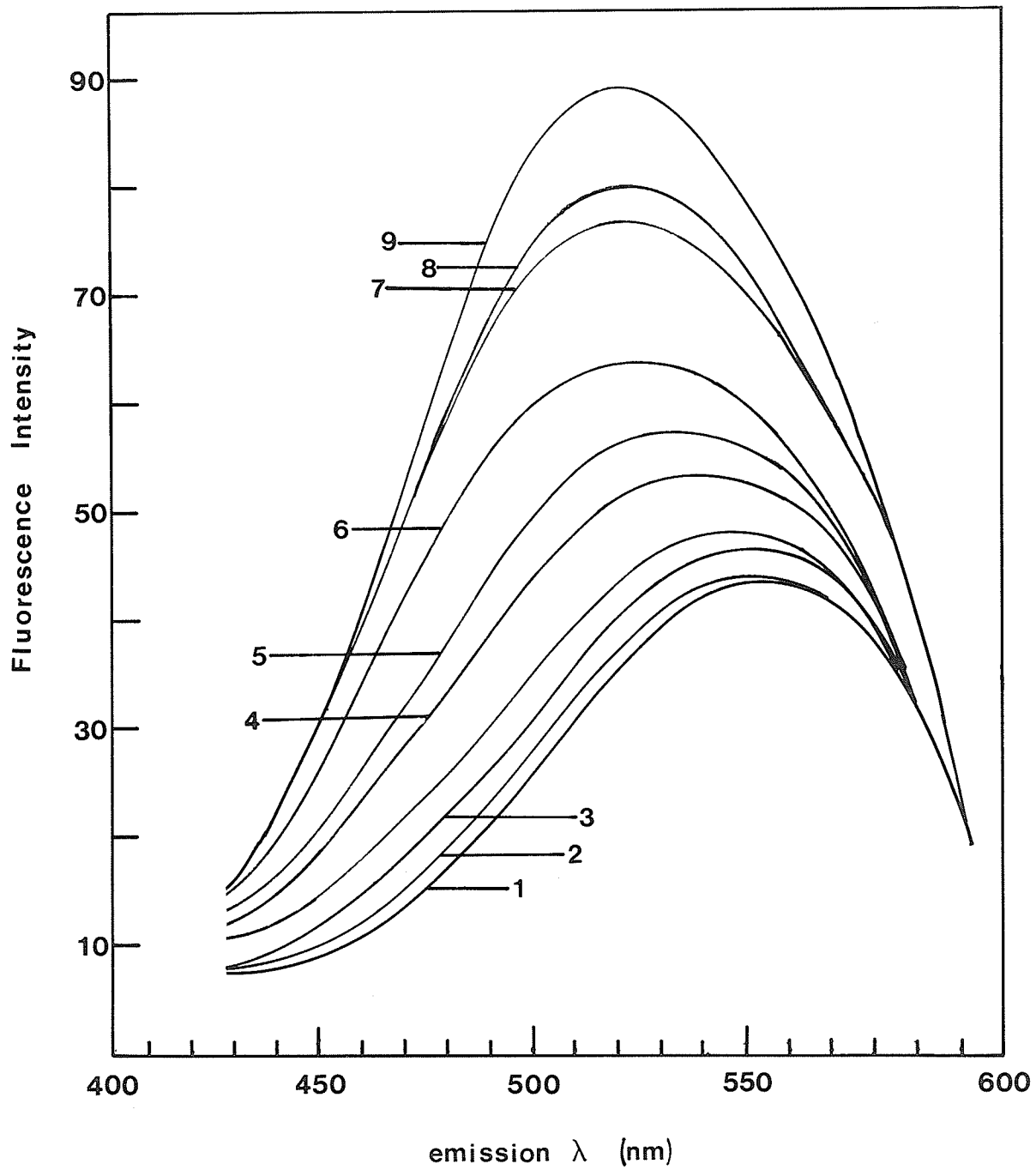
90
70
50
30
10
Fluorescence Intensity
9
8
7
6
5
4
3
2
1
400
450
500
550
600
emission λ (nm)

Fig. 37. Reaction of N-DAZ with T. californica AcChase in the presence of a variety of peripheral-site effectors. Monitored by the scan of the emission spectrum of N-DAZ after 17 hr of reaction with AcChase (2.57×10^{-7} M) at 25°C. A) AcChase + Zn^{2+} (4.74×10^{-4} M) + N-DAZ (2.72×10^{-5} M) ; B) AcChase + N-DAZ (2.72×10^{-5} M); C) AcChase + Mg^{2+} (4.75×10^{-3} M) + N-DAZ (2.72×10^{-5} M); D) Buffer + N-DAZ (2.72×10^{-5} M); The excitation wavelength was 345 nm. 0.3 mL fluorescence cells were used. The buffer was 1.0 mM-Tris-Cl, pH 8.0.

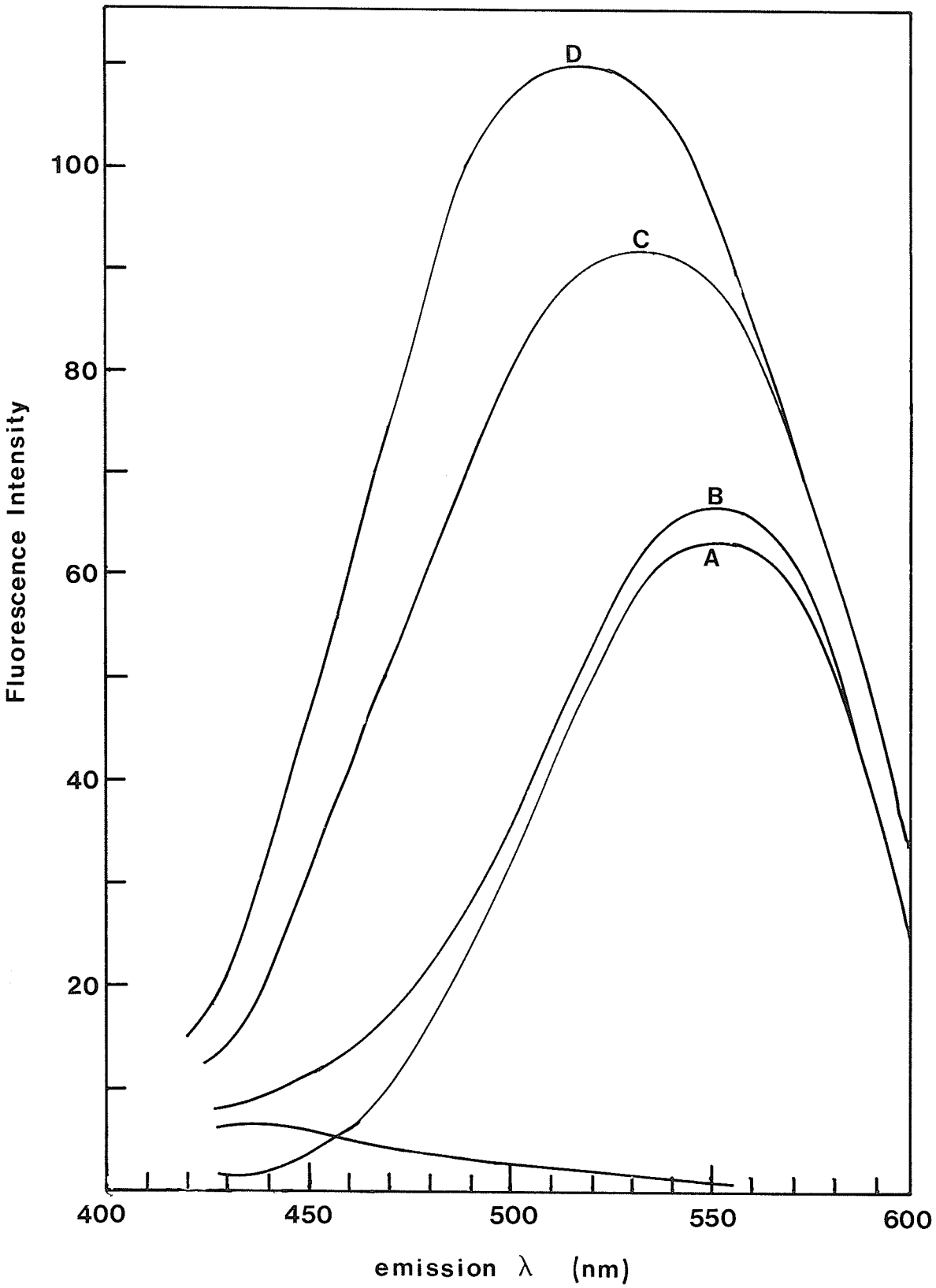
D
C
B
A
100
80
60
40
20
Fluorescence Intensity
400
450
500
550
600
emission λ (nm)

Fig. 38. Fluorescence spectrum of modified *T. californica* AcChase. AcChase (2.57×10^{-7} M) was reacted with N-DAZ (2.5×10^{-5} M) in the presence of Zn^{2+} (1.04×10^{-4} M) for 17 hr at 25°C. The excess N-DAZ and Zn^{2+} were removed by extensive dialysis. The buffer was 1.0 mM-Tris-Cl, pH 8.0. The excitation wavelength was 345 nm. 3.0 mL fluorescence cells were used. (A) dialysed enzyme; (B) N-DAZ + Buffer after 17 hr at 25°C.

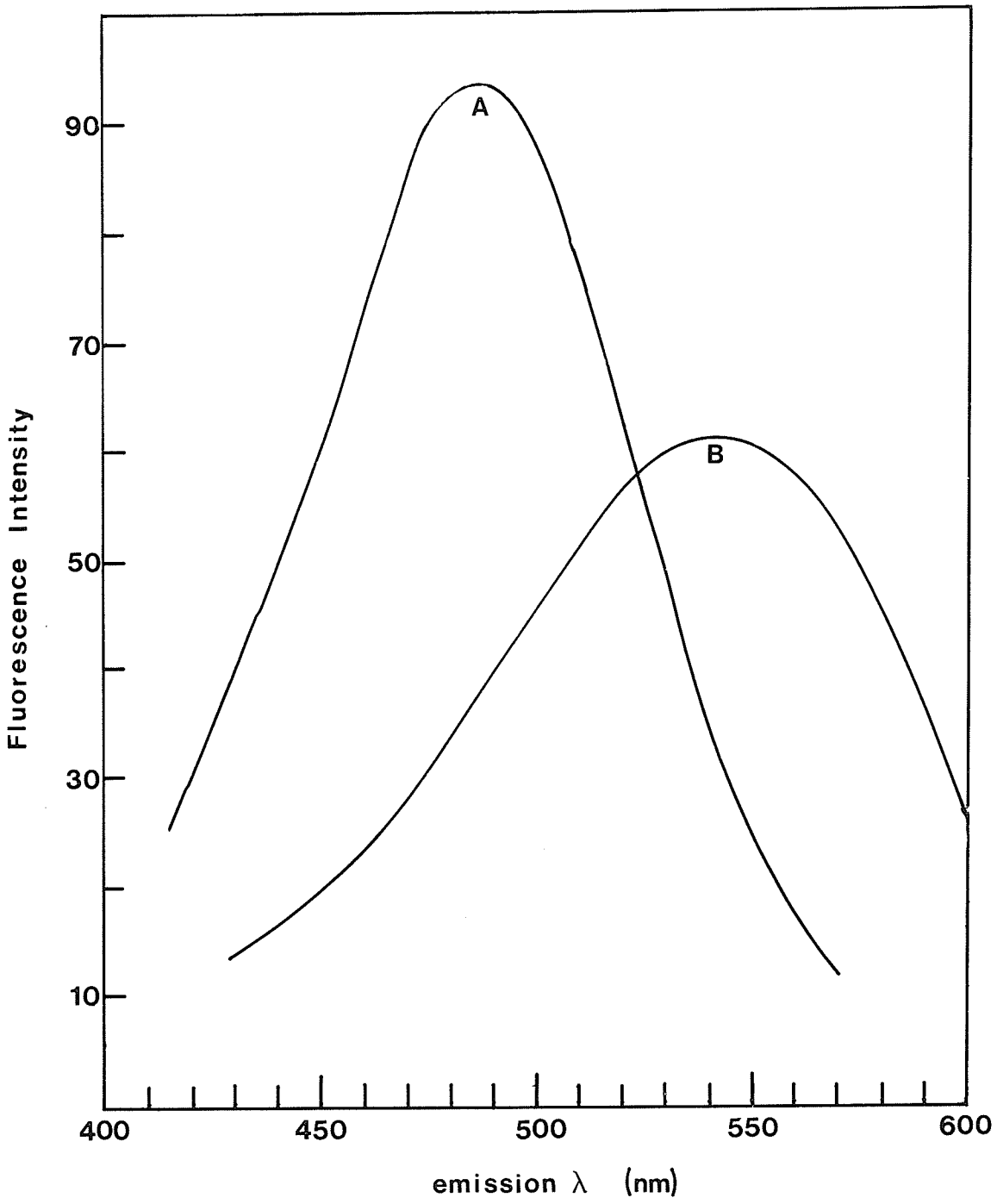
A
B
90
70
50
30
10
Fluorescence Intensity
400
450
500
550
600
emission λ (nm)

AcChase; Fig. 37B) retained only 40% of its activity whereas the enzyme that had the most label (N-DAZ + AcChase plus Zn^{2+}, Fig. 37A) was devoid of AcChase activity.

The reaction of N-DAZ with AcChase plus Zn^{2+} was followed by continuously monitoring the increase in the fluorescence at 500 nm. The reaction was very slow, reaching completion in ∿17 hrs. The pseudo-first order rate constant (k_{obs}) extracted from these data (Fig. 39) was 0.16 hr^{-1} ($t_{1/2}$ of 4.33 hr), approximately 5-fold lower than previously reported for the reaction of N-DAZ with BSA (162).

ii) E. electricus AcChase:

Incubation of E. electricus AcChase with N-DAZ resulted in a very small enhancement in the N-DAZ fluorescence spectrum (Fig. 40B), although the emission maximum was blue shifted by 10 nm. This partially modified enzyme was fully active at the end of 17 hr. Again in the presence of Zn^{2+}, the fluorescence at 500 nm was enhanced by 1.9 fold over that observed with N-DAZ plus enzyme alone (Fig. 40A). Under these conditions the enzyme retained only 23% of its original activity. Neither Hg^{2+} nor 2-PAM had any apparent effect on the reaction of N-DAZ with AcChase. DMB (1×10^{-6} M) was found to inhibit the reaction of N-DAZ with AcChase (Fig. 40C, D and E). The excess N-DAZ was removed (by either dialysis or chromatography) and the resulting protein was then devoid of AcChase activity.

These results suggest that AcChase is most reactive towards N-DAZ in its unreactive conformation (stabilized by Zn^{2+}) and least reactive in the activated form (stabilized by

Fig. 39. Kinetics of the reaction of N-DAZ with T. californica AcChase. Fluorescence at 500 nm was continuously monitored. The excitation wavelength was 345 nm. The reaction mixture contained AcChase (5.72×10^{-7} M), Zn^{2+} (1.0×10^{-4} M) and N-DAZ (2.75×10^{-5} M). 3.0 mL fluorescence cuvettes were used. Dashed line; buffer + N-DAZ (2.75×10^{-5} M).

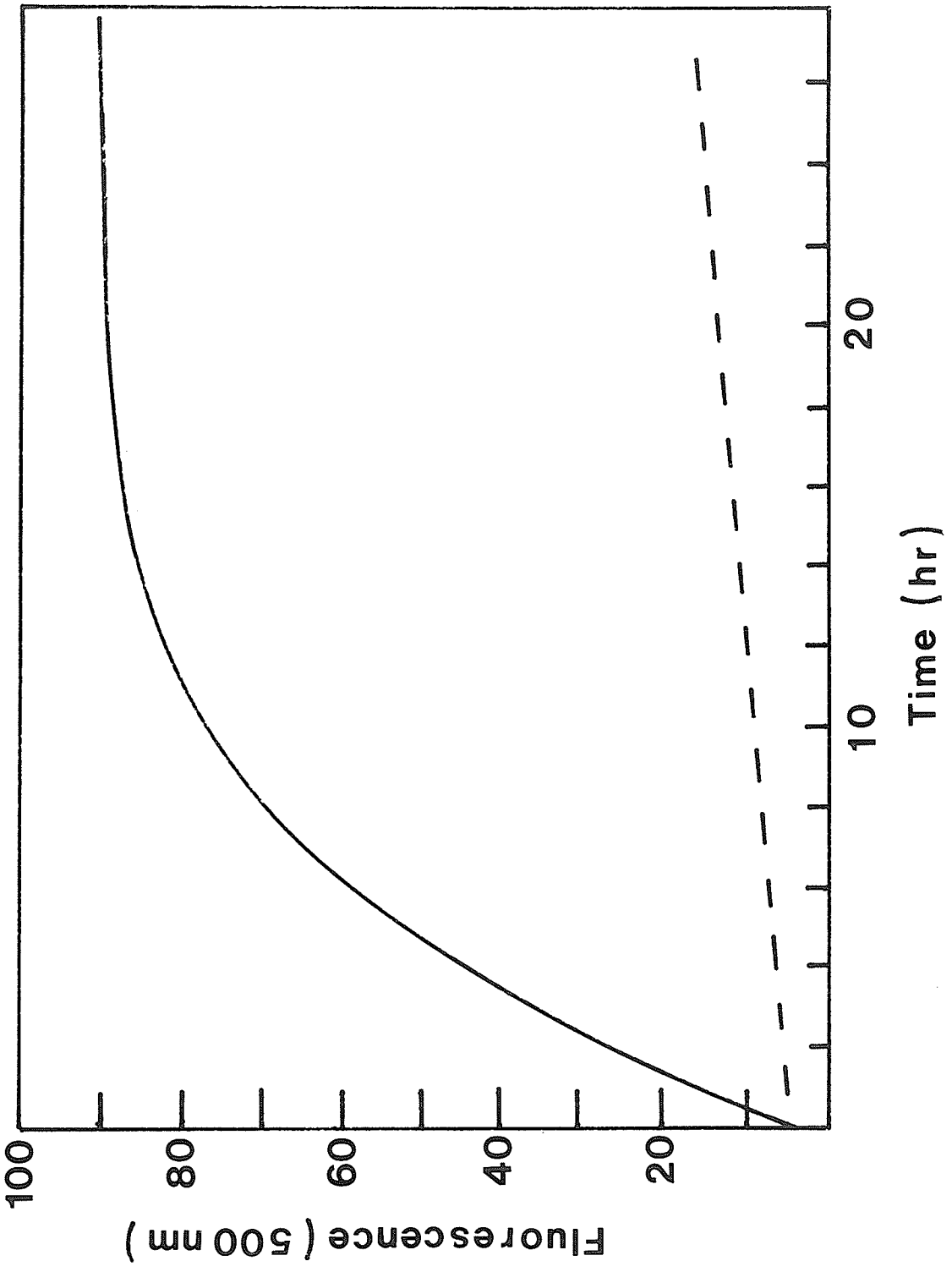
Fluorescence (500 nm)
100
80
60
40
20
10
20
Time (hr)

Fig. 40. Reaction of N-DAZ with *E. electricus* AcChase in the presence of a variety of compounds. Monitored by the scan of the emission spectrum of N-DAZ after 17 hr of reaction with AcChase (2.57×10^{-7} M) at 25°C. (A) AcChase + $ZnSO_4$ (1.0×10^{-4} M) + N-DAZ (2.72×10^{-5} M); (B) AcChase + N-DAZ (2.72×10^{-5} M); (C) AcChase + $HgCl_2$ (5×10^{-5} M) + N-DAZ (2.72×10^{-5} M); (D) AcChase + 2-PAM (1×10^{-4} M) + N-DAZ (2.72×10^{-5} M); (E) AcChase + DMB (1×10^{-6} M) + N-DAZ (2.72×10^{-5}) or Buffer + N-DAZ (2.72×10^{-5} M). The buffer was 1.0 mM-Tris-Cl, pH 8.0. 3.0 mL fluoresence cells were used. The excitation wavelength was 345 nm.

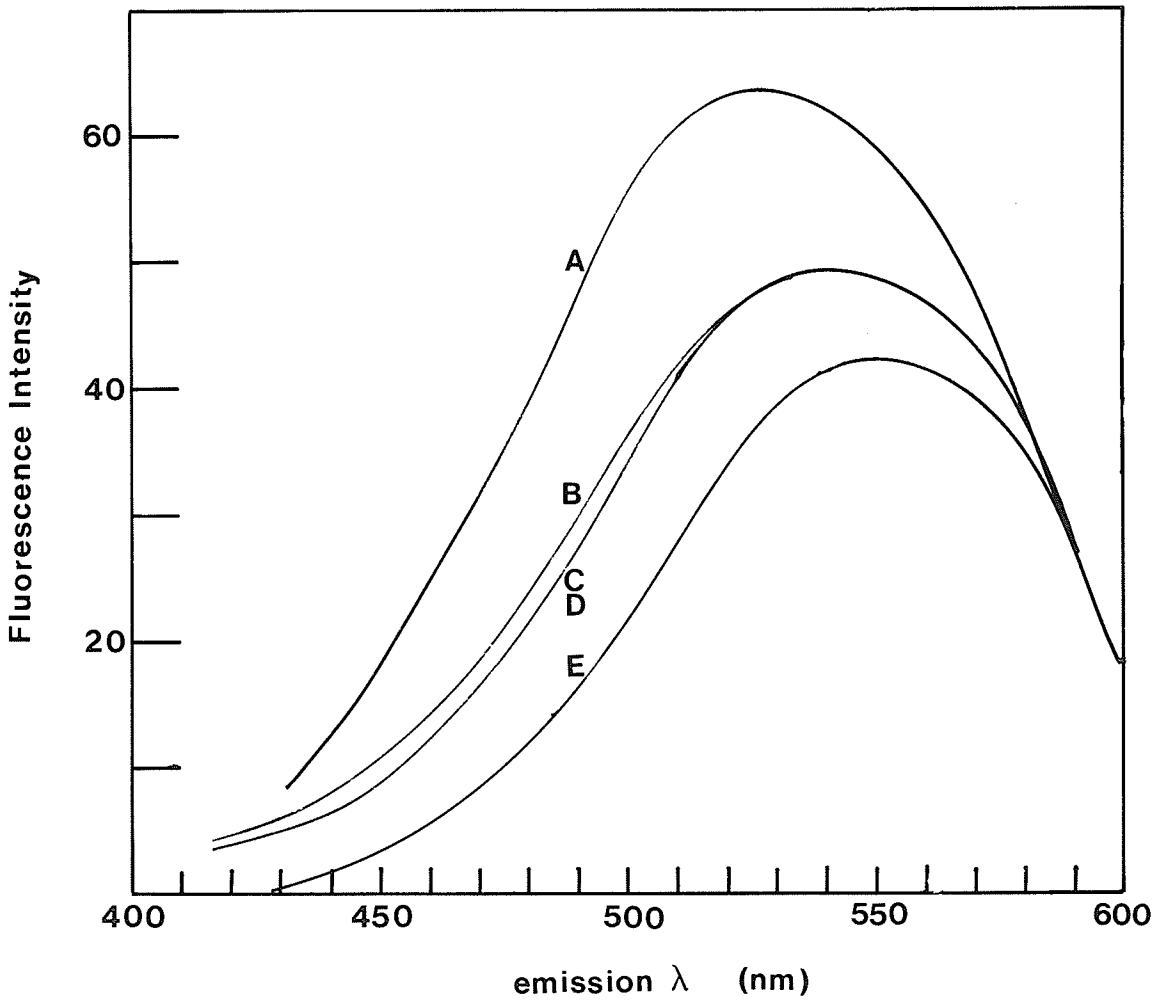
Fluorescence Intensity
60
40
20
A
B
C
D
E
400
450
500
550
600
emission λ (nm)

Mg^{2+} or at high ionic strength).

The modified enzyme samples, containing the highest amount of label (E + Zn^{2+} + N-DAZ), were hydrolyzed in 6 M HCl, in sealed tubes for 4 hr at 110°C, the HCl was removed, the hydrolysate was dissolved in MeOH, and applied to a 20 x 20 cm TLC sheet (EASTMAN silica gel). Two dimensional TLC was then performed using the solvent systems #63 or #64 of Neidweiser (164). A fluorescent, ninhydrin positive spot that did not move in the first (#63) solvent system but had an R_f value of 0.87 in the second (#64) solvent, which is very close to the R_f value obtained with dansyl-S-aminoethyl-cysteine (0.85), subjected to 2 dimensional TLC under identical conditions (Fig. 41). Further tests, to determine the structure of the fluorescent compound in the enzyme hydrolysate, are in progress.

Fig. 41. 2-Dimensional TLC of the hydrolysate of modified AcChase. The modified protein was hydrolysed in 6.0 M HCl at 110°C for 4 hr. The HCl was removed, and the hydrolysate was extracted with methanol and applied onto a silica gel plate (20 x 20 cm). Solvent system in direction 1 was benzene:pyridine:acetic acid (80:20:5 v/v); and in direction 2 was toluene:2-Cl-ethanol:NH_4OH (80:20:5 v/v). Neither dansyl-S-aminoethyl cysteine (A) nor the protein hydrolysate (B) moved in solvent system #1. In solvent system 2: dansyl-S-aminoethyl cysteine (A) resulted in two fluorescent (F) spots with R_f values of 0.65 and 0.85 only the spot with the latter R_f value was ninhydrin positive (N); the protein hydrolysate (B) resulted in one fluorescent spot (F) with an R_f value of 0.85, and was ninhydrin positive (N).

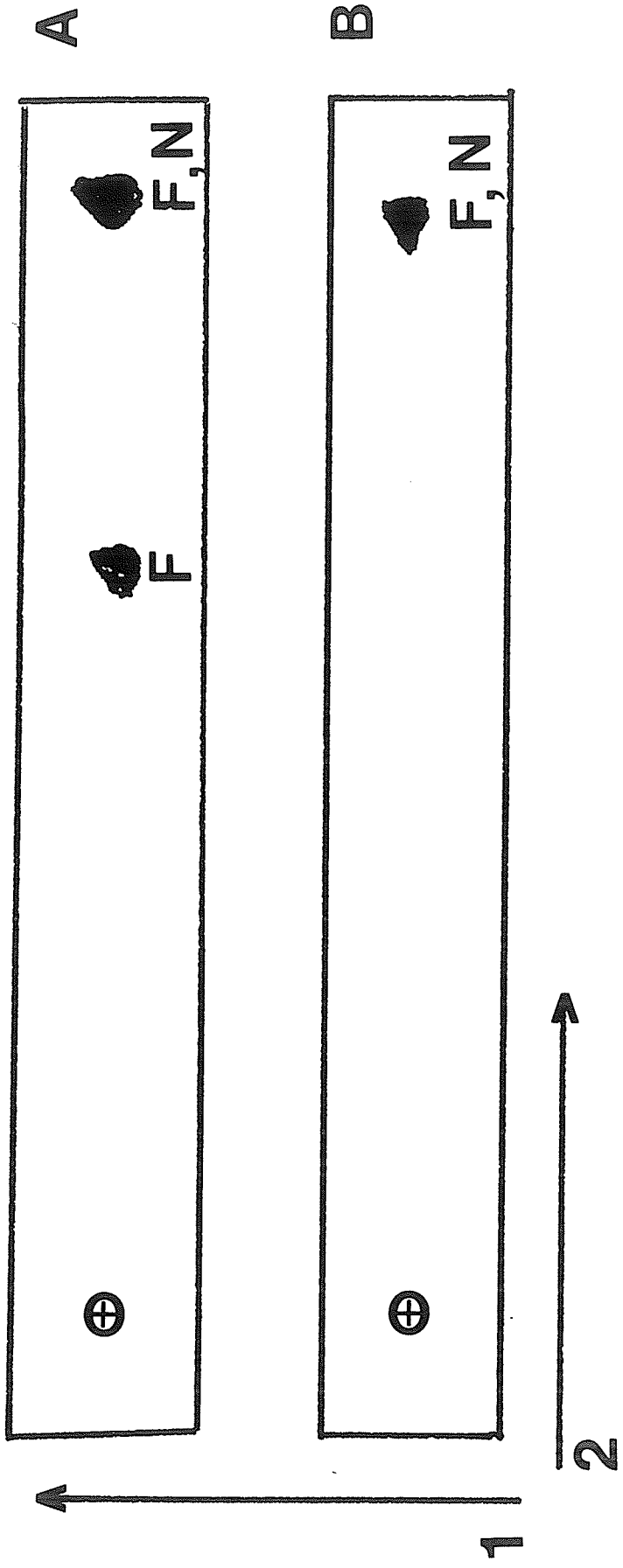
A
B
F,N
F
F,N
1
2

DISCUSSION

Fluorescence titrations:

The specificity of propidium for the peripheral anionic sites of AcChase isolated from T. californica has been elegantly demonstrated by Taylor et al. (130). In these studies four molecules of propidium were shown to bind per molecule of tetrameric (11s) AcChase, with a binding constant of 3×10^{-7} M. The binding was hyperbolic indicating that the four propidium binding sites were identical. Propidium displacement experiments were used to demonstrate binding specificity of other ligands: Propidium was displaced by the ligands gallamine, d-tubocurarine and decamethonium. Active site-directed ligands which display competitive kinetic behaviour (edrophonium and N-methylacridinium) as well as the modification of the active site with bulky sulphonates and phosphates had no effect on the interaction of propidium with AcChase (130, 143).

In the current investigation the use of propidium as a probe for the peripheral anionic sites was extended to AcChase isolated from the electric organs of E. electricus, the electric eel. The AcChases from these two sources are quite distinct with respect to molecular weights and amino acid content. These differences also extend to the catalytic properties of the two enzymes, although qualitatively they display many similarities with respect to substrate and ligand binding specificities. Quantitatively they are somewhat different. T. californica AcChase has a turnover number that is approximately 3-fold less and displays approximately ten-fold lower affinity

for cationic ligands, than E. electricus AcChase under comparable experimental conditions. The present results indicate that these differences extend to propidium binding: Four molecules of propidium were shown to bind per tetrameric (11S) E. electricus AcChase molecule, however, the binding exhibited considerable heterogeneity. Less than two molecules of propidium were bound very tightly, with a dissociation constant of less than 10^{-7} M. The remainder of the propidium molecules were bound less tightly, with a dissociation constant of 4 x 10^{-6} M. There are several possible interpretations of these results. The first explanation that comes to mind is that E. electricus AcChase possesses non-equivalent propidium binding sites. This is plausible in view of the structural asymmetry suggested in the most recent structural model for 11S E. electricus AcChase proposed by Rosenberry and his co-workers (60, 65). In this model two of the subunits are linked to one another by disulphide bridges while the remaining two are linked again by disulphide bridges to a collagen-like tail (as illustrated below).

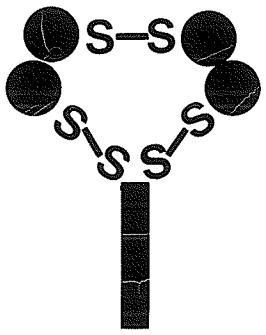

Another possibility is that there is a heterogeneous enzyme population made up of native and partially denatured enzyme. The source of the denaturation could be the proteolytic (or autolytic) step in the isolation procedure: Both T. californica and E. electricus are solubilized from their respective tissues by a limited proteolytic or a prolonged autolytic (in toluene) digestion. The E. electricus enzyme used in this study was obtained from a crude, commercially available preparation (Sigma type VI-S) which is solubilized from the eel electric tissues by autolysis, for up to 2 years under toluene. It is therefore conceivable that under these conditions E. electricus AcChase is more susceptible to autolytic degradation of its polypeptide chains. A third possibility involves the binding of propidium to pre-existing kinetic states which are in equilibrium; one conformation would bind propidium tightly, the other less so. The homogeneous propidium binding observed in the case of T. californica could be accounted for by assuming that only one form dominates or that propidium can bind to either conformation with equal affinity. Evidence for the latter has been presented by Bolger and Taylor (144): Binding of bisquaternary ligands to T. californica AcChase was characterized by a fast bimolecular step plus a slow unimolecular step. Propidium on the other hand displayed only the fast bimolecular step. These results were interpreted in terms of two preexisting conformations of AcChase. Propidium was assumed to bind to either form, therefore only displayed the fast bimolecular step whereas the bisquaternary ligands were thought to

bind to one conformation only. The slow unimolecular step represented the rate of interconversion between enzyme forms (144).

The apparent differences between E. electricus and T. californica enzymes with respect to propidium binding were, in the present study, shown not to extend to the locus of binding. Gallamine, a molecule that has peripheral anionic site specificity for T. californica AcChase (130, 143) or erythrocyte (133) AcChases, was able to displace propidium, while edrophonium, a ligand specific for the anionic subsite of the catalytic site (56), failed to do so. In addition Zn^{2+} a species that has been demonstrated to inactivate T. californica (145) and E. electricus AcChases (see results) and Mg^{2+}, an activator of both T. californica and E. electricus enzymes (129, 133, present study), were tested for their ability to displace propidium from E. electricus AcChase. Zn^{2+} displaced 50% of the bound propidium at its ($Zn(OH)_2$) solubility limit. Mg^{2+} was less effective, displacing approximately 30% of the bound propidium. The Mg^{2+} results are in accord with previous kinetic and spectral evidence that demonstrate that divalent activators combine at the peripheral anionic subsite P_1 whereas gallamine and propidium occupy subsites P_2 through P_4. The subsite specificity of Zn^{2+} has yet to be established although the present results seem to indicate that Zn^{2+} and propidium sites do not exactly overlap.

These studies further demonstrate the usefulness of propidium as a probe for the peripheral sites of AcChase from E. electricus as well as T. californica, although there does appear

to be some (as yet unexplained) differences in the binding characteristics. The inorganic cation Zn^{2+} appears to combine with AcChase at the peripheral anionic sites but whether this interaction leads to the inactivation of the enzyme requires further kinetic evidence.

Steady-State kinetics:

The results obtained from a study of the rates of hydrolysis of AcSCh under steady-state conditions, in the presence or absence of a variety of peripheral or catalytic site specific ligands, indicate that E. electricus exists in at least three kinetically distinct states in equilibrium. These states may be defined as: the low ionic strength state (E); the activated state (E_a); and the inactive state (E_i). In the absence of peripheral site effectors, at low ionic strength the E state predominates, while the conversions to states E_a and E_i require the presence of specific peripheral site ligands and occur in a concerted manner without any apparent intersubunit co-operativity.

The preliminary evidence for the existence of the ionic strength-dependent (E) and (E_a) forms arose from the fact that two distinct sets of data, both displaying Henri-Michaelis-Menten behaviour, were obtained at either low or high ionic strength. The values of K_{app} and k_{cat} at low ionic strength were 4.3×10^{-6} M and $3.5 \pm 1.0 \times 10^{5}$ min^{-1}, respectively and increased to 5.6×10^{-5} M and 9×10^{5} min^{-1} at high ionic strength. The kinetics of hydrolysis of AcSCh at an inter-

mediate ionic strength (0.025 M) did not obey Henri-Michaelis-Menten behaviour and displayed downward curvature in the reciprocal plots, at high substrate concentrations, suggesting kinetic heterogeneity at sub-critical ionic strengths. In addition the organic ligands that were shown to be peripheral site-specific (propidium and gallamine) inhibited the AcSCh hydrolysis at low ionic strength, in an uncompetitive manner, and displayed downward curvature in the double reciprocal plots. The active site-specific compound edrophonium behaved as a classical competitive inhibitor. The downward curvature produced in the presence of propidium or gallamine may be interpreted as an indication of peripheral site-specific ligand-induced kinetic heterogeneity in AcChase. This assumption is given further support by the observation that preincubation of AcChase with either propidium or gallamine prior to the addition of AcSCh resulted in hydrolysis rates that were up to 1.4-fold higher than obtained when AcSCh plus gallamine or propidium were introduced at the same time. Furthermore, the double reciprocal plots in the preincubated case no longer displayed curvature and the initial rates were increased over most of the substrate concentration used. In addition, the inhibition appeared to be more competitive in nature. The activation was observed only upon a 10 minute preincubation of the enzyme with either gallamine or propidium, suggesting that the rate of activation of the enzyme by these ligands was very slow. The slow propidium- or gallamine-induced activation was directly observed in the stop-flow spectrophotometer.

The rate of AcChase-catalyzed hydrolysis of AcSCh increased gradually to a rate approximately 1.36 times that of the initial rate (a few seconds after the mixing of the reagents). In addition to the organic peripheral site-specific ligands, inorganic cations Mg^{2+}, Ca^{2+} and Mn^{2+} were shown to activate AcChase at low ionic strength. The concentration-dependence of the activation process appeared to be hyperbolic with the metal ions examined. The inorganic ligands all increased the AcChase-catalyzed rates of hydrolysis of AcSCh approximately 1.7 times over and above the rates in their absence. The maximal effect was observed at an ionic strength of 0.07 to 0.1 and was identical to the amount of activation observed by Na^{+}. However, the concentration or ionic strength of the divalent cations required for half-maximal activation (a rough estimate of the enzyme-cation dissociation constant) was 30-fold or 12-fold lower, respectively, when compared with monovalent sodium. Therefore the activation of AcChase by cations is thought to result from a specific metal-metal-peripheral anionic site interaction, and a non-specific ionic strength effect; a conclusion supported by the earlier observations of Crone and his colleagues (134, 135), working with erythrocyte AcChase. The activation induced by metal cations was rapid in contrast to the slow activation observed with propidium and gallamine. This provides further support for the existence of separate metal ion (P_1) and organic cation activator sites (P_2 - P_4) (56).

The enzyme was converted to an inactive state (E_i) in

the presence of Zn^{2+}, Cd^{2+}, Pb^{2+} and Hg^{2+}. The inactivation was very slow, requiring about 10 minutes for the onset of maximal inhibition. The concentration-dependence of the inactivation process appeared to be hyperbolic with respect to both metal ions, as measured by the decrease in initial rates of AcSCh hydrolysis. The instantaneous effect of Zn^{2+}, measured under steady-state conditions with rapid-mixing techniques (using a stopped-flow apparatus), was an inhibition of the rates of hydrolysis at AcSCh concentrations $<8 \times 10^{-6}$ M; above this substrate concentration, Zn^{2+} was found to increase the initial rates of hydrolysis. A concentration of Zn^{2+} required to inactivate >95% of the AcSCh hydrolysis rate after a 10 minute preincubation (4×10^{-4} M), increased the instantaneous hydrolysis rates by 1.7-fold. These results, aside from the demonstration that the decrease in the rates of AcSCh hydrolysis does not arise from simple inhibition and therefore is a peripheral anionic site-mediated effect, suggest that Zn^{2+} has two opposing effects on AcChase: an instantaneous conversion of the enzyme to an activated state (E_a) as well as a slow inactivation to an inactive state (E_i). These two opposing effects could result if Zn^{2+} can bind to peripheral activator as well as to peripheral inactivator sites. Zn^{2+} binding at or near propidium binding sites has been demonstrated by the fluorescence displacement experiments described earlier, however the location of the site or sites on the enzyme responsible for inactivation are not known.

T. californica AcChase:

The steady-state rates of hydrolysis of AcSCh catalyzed by T. californica AcChase under low and high ionic strength conditions were significantly different from the results obtained with E. electricus AcChase. The kinetics at low ionic strength obeyed Henri-Michaelis-Menten kinetics up to 12 μM AcSCh. Above this concentration the double reciprocal plots were displaced downward and no substrate inhibition was observed, even with AcSCh concentrations as high as 614 μM. The K_{app} and k_{cat} evaluated from the linear portion of the double reciprocal plots were 1.18×10^{-5} M and 3.1×10^{4} min^{-1} respectively. The kinetics at high ionic strength displayed Henri-Michaelis-Menten behaviour over the entire substrate concentration range with K_{app} and k_{cat} 4.46×10^{-5} M and 2.92×10^{5} min^{-1}, respectively. The initial rates at high ionic strength were higher than the low ionic strength rates for the entire substrate concentration range. This is brought about by the values of k_{cat} at low and high ionic strength, differing by approximately 10-fold. In E. electricus k_{cat} increased by approximately 2.5-fold; as a result enhanced rates at high ionic strength are observed only at AcSCh concentrations above (25-30 μM). A ten-fold increase in k_{cat} going from low to high ionic strength, with T. californica AcChase, was accompanied by an approximately 3.7-fold increase in K_{app} ($K_{app} \sim k_{cat}K_s$). This is in contrast to the E. electricus AcChase where a 2.57-fold increase in k_{cat} is accompanied by a 10-fold increase in K_{app}. It therefore appears that in T. californica AcChase, K_s for AcSCh decreases

whereas in E. electricus AcChase it increases with increasing ionic strength.

The downward curvature in the case of the T. californica AcChase observed at low ionic strength is reminiscent of the biphasic double reciprocal plots obtained at intermediate ionic strength with E. electricus AcChase. One possible explanation of these results is that the equilibrium between active (E) and activated (E_a) forms of T. californica enzyme is less dependent on the presence of activators so that at low ionic strength significant amounts of (E) and (E_a) are present. An alternative explanation could be that AcSCh binds at the peripheral anionic activator sites, thereby converting (E) to (E_a), at high concentrations. However, the nature of steady-state kinetics makes it impossible to distinguish between these two explanations.

Pre-steady state kinetics:

E. electricus AcChase:

The advantage of a pre-steady-state kinetic study over the steady-state approach is that with the former the kinetic parameters K_s, k_2 and k_3 of the proposed catalytic mechanism (Scheme II) may be separately established (see appendix). In addition the amount of active enzyme can be accurately determined. Therefore pre-steady-state kinetics seem ideally suited for a study of the consequences of peripheral site occupation.

In the present study pre-steady-state conditions were obtained by studying the carbamoylation of the enzyme by the

fluorogenic carbamoylating agent M7C (79). With this pseudo-substrate the decarbamoylation rate constant k_3 is much smaller than the carbamoylating rate constant k_2 and as a result there is a pre-steady-state "burst" of fluorescence resulting from the release of the fluorescent compound M7C, upon formation of the carbamoyl enzyme. The amplitude of the carbamoylation phase corresponds to the amount of free, active enzyme, while the pseudo-first order approach to steady-state is a reflection of the carbamoylation rate constant (k_2). The steady-state turnover of M7C can be related to the decarbamoylation rate constant (k_3) (79).

In the M7C concentration range 0.5 to 10 μM, at low ionic strength, the dependence of the pseudo-first order rate constant (k_{obs}) on the substrate concentration was hyperbolic (as predicted by eq. [79a]; appendix). Ligands that have been implicated in peripheral site occupation, propidium and gallamine, increased both the carbamoylation rate constant (k_2) and the decarbamoylation rate constant (k_3). Edrophonium, on the other hand, inhibited the carbamoylation in a competitive manner, once again demonstrating that these two classes of compounds interact with the enzyme in different ways.

Above 10 μM M7C concentration at low and high ionic strength, the dependence of k_{obs} on the M7C concentration was no longer hyperbolic. The rates increased in a non-hyperbolic manner, resulting in a downward displacement of the double reciprocal plots. The increase in k_{obs} was accompanied by an increase in k_3: The extrapolated value of k_2 was increased almost

3-fold, k_3 was almost doubled (∿1.3-fold at high ionic strength). This result, reminiscent of AcSCh kinetics at low ionic strength displayed by T. californica AcChase, could be due to either substrate activation or a second enzyme population becoming activated, at high M7C concentrations. The activation of a second enzyme population would therefore be accompanied by an increase in the total enzyme concentration. The fact that the carbamoylation amplitude (a direct measure of enzyme concentration) remained constant for the entire substrate (M7C) range studied (0.5 to 38 μM), suggests that the observed activation of k_2 and k_3 is due to the conversion of the active enzyme to an activated form (E_a). There are several lines of evidence to indicate that M7C interacts with the same region of the peripheral anionic sites occupied by propidium or gallamine: The effects of propidium or gallamine on k_2 or k_3 are observed only at low M7C concentrations. At high M7C concentrations, where substrate activation is observed, these ligands no longer have any effect on carbamoylation (k_2) or decarbamoylation (k_3) rates. This could only come about if M7C and gallamine or propidium binding subsites (P_2-P_4) are mutually exclusive.

In going from low to high ionic strength conditions, K_s was increased by ∿3.8 fold, k_3 was approximately doubled, while k_2 was unaffected. Inorganic activators appear to induce the same conformational changes as induced by high ionic strength, as the only effect of Ca^{2+} or Mg^{2+} was an approximate tripling of k_3. However, the activation of k_3 by Mg^{2+} or Ca^{2+} was also observed at high ionic strength, further indicating that con-

formational changes induced either by high ionic strength or by specific metal cation binding to peripheral activator sites, although resulting in similar kinetic consequences, are two independent processes. The observation of activation of k_3 (by Mg^{2+} or Ca^{2+}) at high ionic strength is also significant in that it illustrates that the role of peripheral anionic sites in controlling the catalytic activity of the enzyme is not limited to the physiologically unimportant, low ionic strength conditions.

The decarbamoylation rates (k_3) were also activated by Mg^{2+} or Ca^{2+} at high M7C concentrations, where organic activators (propidium or gallamine) were shown to have no effect. This result once again provides evidence for the existence of separate metal and organic cation activator sites.

The effect of inactivating ligands on the pre-steady-state carbamoylation of E. electricus AcChase was a gradual lowering of the carbamoylation amplitude and the decarbamoylation rate. This effect was most readily observed when the enzyme was preincubated with the inactivator for about 10 minutes prior to the introduction of M7C, thus suggesting that the inactivation is very slow and possibly reflects a ligand-induced change in the enzyme conformation. Evidence for Zn^{2+}- and d-tubocurarine-induced slow changes on AcChase has been presented by Epstein et al. (146): T. californica AcChase was modified at the reactive serine with the reagent [1-(dimethylamino)napthalene-5-sulfamido]pentylmethylphosphonofluoridate (a sensitive probe of active-site conformation). In the

presence of Zn^{+2} or d-tubocurarine, the fluorescence of the modified protein was enhanced and the emission maximum shifted to lower wavelengths. The change in fluorescence intensity occurred very slowly, and was comparable with the rate of inhibition of the native enzyme by either Zn^{2+} or d-tubocurarine. Displacement of propidium by Zn^{2+} or d-tubocurarine was rapid with respect to the time course of enzyme inhibition or changes in the fluorescence of the dansylated enzyme, thus suggesting that inactivators combine rapidly with the peripheral anionic sites and induce slow conformational changes that lead to inactivation of the enzyme.

Of the organic ligands tested only d-tubocurarine resulted in the inactivation of E. electricus AcChase. The carbamoylation amplitude decreased in an approximately hyperbolic manner with increasing d-tubocurarine concentrations and reached a minimum at approximately 50% of the initial carbamoylation amplitude. The evidence for d-tubocurarine-induced inactivation being a peripheral effect is two-fold; a) the inactivation is observed at high M7C concentrations, where d-tubocurarine was shown not to affect carbamoylation rates and therefore does not interact with the catalytic sites; b) d-tubocurarine is slightly less effective at decreasing carbamoylation amplitudes at high M7C concentrations where M7C has been implicated in peripheral site occupation. The inability of d-tubocurarine to lower the amplitude below approximately 50% of the initial carbamoylation amplitude (at d-tubocurarine concentrations as high as 5 mM) might be related to an inability of the 11s AcChase to bind

more than two of the bulky d-tubocurarine molecules.

The cationic inhibitors Hg^{2+}, Zn^{2+}, Cu^{2+}, Cd^{2+} and Pb^{2+}, also brought about a decrease in the carbamoylation amplitude. The inactivation was again slow and required a 10 min preincubation for the maximal decrease in carbamoylation amplitudes. The carbamoylation amplitude decreased in a hyperbolic manner with increasing metal ion concentration, and unlike d-tubocurarine, the metal ions were able to abolish all of the carbamoylation amplitude. The amplitude decrease was not dependent on the M7C concentration. The inactivation was observed at both low and high ionic strength; this effect therefore represents one of the few clear-cut examples of a peripheral effect observable at high ionic strength. The apparent dissociation constant for the inactivating metal ions (estimated from the concentration of the cation required to eliminate 50% of the carbamoylation amplitude) were 10-30 fold higher at high ionic strength than at low ionic strength, suggesting that the peripheral anionic sites as well as the catalytic sites are altered in ionic strength-induced conformational changes of the enzyme. The hyperbolic concentration-dependence observed in the inactivation profiles suggest that the peripheral sites on AcChase are equivalent and that the enzyme is converted to the inactive form in a concerted manner without inter-subunit co-operativity.

The effects of the inactivating ligands (Hg^{2+}, Zn^{2+}, Cu^{2+}, Cd^{2+} and Pb^{2+}) were reversible upon addition of EDTA; however, all of the original carbamoylation amplitude could not be

recovered. This prompted a study of the effects of prolonged incubation of the enzyme with a given inactivator. It was observed that prolonged contact of the enzyme with the inactivator resulted in a time-dependent decrease in the amount of recoverable activity. If this experiment was repeated under conditions of O_2-saturation the irreversible inactivation was more rapid but under N_2-saturation was slower. The irreversible inactivation could therefore involve a metal-catalyzed oxidation of an essential enzymic functional group. One functional group, oxidizable under such mild conditions is the sulphydryl group of the amino acid cysteine. These observations led to a study of the reaction of AcChase with sulphydryl-specific reagents and is discussed further, later in this section.

The effects of inorganic and organic peripheral-site activators on the inorganic cation induced inactivation of AcChase was very interesting. The peripheral-site activators (Mg^{2+}, propidium) protected AcChase from Zn^{2+}-induced time-dependant decrease in the carbamoylation amplitude, but failed to reactivate the Zn^{2+}-inactivated enzyme. These results could come about either from a lowering of the peripheral site affinity for activators or from an increase in the affinity for inactivators, in the inactivated state (E_i). The latter possibility would be analogous to the desensitization of the acetylcholine-receptor: Prolonged incubation of the receptor with agonists or antagonists results in a slow conformational change of the receptor to a desensitized state which is characterized

by an increased affinity (by as much as 1000-fold) for agonists or antagonists (28).

The kinetics of conversion to inactive species:

The inactivation of E. electricus AcChase by the inorganic cations Hg^{2+}, Cd^{2+}, Cu^{2+} and Zn^{2+} was biphasic at low ionic strength, irrespective of the method of assay. The kinetics were resolved into two first order processes, characterized by two rate constants of 5.12×10^{-2} sec^{-1} and 4.4×10^{-3} sec^{-1}, respectively. Although the relative amplitudes of the slow phases differed according to the method of assay, the rate constants extracted from the time courses were virtually identical either with the continuous NPA assay or the discontinuous M7C assay.

Pattison and Bernhard (145) were the first to report biphasic inactivation kinetics with the inactivating peripheral site ligands d-tubocurarine, Cu^{2+} and Zn^{2+}. The biphasicity was explained in terms of a two state model for AcChase. In this model AcChase from T. californica was assumed to be in a conformational equilibrium between active (E) and inactive (E_i) kinetic states. Activators of the enzyme such as Mg^{2+}, Cu^{2+}, propidium or gallamine were thought to stabilize the active (E) conformation, whereas inactivators d-tubocurarine, Cu^{2+} and Zn^{2+} would stabilize the inactive (E_i) conformation. The faster rate observed in the inactivation kinetics, under saturating inactivator ligand (L) concentrations, was attributed to the rate of conversion, $E \rightarrow E_iL$. The slower rate constant was thought to represent the conformational transition in the opposite

direction, $E_i \rightarrow E$. In subsequent investigations, Epstein *et al.* (146) were able to detect Zn^{2+}- and d-tubocurarine-induced slow conformational changes, by alterations in the fluorescence of *T. californica* AcChase labelled at the active sites with fluorescent dansyl [1-(dimethylamino)napthalene-5-sulfonamido] phosphonates. The onset of the Zn^{2+}- and d-tubocurarine-induced conformational changes was biphasic, at low ionic strength. The faster of the two rate constants extracted was 2.2×10^{-1} sec^{-1}, similar to that observed kinetically by Pattison and Bernhard (145) (3×10^{-2} sec^{-1}). There was no attempt made on the part of Epstein *et al.* (146) to explain the second slower rate constant. These results were explained in terms of a two-state model (Scheme IV). In this model, *T. californica* AcChase was thought to be in two conformational states, active (E) and inactive (E_i). The rate constant extracted from the Zn^{2+} or d-tubocurarine induced changes in enzyme fluorescence was thought to be the sum of the two slow processes, $EL \rightarrow E_i L$, and $E_i L \rightarrow E$, under saturating inactivating ligand (L) concentrations.

$$\begin{array}{ccccc} & & \text{fast} & & \\ & E+L & \rightleftharpoons & EL & \\ \text{slow} & \uparrow & & \downarrow & \text{slow} \\ & E_i+L & \rightleftharpoons & E_iL & \\ & & \text{fast} & & \end{array}$$

SCHEME IV

It is felt that a more adequate explanation of the bi-phasic inactivation results obtained here with *E. electricus* AcChase, and by Pattison and Bernhard (145) and Epstein *et al.*

(146) with T. californica AcChase, requires the inclusion of a third activated state in the proposed model (Scheme IV).

Extensive evidence for the activated (E_a) state, induced by peripheral activating ligands and stabilized at high ionic strength comes from steady-state and pre-steady-state kinetic data presented here: Under conditions of low ionic strength the steady-state kinetic parameters K_{app} and k_{cat} for AcSCh are 4.3×10^{-6} M and 3.5×10^{5} min^{-1}, respectively. In the presence of 100 mM NaCl the enzyme is converted to a high K_{app} (5.6×10^{-5}M), high k_{cat} (9.6×10^{5} min^{-1}) form. Ca^{2+}, Mg^{2+} and Mn^{2+} also appear to induce this conversion, increasing the steady-state velocities by approximately 1.7-fold. The organic peripheral site ligands have also been shown to activate the enzyme through slow conformational changes; the maximal activation was approximately 1.4-fold. Under pre-steady-state kinetic conditions, the organic ligands M7C, propidium and gallamine were shown to activate both the carbamoylation and decarbamoylation rate constants by approximately 3-fold. Inorganic activators were shown to activate only the decarbamoylation step by ∿3-fold.

The inactivation kinetics under high ionic strength conditions are monophasic, but at low ionic strength are biphasic. The fast rates at high and low ionic strength are virtually identical. This behaviour cannot be accounted for by the two state model.

A more appropriate explanation, which can account for the observed inactivation kinetics, would be that the metal cation-

induced inactivations from the active (E) and the activated (E_a) kinetic states, are characterized by rate constants differing approximately by an order of magnitude. The slow inactivation rate constant, only observed at low ionic strength, is thought to represent the conversion to the active (E) enzyme to the inactive (E_i) form, ($E \rightarrow E_i$); whereas the fast inactivation rate constant observed both at low and high ionic strength is thought to represent the conversion of activated (E_a) enzyme to the inactive (E_i) form ($E_a \rightarrow E_i$). Biphasic inactivation kinetics can therefore be accounted for by the presence of both (E) and (E_a) in significant proportions at low ionic strength. In order for this to happen inactivating ligands must activate the enzyme as well as inactivating it. This has in fact been demonstrated in the present study with Zn^{2+} (as the inactivating ligand): at low ionic strength, with rapid mixing techniques, Zn^{2+} was shown to increase the initial rates of AcSCh hydrolysis by as much as 1.7-fold.

In view of the present evidence, Scheme V is proposed to account for peripheral-site-specific ligand induced kinetic (conformational) states in E. electricus AcChase.

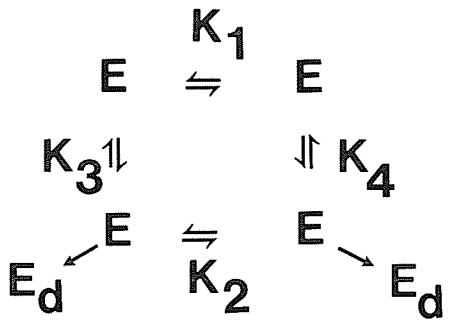

SCHEME V

In this scheme active enzyme (E) predominates at low ionic strength. The activated enzyme (E_a) is stabilized by peripheral site activators or at high ionic strength. The inactivating ligands can bind to activator (P_1) as well as to inactivator subsites of the peripheral anionic sites, the conversion to (E_a) is rapid whereas to (E_i) or to (E_{ia}) is slow. The conversion to the inactive states, (E_i) and (E_{ia}), from the corresponding active (E) and activated (E_a) states proceed with different rates. The conversion, $E_a \rightarrow E_{ia}$, has a larger rate constant than the $E \rightarrow E_i$, conversion, thus resulting in biphasic inactivation kinetics at low ionic strength. Under high ionic strength conditions only the rate constant corresponding to the conversion of $E_a \rightarrow E_{ia}$ is observed. The states E_{ia} and E_i are kinetically indistinguishable. In addition to the reversible steps, metal inactivators of AcChase convert the enzyme to a denatured state (E_d), which is irreversible.

Strong support for Scheme V is provided by the results obtained from the study of the La^{3+}-induced inactivation of the enzyme. Preincubation of E. electricus AcChase with varying amounts of La^{3+} for 10 minutes resulted in a decrease in the carbamoylation amplitude both at low and high ionic strength. The inactivation profile at low ionic strength was very unusual in that the onset of the inactivation was observed at 1 μM La^{3+} and the enzyme was still not completely inactivated at La^{3+} concentrations as high as 10^{-2} M. This effect was not due to the extra contribution to ionic strength made by trivalent cations as Hg^{2+}, made equivalent to La^{3+} in ionic

strength by the addition of appropriate amounts of NaCl, did not alter the Hg^{2+} inactivation profile.

At high ionic strength, the La^{3+}-induced inactivation titration curve was "normal", in the sense that it was complete within two orders of magnitude of La^{3+} concentration.

La^{3+} was also observed to activate the steady-state hydrolysis rates under rapid mixing conditions but the activation occurred at concentrations much lower than observed in the case of Zn^{2+}. This raised the possibility that the magnitudes of dissociation constants K_1 and K_3 (the affinity of the inactivating ligands for the activator and inactivator sites) might control the shape of the observed inactivation profile. An expression for the fraction of active enzyme (f) was derived from Scheme V (see appendix) eq. [46].

$$f = \frac{1 + \frac{[L]}{K_1}}{1 + \frac{[L]}{K_1} + \frac{[L]}{K_3} + \frac{[L]^2}{K_1 K_4}} \qquad [46a]$$

Titration curves were generated by utilizing eq. [46a]. It was observed that if K_1 (Scheme V) exceeded K_3 by 5-fold or less the titration curves generated were similar to that obtained with La^{3+} at low ionic strength. However, if K_1 exceeded K_3 by 7-fold or greater, the titration curves appeared "normal" i.e. the titration (inactivation) was complete within two orders of magnitude of ligand concentration (Fig. 42). The La^{3+} titration data obtained at low ionic strength, were fitted to eq. [46a] by computer; the values of K_1, K_3 and K_4

Fig. 42. Simulation of La^{3+} inactivation profiles using eq. [46a] derived from Scheme V

$$f = \frac{1 + \frac{[La^{3+}]}{K_1}}{1 + \frac{[La^{3+}]}{K_1} + \frac{[La^{3+}]}{K_3} + \frac{[La^{3+}]^2}{K_1 K_4}} \quad [46a]$$

Conditions: $K_4 = 1 \times 10^{-3}$ M; $K_3 = 5 \times 10^{-6}$ M; a) $K_1 = 5 \times 10^{-4}$ M; b) $K_1 = 5 \times 10^{-5}$ M; c) $K_1 = 1 \times 10^{-5}$ M.

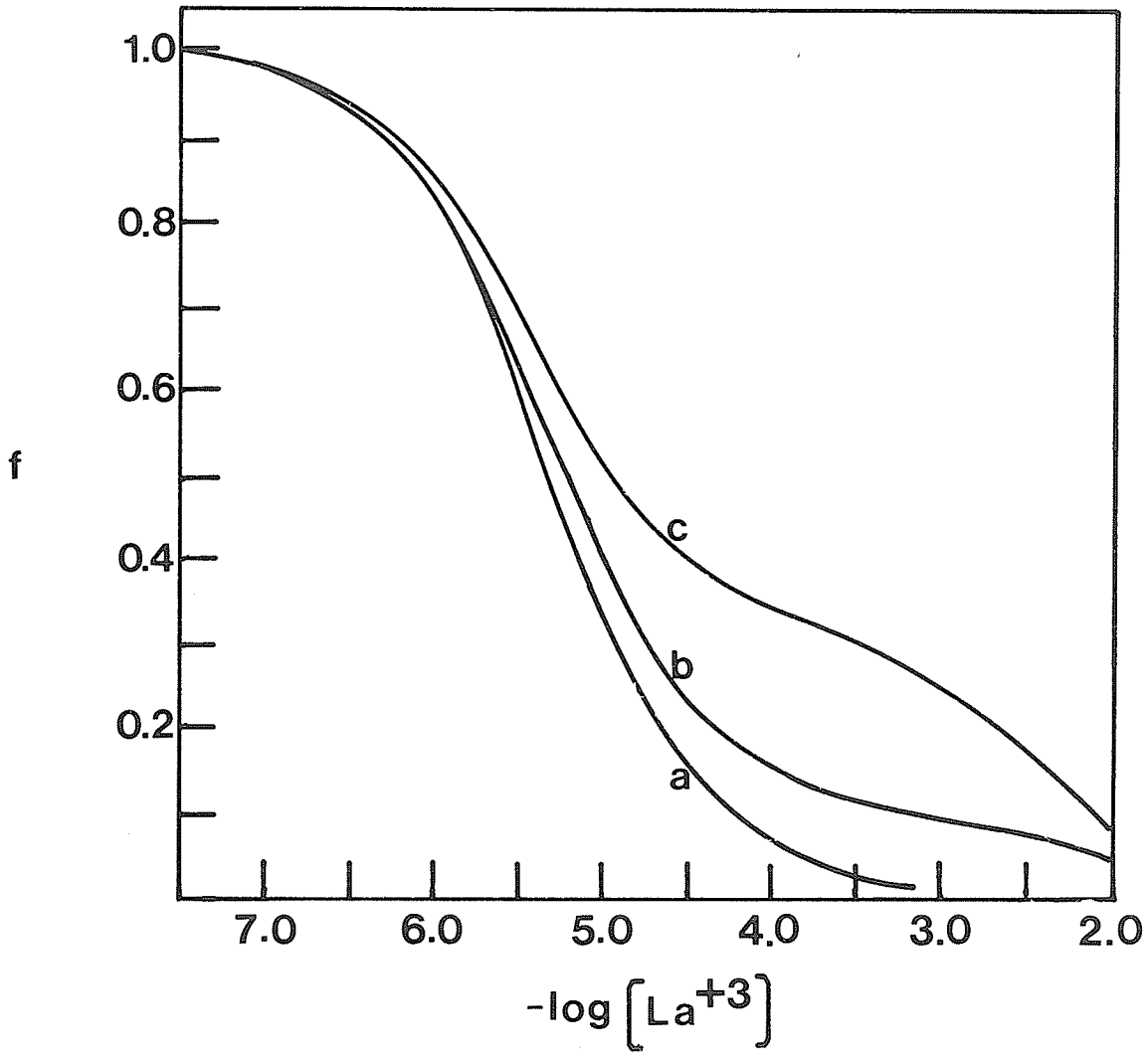
1.0
0.8
0.6
0.4
0.2
f
c
b
a
7.0
6.0
5.0
4.0
3.0
2.0
-log [La+3]

obtained from the computer-fit were 6.5×10^{-6} M, 4.26×10^{-6} M, and 1.52×10^{-3}M, respectively.

T. californica AcChase:

AcChase isolated from one particular lot of T. californica electroplax displayed biphasic carbamoylation rates at low but not at high ionic strength. The carbamoylation at low ionic strength was characterized by two pseudo-first order processes, differing approximately by an order of magnitude. This phenomenon was not due to a time dependant denaturation of the enzyme, as incubation of AcChase at 25°C for up to 11 hrs did not result either in a change in the observed carbamoylation rates or in the relative amplitudes of the two rate processes. The dependance of the fast pseudo-first order carbamoylation rates on the M7C concentration was as predicted (by eq. [79a], see appendix) in the concentration range (0.5 to 10 μM) used. The kinetic parameters extracted from the data had the values K_s = 3.1×10^{-6} M, k_2 = 0.148 sec^{-1} and k_3 = 1.4×10^{-4} sec^{-1}. As in the case of E. electricus AcChase, the peripheral activators Mg^{2+}, Ca^{2+} activated k_3 by 3-fold; propidium activated both k_2 and k_3. Under conditions of high ionic strength K_s and k_2 had the values 3.5×10^{-5} M and 0.23 sec^{-1} in very close correspondance with published values (130). The Zn^{2+} inactivation profiles were independent of ionic strength. This is in contrast to the results obtained with E. electricus AcChase and possibly suggests that with T. californica AcChase the peripheral anionic-inactivator subsites are not altered by ionic strength-induced conformational changes in the enzyme.

The overall conclusion from the fast carbamoylation results is that T. californica AcChase is essentially identical to E. electricus AcChase with respect to carbamoylation kinetics under pre-steady-state conditions.

The slow carbamoylation rates may be due to the presence of a kinetically altered form of the enzyme, perhaps as a result of excessive proteolysis during the isolation of this particular batch of enzyme. The pre-steady-state kinetic parameters extracted from the dependence of the slow pseudo-first order carbamoylation rates on M7C concentration, were K_s = 1.67 x 10^7 M, k_2 = 5 x 10^{-3} sec . These two parameters, which are 12- and 30-fold lower, respectively, than the corresponding values obtained using the fast carbamoylation rates, therefore may result from a partially denatured form of the enzyme. The slow carbamoylation rates were activated but never attained the fast rates in the presence of Mg^{2+}, propidium or M7C. This effect has not been observed with E. electricus or the fast T. californica AcChases. Furthermore the effect of these activators was to decrease the slow phase amplitude and to increase the fast phase amplitude without affecting the total carbamoylation amplitude thus suggesting an activator-induced conversion of the slow enzyme to the fast form, and is assumed to be the result of activators interacting with the peripheral sites of the partially denatured enzyme and thereby converting it to a more "native" like state.

Attempts to induce biphasicity in "monophasic" T. californica AcChase were not successful. Various experiments consisting of alterations in isolation and assay procedures and of the TIAA

(throw in anything available) type, failed to introduce biphasicity in the carbamoylation rates.

Kinetic heterogeneity in AcChase is by no means limited to T. californica enzyme or to the present study. Gentinetta and Brodbeck (139) reported that 18S,8S and 11S E. electricus AcChase isolated and purified in their laboratory, resulted in curved Lineweaver-Burk plots, and the inhibition of all of the molecular forms of the enzyme with iPr_2PF was biphasic. Subsequently, attempts by Barnett and Rosenberry (77) to reproduce Gentinetta and Brodbeck's (139) results failed, the inactivation by iPr_2PF was strictly monophasic. In the current investigations the inactivation by iPr_2PF was also strictly monophasic. The iPr_2PF inactivation kinetics of "monophasic" and "biphasic" T. californica as well as E. electricus AcChase were performed in the hope that iPr_2PF kinetics were more sensitive at detecting kinetic heterogeneity than the carbamoylation kinetics. The kinetic picture that emerged was identical to the carbamoylation results: E. electricus and the "monophasic" T. californica AcChases displayed monophasic iPr_2PF inactivation kinetics whereas the "biphasic" T. californica enzyme displayed biphasic inactivation with iPr_2PF.

An explanation of the intermittent observation of kinetic heterogeneity in AcChase cannot be offered at this point and must await further study.

The chemical modification of AcChase:

There have been many reports of a thiol-like reactivity in AcChase. Some of the earlier evidence is summarized in

Table IX. More recently Massoulié and Rieger (149) have reported that purified T. californica AcChase is inhibited by PCMB. The inactivation was very slow, the half-life of the reaction was approximately 90 minutes. Wins et al. (132) have demonstrated PCMB interacts with AcChase at or near the peripheral anionic sites, as the PCMB inactivation was reversible with Ca^{2+}, a peripheral site-specific ligand. Wilson and Silman (150) have also demonstrated that arsenite inhibition of AcChase was reversible with PCMB, suggesting a possible competition between these two thiol specific reagents for the "thiol-like" group in AcChase. In the present study, the time-dependent loss of activity observed at low concentrations of T. californica AcChase (10^{-11} M) was greatly increased if the enzyme solutions contained DTNB. At high enzyme concentrations (2×10^{-7} M), the enzyme was very stable. Neither the carbamoylation rate nor the amplitude changed upon incubation of the enzyme at 25°C for up to 11 hrs. However, if DTNB was added, there was a slow decrease in the carbamoylation amplitude. Incubation with DTNB for 8 hrs at 25°C resulted in the loss of 25% of the carbamoylation amplitude. These results were interpreted as arising from the modification of free thiol groups in AcChase since DTNB is one of the most specific reagents for the titration of thiol groups in proteins. A DTNB-dependent loss in activity could not be demonstrated with E. electricus AcChase, either with low or high enzyme concentrations. However, the observation that the metal-induced irreversible inactivation was O_2 dependent raised the possibility of free

thiols being at or near the peripheral anionic sites and that in the case of E. electricus AcChase were inaccessible to DTNB. DTNB titrations with both T. californica AcChase and E. electricus AChases were carried out under denaturating conditions. Under these circumstances both enzymes reacted with DTNB; however, the results could not be quantitated as the amount of coloured thionitrobenzoate anion (equal to the free thiol concentration) was quite small (0.02-0.05 absorbance units). Accurate determinations of the free thiol groups using DTNB could be made, either with a very sensitive spectrophotometer or by using very high concentrations of enzyme. Owing to the lack of the former and the prohibitive costs of the latter, an alternative, more sensitive method for the determination of free thiol groups was sought. One such reagent introduced recently by Scouten et al. (162) was the fluorescent, thiol specific compound N-dansylaziridine (N-DAZ).

T. californica AcChase:

The reaction of N-DAZ with T. californica AcChase was characterized by a slow, time dependent enhancement in the N-DAZ fluorescence intensity and blue shift of approximately 10 nm in the fluorescence emission maximum. The magnitude of the fluorescence enhancement was dependent on the reaction conditions used. The largest enhancement (1.6-fold higher than with enzyme plus N-DAZ alone) of the fluorescence spectrum (at 500 nm), was obtained in the presence of Zn^{2+} (1 x 10^{-4} M) while the smallest enhancement was observed if the reaction was performed at high ionic strength or in the pre-

sence of Mg^{2+} (5×10^{-3} M). These results are thought to reflect at least 3 distinct conformational states of the enzyme (in order of reactivity with N-DAZ): The inactivator stabilized, inactive state (E_i), the low ionic strength stabilized, active state (E), and the high ionic strength/activator-stabilized, activated state (E_a).

The kinetics of the AcChase/N-DAZ reaction were studied under pseudo-first order conditions, by continuously monitoring the increase in fluorescence at 500 nm. A pseudo-first order rate constant of 0.16 hr^{-1} was obtained, and was unaffected by Zn^{2+}. This rate constant is approximately 5-fold smaller than that reported for the reaction of N-DAZ with BSA (162). The unreacted N-DAZ was removed by either extensive dialysis or by chromatography on a column of Sepharose 4-B to which L-cysteine was covalently attached.

The resultant modified protein was devoid of AcChase activity and displayed a new peak in its fluorescence spectrum. This peak had an excitation maximum at 345 nm and an emission maximum at 495 nm, and is identical to the spectral properties of S-aminoethyl dansylated BSA (162). The effect of the modification on the catalytic activity of AcChase is not clearly understood: If the enzyme is modified with N-DAZ in the absence of Zn^{2+}, it retains 90% of its original activity at the end of 17 hrs, but upon removal of the excess N-DAZ, the activity drops to only 40% of the original. One possible explanation of this result could be that the dansylation renders the enzyme more susceptible to denaturation (i.e. it

precipitates out of solution, or becomes sensitive to agitation).

E. electricus AcChase:

The reactivity of E. electricus AcChase towards N-DAZ was different from that of T. californica AcChase. Incubation of E. electricus enzyme plus N-DAZ resulted in a very small enhancement in the N-DAZ emission spectrum, although the same spectral changes were observed. Introduction of Zn^{2+} to the reaction mixture again resulted in a greater enhancement of the fluorescence at 500 nm, but in the case of E. electricus AcChase the amount of fluorescence increased by ∿1.9-fold as opposed to ∿1.6-fold with T. californica AcChase. The greater reactivity of T. californica as compared with E. electricus AcChase indicates that the reactive groups are more exposed in the case of the former, possibly explaining the greater tendency of the T. californica enzyme to denaturation or modification with DTNB. Carrying out the modification in the presence of Hg^{2+}, the most tightly bound of the divalent inactivators of AcChase, resulted in a fluorescence enhancement that was 1.9-fold less than that observed in the presence of Zn^{2+}. This possibly indicates an inhibition of the dansylation reaction by Hg^{2+}, the divalent cation that has the highest reported stability constant for thiol containing compounds.

The dansylation results, aside from indicating the possible presence of thiol groups in AcChase, give further support to the proposed model (Scheme V), for a variety of peripheral-site ligand induced kinetic states in AcChase. The enzyme

appears to be most reactive towards N-DAZ in the Zn^{2+}-induced inactive (E_i) state, partially reactive in the active state (E) and least reactive in the high ionic strength/activator induced activated state (E_a). If the differences in reactivity are assumed to be due to the degree of "burial" of these groups within the protein structure then gross conformational changes are implicated. Evidence for extensive peripheral-ligand induced conformational changes in T. californica AcChase have been presented by Epstein et al. (146). The conformational changes were directly measured by the changes in the fluorescence of the enzyme labelled at the active sites with fluorescent dansyl phosphonates. Zn^{2+}, Cu^{2+} and d-tubocurarine were shown to induce slow conformational changes on the enzyme. However Zn^{2+} appeared to enhance the dansyl fluorescence ($\sim$1.1 fold) whereas d-tubocurarine or Cu^{2+} appeared to quench it by up to 2-fold. These results were interpreted as an indication that peripheral-site ligands can induce more than a single conformation at the active centre. Such a conclusion was thought to be reasonable in view of the diverse structures of peripheral-site ligands and their disparate influences on the catalytic behaviour of AcChase (146).

Hydrolysis of the modified T. californica and E. electricus AcChases and the subsequent 2-dimensional TLC of the hydrolysates yielded a fluorescent, ninhydrin-positive compound that displayed R_f values nearly identical to those of a sample of dansyl-s-aminoethyl cysteine.

Further characterization of this compound is essential

in view of the recent report by Sturgill et al. (163) that 3 mol of N-DAZ were incorporated per mol of BSA, even though BSA is known to contain only 1 free thiol group. The extra label was thought to be the result of the covalent reaction of N-DAZ with lysine or arginine as well as the thiol group of BSA.

Summary and conclusions:

The existence of a peripheral anionic region on E. electricus AcChase, with a high affinity for specific cationic ligands was demonstrated by fluorescence binding and displacement studies. In these studies the peripheral site specificity of propidium, gallamine or Zn^{2+} was established. Two classes of binding sites were evident from the propidium binding experiments, and may arise either from structural asymmetry in the enzyme or from heterogeneity in enzyme populations.

Steady-state kinetic studies indicated that eel enzyme existed in two distinct kinetic forms stabilized at either low or high (physiological) ionic strength. At intermediate ionic strength kinetic heterogeneity was evident, suggesting that these kinetic forms are reversibly linked. The k_{cat} and K_{app} of the high ionic strength form were ∿3- and 12-fold higher respectively than the corresponding parameters for the low ionic strength form. The peripheral site ligands gallamine, propidium, Mg^{2+}, Ca^{2+} were shown to activate the low ionic strength form of the enzyme (E) to the high ionic strength activated form (E_a). The cation Zn^{2+} was shown to have two

opposing effects on the steady-state kinetics: an instantaneous activation of the steady-state rates of hydrolysis as well as a slow inactivation of the enzyme. This may be a general metal ion effect with consequences which depend upon the relative affinities of the various binding sites for a particular metal ion.

The pre-steady-state kinetics enabled a more comprehensive study of the consequences of peripheral site occupation on the proposed kinetic mechanism of AcChase. M7C as well as carbamoylating the active site of AcChase was found to interact with the peripheral sites, activating both the carbamoylation rate constant (k_2) and the decarbamoylation rate constant (k_3). The other organic peripheral ligands propidium and gallamine were also shown to activate both k_2 and k_3. The value of K_s was also increased by ~6-fold in going from low to high ionic strength. The inorganic activators Ca^{2+}, Mg^{2+} were shown to affect only k_3.

Zn^{2+}, d-tubocurarine, Cu^{2+}, Hg^{2+}, Cd^{2+} induced the conversion of AcChase to an inactive form. This inactivation was partially reversible with EDTA but a slow metal cation, O_2 dependent irreversible step was evident. The activating ligands Ca^{2+}, gallamine and propidium inhibited the Zn^{2+} induced inactivation but were not able to reverse the inactivation after the enzyme was inactivated, indicating a possible increase in affinity of the peripheral sites in the inactive state, analogous to the desensitization observed with the AcCh-receptor.

The kinetics of the metal-induced inactivation were bi-

phasic at low but not at high ionic strength. The fast rates under both ionic strength conditions were identical, and were thought to represent the same process i.e. the inactivation of "activated" enzyme, $E_a \rightarrow E_{ia}$. On the other hand, the slow rate observed at low ionic strength was thought to represent the inactivation of "active" enzyme, $E \rightarrow E_i$. The biphasic inactivation at low ionic strength may then be explained by assuming that both active and activated enzyme are present in significant amounts at low ionic strength. This could come about if the inactivating ligand activates the enzyme as well as inactivating it. This has been demonstrated with La^{3+} and Zn^{2+}. In view of these results a model (Scheme V) was proposed to account for the kinetic consequences of peripheral site occupation by activating and inactivating peripheral-site specific ligands. This model is particularly successful in accommodating the La^{3+} inactivation results, which demonstrate that the inactivation profile is dependent on the affinity of inactivating ligands for the activating as well as for the inactivating peripheral sites. If the affinity of the inactivating ligand for the activating sites exceeded its affinity for the inactivating sites by 5-fold or less the inactivation profile is spread out as in the case of La^{3+}. However if the affinity of the inactivating ligand for the activating sites is 7-fold or greater than its affinity for the inactivating sites the inactivation at low ionic strength is "normal" in that it is complete within two orders of magnitude of the ligand concentration. Activating species such as Mg^{2+} and

Ca^{2+} thus appear to have a very low affinity for the "inactivator" binding site.

T. californica AcChase displayed non-hyperbolic steady-state kinetics at low ionic strength; the Lineweaver-Burk plots were displaced downwards at high AcSCh concentrations suggesting that AcSCh possibly acts as a peripheral site activator in T. californica but not in E. electricus AcChase.

The pre-steady-state kinetic properties of T. californica enzyme were qualitatively identical to those of E. electricus AcChase. Organic ligands activated both k_2 and k_3 whereas inorganic ligands only affected k_3. One particular enzyme lot displayed biphasic carbamoylation rates which may have arisen as a result of partial denaturation of the enzyme during the isolation process.

T. californica and E. electricus enzymes were modified by reaction with DTNB and N-DAZ, two thiol-specific reagents. A fluorescent, ninhydrin-positive compound with identical R_f values to those of dansyl-S-aminoethyl cysteine was isolated from the hydrolysates of the enzyme modified with N-DAZ. While strongly suggestive of the presence of free thiol groups in AcChase, conclusive proof must await further characterization of this compound.

Both enzymes were most reactive towards N-DAZ in the inactive (E_i) state, partially reactive in the active (E) state, and the least reactive in the activated state (E_a), further illustrating the existence of at least three, peripheral-site specific, ligand-induced conformational states of AcChase.

APPENDIX

1) Determination of free and bound ligand in the propidium titrations and the analysis of the binding data by means of Scatchard plots:

a) Determination of free and bound ligand in fluorescence titrations (130):

For dilute solutions the fluorescence intensity of a fluorescent compound is given by eq. [1a]

$$I = \gamma[F] \qquad [1a]$$

where I = fluorescence intensity

$[F]$ = concentration of the fluorescent ligand

γ = intensity coefficient.

In the presence of enzyme some of F will be bound so that

$$[F_o]_{tot} = [F_f] + [F_b] \qquad [2a]$$

where $[F_f]$ and $[F_b]$ are the concentrations of free and bound ligand respectively, and the observed intensity is now given by eq. [3a].

$$I_T = I_b + I_f \qquad [3a]$$

$$I_b = \gamma'[F_b] \qquad [4a]$$

$$I_f = \gamma[F_f] \qquad [5a]$$

where γ' and γ are the intensity coefficients and I_b and I_f are the fluorescence intensities of free and bound ligand respectively.

Substituting eq. [3a] for I_b and I_f

$$I_T = \gamma[F_f] + \gamma'[F_b] \qquad [6a]$$

or $= \gamma[F_f] + \gamma'([F_o] - [F_f])$ [7a]

$= \gamma [F_o] + (\gamma - \gamma') [F_f]$ [8a]

Therefore the concentration of free ligand is given by eq. [9a]:

$$[F_f] = \frac{I_T - \gamma' [F_o]}{\gamma - \gamma'} \quad [9a]$$

Similarly

$$I_T = \gamma'[F_b] + \gamma([F_o] - [F_b]) \quad [10a]$$

$$= \gamma'[F_b] + \gamma[F_o] - [F_b] \quad [11a]$$

rearranging and solving for $[F_b]$

$$F_b = \frac{[I_T] - \gamma[F_o]}{(\gamma' - \gamma)} \quad [12a]$$

γ can be determined from the slope of an I_T vs. $[F_f]$ (i.e. in the absence of enzyme). γ' can be determined the limiting slope of an I_T vs. $[F_o]$ curve under the conditions where $E_o >> F_o$.

b) Analysis of the by means of a Scatchard plot:

The average number of moles of fluorescent ligand bound to an enzyme containing n binding sites is given by

$$\bar{v} = \frac{[F_b]}{[E_o]} = \frac{nK[F_f]}{1 + K[F_f]} \quad [13a]$$

where K is the binding constant for the ligand-enzyme complex, all sites being assumed to be equivalent.

Eq. [13a] can be rearranged

$$\bar{v} + \bar{v} K[F_f] = nK[F_f] \quad [14a]$$

$$\text{or} \quad \frac{\bar{v}}{[F_f]} = nK - \bar{v}K \qquad [15a]$$

replacing $\bar{v}$ by $\frac{[F_b]}{[E_o]}$

$$\frac{[F_b]}{E_o[F_f]} = nK - \frac{[F_b]}{[E_o]} K \qquad [16a]$$

$$\frac{[F_o]}{[F_f]} = nK[E_o] - [F_b]K \qquad [17a]$$

thus a plot of $[F_b]/[F_f]$ vs. $[F_b]$ will have a slope of $-K$, a vertical intercept of $nK[E_o]$ and a horizontal intercept of $n[E_o]$. If $[E_o]$ is known n and K can readily be determined.

2) Analysis of the competitive data from the propidium displacement experiments (130):

If both propidium [P] and a displacing ligand (D) are present two competing equilibria will be set up

$$[E_o] + [P] \overset{K_p}{\rightleftharpoons} [EP]$$

$$K_p = \frac{[E]\ [P]}{[EP]} \qquad [18a]$$

$$[E_o] + [D] \overset{K_D}{\rightleftharpoons} [ED]$$

$$K_D = \frac{[E][D]}{[ED]} \qquad [19a]$$

If $[P] >> K_p$ and $[E_o]$ then the concentration of free enzyme [E] is negligible.

When both propidium and displacing ligand are present the fractions of enzyme present as [EP] and [ED] are given by eq. [20a] and [21a] respectively.

$$Y = \frac{[EP]}{[EP] + [ED]} \qquad [20a]$$

$$1-Y = \frac{[ED]}{[EP] + [ED]} \qquad [21a]$$

The the contribution to the observed fluorescence by EP (bound propidium) is $f_P Y$ and the contribution of free propidium is $f_D(1-Y)$ eq. 22a

$$f = f_P Y - f_D(1-Y) \qquad [22a]$$

where f, f_P and f_D is the observed fluorescence, fluorescence of fully bound propidium and the fluorescence of free propidium (when displaced from the enzyme under conditions of saturation with displacing ligand)

Rearranging eq. [22a]

$$f = f_P Y + f_D - f_D Y \qquad [23a]$$

$$= f_D + (f_P - f_D)Y \qquad [24a]$$

substituting for Y in eq. [20a]

$$f = f_D + (f_P - f_D)\frac{[EP]}{([EP] + [ED])} \qquad [25a]$$

expanding and rearranging

$$f[EP] + f[ED] = f_D[EP] - f_D[EP] + f_D[ED] + f_P[EP] \qquad [26a]$$

$$\frac{(f_P - f)}{(f - f_D)} = \frac{[ED]}{[EP]} \qquad [27a]$$

substituting for [ED] and [EP] from eq. [18a] and [19a]

$$\frac{(f_P - f)}{(f - f_D)} = \frac{[D]}{[P]} \cdot \frac{K_P}{K_D} \qquad [28a]$$

Therefore a plot $\log \frac{(f_P - f)}{(f - f_D)}$ vs. $\log \frac{[D]}{[P]}$ should be linear with a slope of unity and intercept $\log (K_P/K_D)$. Since K_P can be evaluated as described above, K_D can be evaluated.

The concentrations of [D] and [P] are evaluated as follows:

$$f = f_D + (f_P - f_D)Y \qquad [29a]$$

$$\frac{(f - f_D)}{(f_P - f_D)} = Y \qquad [30a]$$

$$\text{Therefore } [P]_{bound} = Y[E_o] \qquad [31a]$$

$$\text{Then } [P] = [P_o] - \frac{(f - f_D)}{(f_P - f_D)}[E_o] \qquad [32a]$$

Fraction of sites saturated with D = 1-Y

$$[D]_{bound} = 1 - \frac{(f - f_D)}{(f_P - f_D)} [E_o] \qquad [33a]$$

$$= \frac{f_P - f_D - f + f_D}{f_P - f_D} [E_o] \qquad [34a]$$

$$= \frac{(f_P - f)}{(f_P - f_D)} [E_o] \qquad [35a]$$

$$\text{Therefore } [D] = [D_o] - \frac{(f_P - f)}{(f_P - f_D)} [E_o] \qquad [36a]$$

3) <u>Derivation of an expression for the fraction of active enzyme from Scheme V</u>

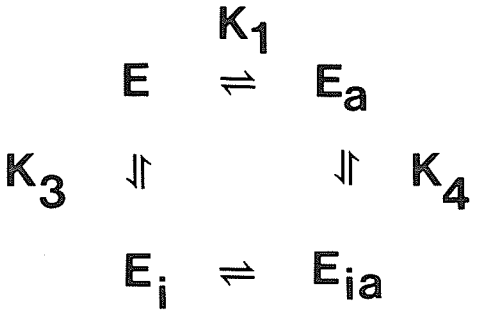

SCHEME V

L represents a ligand capable of occupying both the peripheral activator and inactivator sites. E, E_a, E_i and E_{ia} represent free enzyme, enzyme with activator site occupied, enzyme with inactivator site occupied and enzyme with both activator and inactivator sites occupied.

$$K_1 = \frac{[E]\ [L]}{[E_a]} \qquad [37a]$$

$$K_3 = \frac{[E]\ [L]}{[E_i]} \qquad [38a]$$

$$K_4 = \frac{[E_a]\ [L]}{[E_{ia}]} \qquad [39a]$$

$$E_t = E + E_a + E_i + E_{ia} \qquad [40a]$$

Therefore the fraction of active enzyme is given by $E + E_a/E_t = f$ from eq. [37a].

$$E_a = \frac{[E]\ [L]}{K_1} \qquad [41a]$$

From eq. [38a]

$$E_i = \frac{[E]\ [L]}{K_3} \qquad [42a]$$

From eq. [39a]

$$E_{ia} = \frac{Ea\ [L]}{K_4} \qquad [43a]$$

Substituting eq. [41a] in [43a]

$$E_{ia} = \frac{E\ [L]^2}{K_1\ K_4} \qquad [44a]$$

Therefore

$$\frac{E_a + E}{E_t} = f = \frac{[E] + \frac{[E][L]}{K_1}}{[E] + \frac{[E][L]}{K_1} + \frac{[E][L]}{K_3} + \frac{E[L^2]}{K_1 K_4}} \qquad [45a]$$

eliminating [E]

$$f = \frac{1 + \frac{[L]}{K_1}}{1 + \frac{[L]}{K_1} + \frac{[L]}{K_3} + \frac{[L]^2}{K_1 K_4}} \qquad [46a]$$

4) Determination of an expression for the pre-steady-state carbamoylation of AcChase by M7C (165):

The mechanism of carbamyl ester hydrolysis is given by eq. 47a

$$E + S \overset{K_s}{\rightleftharpoons} ES \overset{k_2}{\underset{P_1}{\rightleftharpoons}} ES' \xrightarrow{k_3} E + P_2 \qquad [47a]$$

P_1 = M7H

Under steady-state conditions ([S]>>[E_o] and [S] is a constant)

$$K_m = \frac{k_3}{k_2 + k_3} \cdot K_s \qquad [48a]$$

$$k_{cat} = \frac{k_2 k_3}{k_2 + k_3} \qquad [49a]$$

The rate expressions for ES, ES' and P_1 and P_2 can then be written

$$\frac{d[ES]}{dt} = k_1[E][S] - (k_2 + k_{-1})[ES] \qquad [50a]$$

$$\frac{d[P_1]}{dt} = k_2[ES] \qquad [51a]$$

$$\frac{d[P_2]}{dt} = k_3[ES'] \qquad [52a]$$

$$\frac{d[ES']}{dt} = k_2[ES] - k_3[ES'] \qquad [53a]$$

[ES] is the highest at t=0 then decreases to a steady-state rate.

$$[E_o] = [E] + [ES] + [ES'] \qquad [54a]$$

$$\text{since} \quad K_s = \frac{[E][S]}{[ES]} \qquad [55a]$$

$$\text{then} \quad [E_o] = [ES]\frac{K_s}{[S]} + [ES] + [ES'] \qquad [56a]$$

$$[E_o] = [ES](1 + \frac{K_s}{[S]}) + [ES'] \qquad [57a]$$

substituting in [53a] to get an equation only in [ES']

$$[ES] = \frac{[E_o] - [ES']}{1 + \frac{K_s}{[S]}} \qquad [58a]$$

$$\frac{d[ES]'}{dt} = \frac{k_2}{1 + \frac{K_s}{[S]}} ([E_o] - [ES']) - k_3[ES]' \qquad [59a]$$

$$= \frac{k_2\ E_o}{1 + \frac{K_s}{[S]}} - (k_3 - \frac{k_2}{1 + \frac{K_s}{[S]}})\ [ES'] \qquad [60a]$$

$$\text{if} \quad a = \frac{k_2\ [E_o]}{1 + \frac{K_s}{[S]}} \qquad [61a]$$

$$\text{and} \quad b = k_3 + \frac{k_2}{1 + \frac{K_s}{[S]}} \qquad [62a]$$

then eq. [60a] simplifies to

$$\frac{d[ES']}{dt} = a - b\ [ES'] \qquad [63a]$$

$$\frac{d[ES']}{(a-b)[ES']} = \qquad [64a]$$

integrating and evaluating the constants

$$\frac{\ln\ (a-b\ [ES'])}{a} = -bt \qquad [65a]$$

taking the antilog of both sides

$$[ES'] = \frac{a}{b}\ (1 - e^{-bt}) \qquad [66a]$$

now substituting [66a] and in [58a] to get an expression all in [ES]

$$[ES] = \frac{E_o - \frac{a}{b}\ (1 - e^{-bt})}{1 + \frac{K_s}{[S]}} \qquad [67a]$$

now substitute in rate expression for P_1 (eq. [51a])

$$\frac{d[P_1]}{dt} = \frac{E_o - \frac{a}{b}\ (1 - e^{-bt})}{1 + \frac{K_s}{[S]}} \cdot k_2 \qquad [68a]$$

integrate and evaluate the constant

$$[P_1] = \frac{k_2}{1 + \frac{K_s}{[S]}}\ [E_o] - \frac{a}{b}\ t + \frac{a}{b^2}\ (1 - e^{-bt}) \qquad [69a]$$

substituting for a and b

$$P_1 = \frac{k_{cat}[E_o][S_o]}{[S_o] + K_m}\ t + [E_o]\left[\frac{\frac{k_2}{k_2 + k_3}}{1 + \frac{K_m}{[S_o]}}\right]^2 X$$

$$\left(1 - \exp\left(-\frac{(k_2 + k_3)[S_o] + k_3K_s}{K_s + [S_o]}\ t\right)\right) \qquad [70a]$$

The total enzyme and M7C concentration are E_o and S_o, t is the time. As t increases, the exponential approaches zero and eq. [70a] reduces to

$$[P_1] = \Pi + A \qquad [71a]$$

where

$$A = \frac{k_{cat}\,[E_o][S_o]}{[S_o] + K_m} \qquad [72a]$$

and

$$\Pi = [E_o]\left[\frac{k_2}{\frac{k_2 + k_3}{K_m}}{1 + \frac{K_m}{[S_o]}}\right]^2 \qquad [73a]$$

In the titration experiments $[S_o] >> K_s\ k_3/k_2$ eq. [73a] reduces to $\Pi = [E_o]$ [74a] and thus is a measure of enzyme normality.

The observed pseudo-first order rate constant of carbamoylation (k_{obs}) can be evaluated according to the first-order rate equation

$$\ln(I_{ss} - I_{press}) = k_{obs}t + \log I_{ss} \quad (t = 0) \qquad [75a]$$

where $(I_{ss} - I_{press})$ is the difference at time t between the calculated fluorescence on the extrapolated steady-state line and the measure pre-steady-state burst in M7H production.

A plot of $\ln (I_{ss} - I_{press})$ vs. t yields a line with a slope of $-k_{obs}$ and $\ln (I_{ss})$ as the vertical intercept (t = 0).

The value of k_{obs} can then be related to any substrate

concentration $[S_o]$, according to eq. [76a]

$$k_{obs} = \frac{(k_2 + k_3)\ [S_o]\ k_3 K_s}{K_s + [S_o]} \qquad [76a]$$

if $k_2 >> k_3$ and $[S_o] > K_s$ then [77a]

reduces to

$$k_{obs} = \frac{k_2\ [S_o]}{[S_o] + k_2} \qquad [78a]$$

and in its reciprocal form

$$1/k_{obs} = 1/k_2 + \frac{K_s}{k_2\ [S]} \qquad [79a]$$

permits the evaluation of K_s and k_2. A plot of $1/k_{obs}$ vs. $1/[S]$ will have a slope of K_s/k_2 and a vertical intercept ($[S_o] = 0$) of $1/k_2$. The decarbamoylation rate constant k_3 can be evaluated from eq. [80a]

$$\frac{d[P_1]}{dt} = V_{ss} = A = \frac{\frac{k_2\ k_3}{k_2 + k_3}\ [E_o][S]}{[S_o] + \frac{K_s k_3}{k_2 + k_3}} \qquad [80a]$$

If $[S_o] > K_s$ and $k_2 >> k_3$ then eq. [80a] reduces to eq. [81a]

$$V_{ss} = k_3\ [E_o] \qquad [81a]$$

and since $[E_o]$ can be determined from the amplitude of the burst eq. [73a] k_3 can be easily evaluated.

BIBLIOGRAPHY

1) Hunt, R. and Traveau, R. (1906) Brit. Med. J., 2, 1788.

2) Stedman, E., Stedman, E. and Easson, L.H. (1932) Biochem. J. 26, 2056.

3) Glick, D. (1939) J. Biol. Chem. 130, 527.

4) Glick, D. (1938) J. Biol. Chem. 125, 729.

5) Glick, D. (1941) J. Biol. Chem. 137, 357.

6) Alles, G.A. and Hawes, R.C. (1940) J. Biol. Chem. 133, 375.

7) Nachmansohn, D. and Wilson, I.B. (1951) Advances in Enzymology 12, 259.

8) Nachmansohn, D. and Rothenberg, M.A. (1945) J. Biol. Chem. 158, 653.

9) Nachmansohn, D., Rothenberg, M.A. and Feld, E.A. (1947) J. Biol. Chem. 174, 197.

10) Augustinson, K.B. and Nachmansohn, D. (1949) Science 110, 98.

11) Dale, H.H., Feldberg, W. and Vogt, M. (1936) J. Physiol. (London) 86, 353.

12) Katz, B. and Miledi, R. (1965) Proc. Roy. Soc. (London) ser. B 161, 453.

13) Randic, M. and Straughan, D.W. (1964) J. Physiol. (London) 173, 130.

14) DelCastillo, J. and Katz, B. (1955) J. Physiol. (London) 124, 386.

15) Katz, B. (1966) Nerve Muscle and Synapse. New York: McGraw.

16) Katz, B. (1969) The release of Neural transmitters. Springfield, Ill: Thomas.

17) Katz, B. and Miledi, R. (1969) J. Physiol. 203, 459.

18) Katz, B. and Miledi, R. (1969) J. Physiol. 203, 689.

19) Katz, B. and Miledi, R. (1967) J. Physiol. 192, 407.

20) Palade, G. and Palay, S. (1955) Anat. Rec. 118, 335.

21) De Robertis, E.D.P. and Bennett, H.S. (1955) J. Biophys. Biochem. Cytol. 1, 47.

22) Hall, Z.W. (1972) Ann. Rev. Biochem. 41, 925.

23) Sheridan, M.N., Whittaker, V.P. and Israel, M. (1966) Z. Zellforsch 74, 291.

24) Nachmansohn, D. (1975) Chemical and Molecular Basis of Nerve Activity, New York: Academic Press.

25) Neumann, E., Nachmansohn, D. and Katchalsky, A. (1973) Proc. Nat. Acad. Sci. 70, 727.

26) Nachmansohn, D. (1970) Science 168, 1059.

27) Nachmansohn, D. (1971) Proc. Nat. Acad. Sci. 7, 241.

28) Karlin, A. (1974) Life Sci. 14, 1385.

29) Raftery, M.A., Hunkapiller, M.W., Strader, C.D. and Hood, L.E. (1980) Science 208, 1455.

30) Karlin, A. and Cowburn, D.A. (1973) Proc. Nat. Acad. Sci. 70, 3636.

31) Klett, R.P., Fulpius, B.W., Smith, Reich, E., Posani, L.D. (1973) J. Biol. Chem. 248.

32) Olsen, R., Meunier, J.-C and Changeux, J.-P. (1973) FEBS lett. 28, 96.

33) Biesecker, G. (1973) Biochemistry 12, 4403.

34) Elderfrawi, M.E. and Elderfrawi, A.T. (1973) Arch. Biochem. Biophys. 159, 362.

35) Schmidt, J. and Raftery, M.A. (1973) Biochemistry 12, 852.

36) Karlsson, E., Heilbronn, E. and Widlund, L. (1972) FEBS lett. 28, 107.

37) Devine-Strader, C.B., Revel, J.P. and Raftery, M.A. (1979) J. Cell. Biol. 83, 499.

38) Changeux, J.-P. and Podleski, T.R. (1968) Proc. Nat. Acad. Sci. 59, 944.

39) Monod, J., Wyman, J. and Changeux, J.-P. (1965) J. Mol. Biol. 12, 88.

40) Katz, B. and Thesleft, S. (1957) J. Physiol. 138, 63.

41) Rang, H.P. and Ritter, J.M. (1970) Molec. Pharm. 6, 303.

42) Rang, H.P. and Ritter, J.M. (1970) Molec. Pharm. 6, 357.

43) Weiland, G., Georgia, B., Lappi, S., Chignell, L.F. and Taylor, P. (1977) J. Biol. Chem. 252, 7648.

44) Bonner, R., Barrante, F.J. and Javin, T.M. (1976) Nature 263, 429.

45) Grunhagen, H.H. and Changeux, J.-P. (1976) J. Mol. Biol. 106, 517.

46) Quast, U., Schimerlik, M.I., Lee, T., Vitzemann, V., Blanchar, S. and Raftery, M.A. (1978) Biochemistry, 17, 2406.

47) Damle, V.N. and Karlin, A. (1980) Biochemistry 19, 3924.

48) Quast, U. (1980) Proc. Nat. Acad. Sci. 77, 3052.

49) Mendez, B., Valenzuela, P., Martial, J.A. and Baxter, J.D. (1980) Science 209, 695.

50) Main, A.R., Tarkan, E., Aull, J.L. and Soucie, W.G. J. Biol. Chem. 247, 566.

51) Massoulié, J. (1980) T.I.B.S. 5, 160.

52) Dellborn, W.D. and Rosenberg, P. (1957) Arch. Biochem. Biophys. 66, 263.

53) Nachmansohn, D. and Feld, E. (1947) J. Biol. Chem. 17, 715.

54) Wilson, I.B. and Cohen, M. (1953) Biochim. Biophys. Acta 11, 147.

55) Kremzner, L.T. and Rosenberg, P. (1971) Biochem. Pharm. 20, 2953.

56) Rosenberry, T.L. (1975) Advances in Enzymology 43, 103.

57) Rothenberg, M.A. and Nachmansohn, D. (1947) J. Biol. Chem. 168, 223.

58) Dudai, Y., Silman, I., Kalderon, N., Blumberg, S. (1977) Biochim. Biophys. Acta 268, 138.

59) Bon, S., Cartaud, J. and Massoulie, J. (1978) Eur. J. Biochem. 85, 1.

60) McCann, W.F.X. and Rosenberry, T.L. (1977) Arch. Biochem. Biophys. 183, 347.

61) Massoulié, J. and Bon, S. (1976) Eur. J. Biochem. 68, 531.

62) Carson, S., Bon, S., Vigny, M., Massoulie, J. and Fardeau, M. (1979) F.E.B.S. Lett. 97, 348.

63) Dudai, Y. and Silman, I. (1974) J. Neurochem. 23, 1177.

64) Taylor, P., Jones, J.W. and Jacobs, N.M. (1974) Molec. Pharm. 10, 78.

65) Rosenberry, T.L. and Richardson, J.M. (1977) Biochemistry 16, 3550.

66) Webb, G. (1978) Can. J. Biochem. 56, 1124.

67) Bon, S. and Massoulié, J. (1978) Eur. J. Biochem. 89, 89.

68) Lawler, H.C. (1959) J. Biol. Chem. 234, 799.

69) Kremzner, L.T. and Wilson, I.B. (1964) Biochemistry 3, 1902.

70) Rosenberry, T.L., Cheng, H.W. and Chen, Y.T. (1972) J. Biol. Chem. 247, 1555.

71) Wilson, I.B. and Cabib, J.E. (1954). J. Amer. Chem. Soc. 76, 5154.

72) Krupka, R.M. (1966) Biochemistry 5, 1983.

73) Ellman, G.L., Courtney, K.D., Andres Jr., V. and Featherstone, R.M. (1961) Biochem. Pharm. 7, 88.

74) Boyne, A.F. and Ellman, G.L. (1972) Anal. Biochem. 46, 639.

75) Riddles, P.W., Blakely, R.L. and Zerner, B. (1979) Anal. Biochem. 94, 75.

76) Brownstone, C. and Watts, D.J. (1973) Biochem. J. 131, 369.

77) Barnett, P. and Rosenberry, T.L. (1979) Biochim. Biophys. Acta 567, 154.

78) Lange, C. (1978) Eur. J. Med. Chem. 11, 303.

79) Rosenberry, T.L. and Bernhard, S.A. (1971) Biochemistry 10, 4114.

80) Gordon, M.A., Carpenter, D.E., Barret, H.W. and Wilson, I.B. (1978) Anal. Biochem. 85, 519.

81) Vigny, M., Bon, S., Massoulié, J. and Letterier, F. (1975) Eur. J. Biochem. 85, 317.

82) Rieger, F., Bon, S., Massoulié, J. and Cartaud, J. (1973) Eur. J. Biochem. 34, 539.

83) Cartaud, J., Bon, S., Massoulié, J. (1978) J. Cell. Biol. 77, 315.

84) Bon, S., Cartaud, J., Massoulié, J. (1978) Molec. Biol. Rep. 4, 61.

85) Grafius, M.A. and Millar, D.B. (1965) Biochim. Biophys. Acta. 110, 540.

86) Lwebuga-Mukasa, J.S., Lappi, S. and Taylor, P. (1975) Biochemistry 15, 1425.

87) Rotundo, D.M. and Fambrough, D.M. (1978) J. Biol. Chem. 254, 4790.

88) Bon, S., Vigny, M. and Massoulié, J. (1979) Proc. Nat. Acad. Sci. 76, 2564.

89) Viratelle, O.M. and Bernhard, S.A. (1980) Biochem. 19, 4999.

90) Bon, S. and Massoulié, J. (1976) F.E.B.S. Lett. 67, 99.

91) Schaffer, N.K., Michel, H.O. and Bridges, A.F. (1973) Biochemistry 12, 2946.

92) Leuzinger, W. and Baker, A.L. (1967) Proc. Nat. Acad. Sci. 57, 446.

93) Leuzinger, W., Baker, A.L. and Cauvin, E. (1968) Proc. Nat. Acad. Sci. 59, 620.

94) Crothia, C. and Leuzinger, W. (1975) J. Molec. Biol. 91, 55.

95) Adams, D.H. and Whittaker, V.P. (1950) Biochim. Biophys. Acta. 4, 543.

96) Wilson, I.B. and Bergman, F. (1950) J. Biol. Chem. 185, 479.

97) Krupka, R.M. and Hellenbrand (1974) Biochim. Biophys. Acta. 370, 208.

98) Hasan, F.B., Cohen, S.G. and Cohen, J.B. (1980) J. Biol. Chem. 255, 3898.

99) Molte, H.-J., Rosenberry, T.L. and Neumann, E. (1980) Biochemistry 19, 3705.

100) Shininsky, M., Dudai, Y. and Silman, I. (1973) F.E.B.S. Lett. 30, 125.

101) Belleau, B. and Tani, H. (1966) Molec. Pharm. 2, 411.

102) Beddoe, F. and Smith, H.J. (1967) Nature 26, 706.

103) O'Brien, R.D. (1969) Biochem. J. 113, 713.

104) Purdie, J.E. and McIvor, R.A. (1966) Biochim. Biophys. Acta. 128, 590.

105) Purdie, J.E. (1969) Biochim. Biophys. Acta. 185, 122.

106) Belleau, B. and DiTullio, V. (1970) J. Amer. Chem. Soc. 92, 6320.

107) Wolfsy, L. and Michaeli, D. (1967) Proc. Nat. Acad. Sci. 58, 2296.

108) Meunier, J.-C. and Changeux J.-P. (1969) F.E.B.S. Lett. 2, 224.

109) Podleski, T.R., Meunier, J.-C. and Changeux, J.-P. (1969) Proc. Nat. Acad. Sci. 63, 1239.

110) Bender, M.L. and Kezdy, F.S. (1964) J. Amer. Chem. Soc. 86, 3704.

111) Krupka, R.M. (1965) Biochemistry, 4, 429.

112) Krupka, R.M. (1966) Biochemistry, 5, 1988.

113) Fersht, A.R., Blow, D.M. and Fastrez, J. (1973) Biochemistry 12, 2035.

114) Rosenberry, T.L. (1975) Proc. Nat. Acad. Sci. 72, 3834.

115) Koshland, Jr., D.E. and Neet, K.E. (1968) Ann. Rev. Biochem. 37, 359.

116) Krupka, R.M. and Laidler, K.J. (1961) J. Amer. Chem. Soc. 83, 1454.

117) Krupka, R.M. and Laidler, K.J. (1961) J. Amer. Chem. Soc. 83, 1448.

118) Krupka, R.M. (1966) Molec. Pharm. 2, 558.

119) Greenspan, C.M. and Wilson, I.B. (1970) Molec. Pharm. 6, 460.

120) Heilbron, E. (1965) Acta. Chem. Scand. 19, 1333.

121) Rosenberry, T.L. and Bernhard, S.A. (1972) Biochemistry 11, 4308.

122) Goldstein, A. (1951) Arch. Biochem. Biophys. 34, 169.

123) Wilson, I.B., Hatch, M.A. and Ginsburg, S. (1960) J. Biol. Chem. 235, 2312.

124) Hart, G.J. and O'Brien, R. (1973) Biochemistry 12, 2940.

125) Froede, L.C. and Wilson, I.B. (1971) The Enzymes 5, Academic Press, N.Y. p. 87

126) Wilson, I.B. and Ginsburg, S. (1951) Biochim. Biophys. Acta. 18, 168.

127) Barnett, P. and Rosenberry, T.L. (1977) J. Biol. Chem. 252, 7200.

128) Changeux, J.-P. (1966) Molec. Pharm. 2, 369.

129) Kitz, R.J., Braswell, L.M. and Ginsburg, S. (1970) Molec. Pharm. 6, 108.

130) Taylor, P. and Lappi, S. (1975) Biochemistry 14, 1989.

131) Mooser, G., Schulman, H. and Sigman, D.S. (1972) Biochemistry 11, 1595.

132) Wins, P., Schonfeniels, E. and Foidart, J.-M. (1970) Life Sci. 9, 259.

133) Roufogalis, B.D. and Quist, E.E. (1972) Molec. Pharm. 8, 41.

134) Crone, H.D. (1973) J. Neurochem. 20, 225.

135) Dawson, R.M. and Crone, H.D. (1973) J. Neurochem. 21, 247.

136) Roufogalis, B.D. and Wickson, V.M. (1972) J. Biol. Chem. 248, 2254.

137) Roufogalis, B.D. and Wickson, V.M. (1975) Molec. Pharm. 11, 352.

138) Wermuth, B. and Brodbeck, U. (1973) Eur. J. Biochem. 37, 377.

139) Gentinetta, R. and Brodbeck, U. (1976) Biochim. Biophys. Acta. 438, 437.

140) Taylor, P. and Jacobs, N.M. (1974) Molec. Pharm. 10, 93.

141) Mooser, G. (1972) Ph.D. dissertation. Univ. of California (L.A.)

142) Mooser, G. and Sigman, D.S. (1974) Biochemistry 13, 2299.

143) Taylor, P., Luebuga-Mukasa, Lappi, S. and Rademacher, J. (1974) Molec. Pharm. 10, 703.

144) Bolger, M.B. and Taylor, P. (1979) Biochemistry 18, 3622.

145) Pattison, S. and Bernhard, S. (1978) Proc. Nat. Acad. Sci. 75, 3613.

146) Epstein, D.J., Berman, H.A. and Taylor, P. (1979) Biochemistry 18, 4749.

147) Berman, H.A., Yguerabide, J. and Taylor, P. (1980) Biochemistry 19, 2226.

148) Mounter, L.A. and Whittaker, V.P. (1952) Biochem. J. 53, 167.

149) Massoulié, J. and Rieger, F. (1969) Eur. J. Biochem. 11, 441.

150) Wilson, A.B. and Silman, I. (1977) Biochemistry 16, 2701.

151) Friedman, M. (1973) The Chemistry and Biochemistry of the Sulphydryl group in Amino Acids, Peptides and Proteins. Pergamon: Toronto. pp. 341.

152) Jocelyn, P.C. (1972) Biochemistry of the SH group. Academic: N.Y. pp. 137.

153) Barlow, R.B. and Ing, H.P. (1948) Nature 161, 718.

154) Massart, L. and Dufait, R. (1939) Enzymologia 6, 282.

155) Thompson, R.H.S. (1948) J. Physiol. 105, 370.

156) Mackworth, J.F. (1948) Biochem. J. 42, 82.

157) Barron, E.S.G., Miller, Z.B., Bartlett, G.R., Meyer, T. and Singer, T.P. (1947). Biochem. J. 410, 69.

158) Barron, E.S.G. and Singer, T.P. (1943) Science 97, 356.

159) Nachmansohn, D. and Lederer, E. (1939) Bull. Soc. Chim. Biol., Paris 21, 797.

160) Wels, P. and Repke, K. (1947) Arch. exp. Path. Pharmak. 204, 323.

161) Stadie, W.C., Riggs, B.C. and Haugaard, N. (1945) J. Biol. Chem. 161, 175.

162) Scouten, W.H., Lubcher, R. and Baughman, W. (1974) Biochim. Biophys. Acta. 336, 421.

163) Sturgill, T.W., Baskin, G.S. and Taylor, R.P. (1977) Biochim. Biophys Acta. 485, 236.

164) Neiderweiser, A. (1972) In Methods in Enzymology (Hirs, C.H.W. and Timasheff, S.N., eds) 25B, pp. 60-69.

165) Bender, M.L. Kezdy, F.J. and Wedler, F. (1967) J. Chem. ed. 44, 84.